ASSESSING THE INFLUENCE OF HILLY LANDSCAPE CHARACTERISTICS ON RIVER WATER QUALITY: A CASE OF TLAWNG RIVER

BACHELOR OF PLANNING

K VANLALRORELFAMKIMI
2020BPLN036

SCHOOL OF PLANNING AND ARCHITECTURE, BHOPAL
Neelbad Road, Bhauri, Bhopal (M.P.) 462030

May 2025

(This page has been left blank intentionally.)

ASSESSING THE INFLUENCE OF HILLY LANDSCAPE CHARACTERISTICS ON RIVER WATER QUALITY: A CASE OF TLAWNG RIVER

Thesis submitted in partial fulfilment of the requirements for the award of the degree of

BACHELOR OF PLANNING

By

K VANLALRORELFAMKIMI
2020BPLN036

Under the Guidance of
Ar. Mrunmayi Wadwekar

SCHOOL OF PLANNING AND ARCHITECTURE, BHOPAL
Neelbad Road, Bhauri, Bhopal (M.P.) 462030

May 2025

(This page has been left blank intentionally.)

DECLARATION

I, **K Vanlalrorelfamkimi**, Scholar No. **2020BPLN036,** hereby declare that the thesis entitled **'Assessing the Influence of Hilly Landscape Characteristics on River Water Quality: A Case of Tlawng River'** submitted by me in partial fulfilment for the award of Bachelor of Planning at School of Planning and Architecture, Bhopal, India, is a record of bona fide work carried out by me. The matter/result embodied in this thesis has not been submitted to any other University or Institute for the award of any degree or diploma.

_____

Signature of the Student
Date: May 2025

CERTIFICATE

This is to certify that the declaration of K Vanlalrorelfamkimi is true to the best of my knowledge and that the student has worked under my guidance in preparing this thesis.

RECOMMENDED

_____

Signature of the Guide
Ar. Mrunmayi Wadwekar

ACCEPTED

_____

Signature of Head
Department of Urban & Regional Planning
Dr. Sheuli Mitra

May 2025, Bhopal

(This page has been left blank intentionally.)

Acknowledgement

I would like to take this opportunity to sincerely thank everyone who played a role in helping me reach the point where this completed thesis is in your hands. This achievement would not have been possible without the unwavering support, guidance, and encouragement I received along the way.

I extend my heartfelt thanks to my thesis advisor, Ar. Mrunmayi Wadwekar, for her invaluable mentorship throughout this journey. Her expertise, thoughtful guidance, and constructive feedback were instrumental in shaping the course of my work. I am also thankful to my thesis coordinators, Dr. Ashfaque Alam and Dr. Paulose N. Kuriakose, whose insights and encouragement at critical moments provided great motivation and clarity.

My gratitude also goes out to all the faculty members of the Planning Department at SPA-B. Their teaching and inspiration over the past four years have left a lasting impact on both my academic and personal growth.

I am especially grateful to the National Institute of Urban Affairs (NIUA) for selecting my work for their Student Thesis Competition. Their support provided not just financial sponsorship but also the enriching opportunity to engage with professionals in the field and gain from their knowledge.

I owe a deep debt of gratitude to my family. Their boundless love, patience, and belief in my potential have been my strongest pillars of strength throughout this journey. To my friends—thank you for being my sounding boards, my safe space, and my source of encouragement during tough times. A special note of thanks to Aastha, whose guidance and experience were immensely helpful, and to Fathima,who has been with me throughout the journey. Finally and deaarly, I am profoundly thankful to God for granting me the resilience, faith, and strength needed to persevere.

To everyone who supported me in big ways or small—through kind words, critical input, or simply your presence—thank you from the bottom of my heart.

(This page has been left blank intentionally.)

Abstract

Rivers globally are degrading due to pollution, climate change, and unsustainable practices, with anthropogenic stressors like industrial discharge and agricultural runoff dominating research. In India, the Ganges and its tributaries exemplify this crisis, suffering from severe contamination despite large-scale initiatives like Namami Gange. However, studies overwhelmingly focus on human-driven factors, neglecting the role of natural landscape characteristics in shaping water quality. Critical gaps persist in understanding how topography, slope gradients, and hydrological connectivity in low-order streams—vital for local communities—interact with broader river systems. These smaller, ecologically significant streams remain excluded from national assessments, particularly in India's Northeast Himalayan foothills, where unique hydrological dynamics and fragile ecosystems demand urgent attention.

This study aims to analyse how natural landscape characteristics and non-point source pollution interact to influence river water quality. By focusing on hilly terrains, the research emphasizes the role of inherent natural features—such as topography, slope gradients, and catchment hydrology—in shaping water quality dynamics. Hilly regions, often overlooked in favor of large river systems, serve as critical case studies to isolate natural drivers while addressing the understudied role of low-order streams in sustaining local ecosystems and livelihoods. The study's uniqueness lies in its focus on cause-and-effect mechanisms between landscape attributes and gradual water quality degradation, offering nuanced insights into how terrain-specific processes amplify or mitigate pollution. These findings will advance scientific understanding of natural-environment interactions and provide actionable frameworks for sustainable watershed management in ecologically fragile, data-deficient regions like India's Northeast Himalayan foothills.

The first objective involves a systematic review of existing literature to identify mechanisms linking landscape characteristics to river water quality. This includes analyzing case studies on how natural features and non-point source pollution influence pollutant mobilization, transport, and retention. Key water quality parameters affected by these mechanisms and critical landscape metrics (quantified spatial attributes) are synthesized to define their interdependencies. This phase establishes a conceptual framework for subsequent data collection and analysis.

The second objective focuses on selecting a representative hilly river system in India's Northeast, Tlawng River, in Aizawl, Mizoram, prioritizing low-order streams with limited

prior research. Data is collected through field remote sensing, and secondary sources, and based on its availability and relevance, key ecological and water quality parameters are finalized.

The third objective involves analyzing temporal and spatial relationships between landscape characteristics and water quality through three steps: (1) mapping land cover changes (2017–2024) and corresponding water quality trends to establish baseline dynamics, (2) conducting correlation tests to determine the influence landscape metrics exert on specific water quality parameters, and (3) applying linear regression to quantify the percentage of water quality variation attributable to measurable changes in landscape metrics (e.g., slope gradients, vegetation cover). This approach isolates the role of natural landscape drivers in shaping river health while identifying dominant mechanisms linking land and terrain features to pollutant dynamics.

The study reveals that natural landscape characteristics—particularly slope gradients, topographical connectivity, and catchment hydrology—exert significant influence on river water quality in hilly terrains. Temporal analysis shows a strong correlation between land cover changes and shifts in water quality parameters over 2017–2024. Statistical modelling indicates that steeper slopes amplify pollutant mobilization, while fragmented riparian zones reduce pollutant retention, accelerating degradation. Regression results quantify the degree to which measurable changes in landscape metrics correspond to variations in water quality, highlighting terrain-specific mechanisms driving pollution. These findings underscore the critical role of natural landscape dynamics in mediating water quality, independent of anthropogenic stressors, and provide a foundation for targeted watershed management in ecologically fragile hilly regions.

This study establishes that natural landscape characteristics significantly shape river water quality in hilly areas, offering a critical counterpoint to anthropocentric pollution research. By isolating terrain-driven mechanisms—such as slope-induced erosion and hydrological connectivity—it advances understanding of how intrinsic landscape features mediate water quality degradation.

Keywords: hill; river; landscape metrics; watershed; cause-effect

सारांश

विश्व स्तर पर नदियाँ प्रदूषण, जलवायु परिवर्तन और अवहनीय प्रथाओं के कारण खराब हो रही हैं, जिसमें औद्योगिक निर्वहन और कृषि अपवाह जैसे मानवजनित दबाव अनुसंधान पर हावी हैं। भारत में, गंगा और उसकी सहायक नदियाँ इस संकट का उदाहरण हैं, जो नमामि गंगे जैसी बड़े पैमाने की पहलों के बावजूद गंभीर संदूषण से पीड़ित हैं। हालाँकि, अध्ययन अत्यधिक रूप से मानव-चालित कारकों पर ध्यान केंद्रित करते हैं, जल गुणवत्ता को आकार देने में प्राकृतिक भूदृश्य विशेषताओं की भूमिका की उपेक्षा करते हैं। निम्न-क्रम की धाराओं में – जो स्थानीय समुदायों के लिए महत्वपूर्ण हैं – स्थलाकृति, ढलान प्रवणता, और जलविज्ञानीय संपर्क कैसे व्यापक नदी प्रणालियों के साथ परस्पर क्रिया करते हैं, इसे समझने में महत्वपूर्ण कमियाँ बनी हुई हैं। ये छोटी, पारिस्थितिक रूप से महत्वपूर्ण धाराएँ राष्ट्रीय मूल्यांकनों से बाहर रहती हैं, विशेष रूप से भारत के पूर्वोत्तर हिमालय की तलहटी में, जहाँ अद्वितीय जलविज्ञानीय गतिशीलता और नाजुक पारिस्थितिकी तंत्र तत्काल ध्यान देने की मांग करते हैं।

इस अध्ययन का उद्देश्य यह विश्लेषण करना है कि प्राकृतिक भूदृश्य विशेषताएँ और गैर-बिंदु स्रोत प्रदूषण नदी जल की गुणवत्ता को कैसे प्रभावित करने के लिए परस्पर क्रिया करते हैं। पहाड़ी इलाकों पर ध्यान केंद्रित करके, यह शोध जल गुणवत्ता की गतिशीलता को आकार देने में अंतर्निहित प्राकृतिक विशेषताओं – जैसे स्थलाकृति, ढलान प्रवणता, और जलग्रहण क्षेत्र जलविज्ञान – की भूमिका पर जोर देता है। पहाड़ी क्षेत्र, जिन्हें अक्सर बड़ी नदी प्रणालियों के पक्ष में अनदेखा किया जाता है, प्राकृतिक चालकों को पृथक करने के लिए महत्वपूर्ण केस स्टडी के रूप में काम करते हैं, साथ ही स्थानीय पारिस्थितिकी तंत्र और आजीविका को बनाए रखने में निम्न-क्रम की धाराओं की कम अध्ययन की गई भूमिका को भी संबोधित करते हैं। अध्ययन की विशिष्टता भूदृश्य विशेषताओं और क्रमिक जल गुणवत्ता गिरावट के बीच कारण-और-प्रभाव तंत्र पर इसके फोकस में निहित है, जो भू-भाग विशिष्ट प्रक्रियाएँ कैसे प्रदूषण को बढ़ाती या कम करती हैं, इस पर सूक्ष्म अंतर्दृष्टि प्रदान करती है। ये निष्कर्ष प्राकृतिक-पर्यावरण अंतःक्रियाओं की वैज्ञानिक समझ को आगे बढ़ाएंगे और भारत के पूर्वोत्तर हिमालय की तलहटी जैसे पारिस्थितिक रूप से नाजुक, डेटा-कमी वाले क्षेत्रों में सतत जलग्रहण क्षेत्र प्रबंधन के लिए कार्रवाई योग्य ढाँचे प्रदान करेंगे।

पहले उद्देश्य में भूदृश्य विशेषताओं को नदी जल गुणवत्ता से जोड़ने वाले तंत्रों की पहचान करने के लिए मौजूदा साहित्य की एक व्यवस्थित समीक्षा शामिल है। इसमें इस बात का विश्लेषण करने वाले केस स्टडीज़ शामिल हैं कि कैसे प्राकृतिक विशेषताएँ और गैर-बिंदु स्रोत प्रदूषण, प्रदूषकों की गतिशीलता, परिवहन और प्रतिधारण को प्रभावित करते हैं। इन तंत्रों से प्रभावित होने वाले प्रमुख जल गुणवत्ता पैरामीटर और महत्वपूर्ण भूदृश्य मेट्रिक्स (मात्रात्मक स्थानिक विशेषताएँ) उनकी अंतर्निर्भरताओं को परिभाषित करने के लिए संश्लेषित किए जाते हैं। यह चरण बाद के डेटा संग्रह और विश्लेषण के लिए एक वैचारिक ढाँचा स्थापित करता है।

दूसरा उद्देश्य भारत के पूर्वोत्तर में एक प्रतिनिधि पहाड़ी नदी प्रणाली, आइजोल, मिजोरम में त्लावंग नदी का चयन करने पर केंद्रित है, जिसमें सीमित पूर्व अनुसंधान वाली निम्न-क्रम की धाराओं को प्राथमिकता दी गई है। डेटा क्षेत्र

दूरसंवेदन (फील्ड रिमोट सेंसिंग) और द्वितीयक स्रोतों के माध्यम से एकत्र किया जाता है, और इसकी उपलब्धता और प्रासंगिकता के आधार पर, प्रमुख पारिस्थितिक और जल गुणवत्ता मापदंडों को अंतिम रूप दिया जाता है।

तीसरे उद्देश्य में भूदृश्य विशेषताओं और जल गुणवत्ता के बीच लौकिक और स्थानिक संबंधों का विश्लेषण तीन चरणों के माध्यम से शामिल है: (1) आधारभूत गतिशीलता स्थापित करने के लिए भू-आवरण परिवर्तनों (2017-2024) और संगत जल गुणवत्ता प्रवृत्तियों का मानचित्रण करना, (2) विशिष्ट जल गुणवत्ता मापदंडों पर भूदृश्य मेट्रिक्स के प्रभाव को निर्धारित करने के लिए सहसंबंध परीक्षण आयोजित करना, और (3) भूदृश्य मेट्रिक्स (जैसे, ढलान प्रवणता, वनस्पति आवरण) में मापने योग्य परिवर्तनों के कारण जल गुणवत्ता भिन्नता के प्रतिशत को निर्धारित करने के लिए रैखिक प्रतिगमन लागू करना। यह दृष्टिकोण नदी के स्वास्थ्य को आकार देने में प्राकृतिक भूदृश्य चालकों की भूमिका को पृथक करता है, साथ ही भूमि और भू-भाग की विशेषताओं को प्रदूषक गतिशीलता से जोड़ने वाले प्रमुख तंत्रों की पहचान करता है।

अध्ययन से पता चलता है कि प्राकृतिक भूदृश्य विशेषताएँ – विशेष रूप से ढलान प्रवणता, स्थलाकृतिक संपर्क, और जलग्रहण क्षेत्र जलविज्ञान – पहाड़ी इलाकों में नदी जल की गुणवत्ता पर महत्वपूर्ण प्रभाव डालती हैं। लौकिक विश्लेषण 2017-2024 के दौरान भू-आवरण परिवर्तनों और जल गुणवत्ता मापदंडों में बदलाव के बीच एक मजबूत सहसंबंध दिखाता है। सांख्यिकीय मॉडलिंग इंगित करता है कि तीव्र ढलान प्रदूषक गतिशीलता को बढ़ाते हैं, जबकि खंडित नदीतटीय क्षेत्र प्रदूषक प्रतिधारण को कम करते हैं, जिससे गिरावट तेज होती है। प्रतिगमन परिणाम उस डिग्री को निर्धारित करते हैं जिस तक भूदृश्य मेट्रिक्स में मापने योग्य परिवर्तन जल गुणवत्ता में भिन्नताओं के अनुरूप होते हैं, जो प्रदूषण को चलाने वाले भू-भाग-विशिष्ट तंत्रों पर प्रकाश डालते हैं। ये निष्कर्ष मानवजनित दबावों से स्वतंत्र, जल गुणवत्ता में मध्यस्थता करने में प्राकृतिक भूदृश्य गतिशीलता की महत्वपूर्ण भूमिका को रेखांकित करते हैं, और पारिस्थितिक रूप से नाजुक पहाड़ी क्षेत्रों में लक्षित जलग्रहण क्षेत्र प्रबंधन के लिए एक आधार प्रदान करते हैं।

यह अध्ययन स्थापित करता है कि प्राकृतिक भूदृश्य विशेषताएँ पहाड़ी क्षेत्रों में नदी जल की गुणवत्ता को महत्वपूर्ण रूप से आकार देती हैं, जो मानव-केंद्रित प्रदूषण अनुसंधान के लिए एक महत्वपूर्ण प्रति-बिंदु प्रस्तुत करता है। भू-भाग चालित तंत्रों – जैसे ढलान-प्रेरित कटाव और जलविज्ञानीय संपर्क – को पृथक करके, यह समझने में मदद करता है कि आंतरिक भूदृश्य विशेषताएँ जल गुणवत्ता गिरावट में कैसे मध्यस्थता करती हैं।

Contents

List of Figures

List of Tables

List of Abbreviations

AI-	Aggregation Index
AMC-	Aizawl Municipal Corporation
BIS-	Bureau of Indian Standards
BOD-	Biochemical Oxygen Demand
Ca^{2+}-	Calcium
CPHEEO-	Central Public Health and Environmental Engineering Organisation
DO-	Dissolved Oxygen
EC-	Electrical Conductivity
ED-	Edge Density
GAWSS-	Greater Aizawl Water Supply Scheme
ICMR-	Indian Council of Medical Research
LPI-	Largest Patch Index
LPCD-	Liters Per Capita per Day
LSI-	Landscape Shape Index
LULC -	Land Use/Land Cover
MIRSAC	Mizoram Remote Sensing Application Centre
NH_3-	Ammonia
NO_2^--	Nitrite
PD-	Patch Density
PHED-	Public Health and Engineering Department
PO_4^{3-}-	Phosphate
SHDI-	Shannon's Diversity Index
SHEI-	Shannon's Evenness Index
S%-	Slope Percentage
SP	Stream Proximity
TSS	Total Suspended Solids
USPH	United States Public Health Standards

1 Chapter I: Introduction

This chapter establishes the context for the research undertaken in the thesis. It begins by outlining the global challenges faced by rivers, followed by a focus on Indian rivers, their existing challenges, and current research. It then identifies critical research gaps and understudied areas, with a particular emphasis on rivers in hilly regions. This leads to the formulation of research questions, which guide the thesis in defining its overarching aim and specific objectives, and the methods to achieve them.

1.1 Background

River systems worldwide face severe degradation from pressures like pollution and climate change, threatening ecosystems and human well-being (Akhtar et al., 2021; Wurtsbaugh et al., 2019). While developed regions address these through frameworks emphasizing land use and ecological buffers (e.g., European Water Framework Directive, US Clean Water Act; see Allan, 2004), rapidly developing areas in South and Southeast Asia face acute stress. Here, agricultural runoff, industrial effluents, and urbanization severely compromise water quality with pollutants like nitrates and heavy metals (Matta et al., 2022; Pandey & Singh, 2017)

India's major rivers, such as the Ganges and Brahmaputra, exemplify this crisis, critically threatened by pollution from sewage, agriculture, and industry (Pandey & Singh, 2017; Samal & Gedam, 2021). Current conservation efforts (e.g., Namami Gange) primarily target anthropogenic, point-source pollution in large, high-order rivers, often with mixed success. This approach frequently overlooks the significant influence of natural landscape characteristics on water quality dynamics.

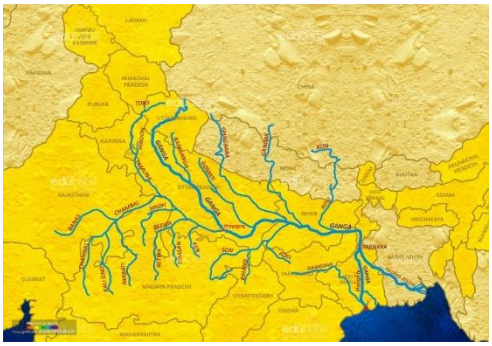

Figure 1 Ganga and its Tributaries

Research increasingly shows that landscape characteristics, such as slope, vegetation, and hydrological connectivity, significantly influence pollutant transport and water quality, especially in complex terrains. Slopes can accelerate erosion and nutrient runoff, while intact riparian zones can buffer pollutants) . However, studies focusing on these natural drivers, particularly in India's ecologically sensitive northeastern Himalayan foothills, are scarce compared to those on anthropogenic stressors. In these hilly catchments, not only land use/land cover (LULC) but also topographical attributes (e.g., slope percentage) and catchment hydrology (e.g., stream proximity, drainage patterns) interact synergistically to determine river water quality.

This thesis aims to address this gap by investigating the relationship between diverse landscape characteristics (quantified as metrics) and river water quality in such hilly terrains. The study will explore how topography, LULC, and catchment hydrology collectively shape river health, providing insights for sustainable watershed management in these under-researched regions.

1.2 Need of the Study

1.2.1 Problem Statement

Global riverine ecosystems are in crisis, facing escalating pressures from pollution, hydrological alterations, and climate change, which severely impact biodiversity and human well-being (Akhtar et al., 2021; Wurtsbaugh et al., 2019). India confronts a formidable challenge with its major rivers, including the Ganges and Brahmaputra, experiencing acute degradation. These vital water sources are heavily polluted by untreated urban sewage, intensive agricultural runoff, and industrial effluents (Pandey & Singh, 2017; Samal & Gedam, 2021b). Current national conservation strategies, such as the Namami Gange programme, predominantly focus on mitigating anthropogenic, point-source pollution in large, high-order river systems, often through wastewater treatment and industrial regulation. While important, these interventions have yielded mixed results, indicating that solely addressing direct pollutant inputs is often insufficient for comprehensive river restoration. A significant issue is that these approaches frequently overlook the profound and often complex influence of natural landscape characteristics on river water quality dynamics, especially in diverse and sensitive terrains.

1.2.2 Research Gap

While the influence of land use and land cover (LULC) on stream ecosystems is widely recognized (J. D. Allan, 2004), and several studies have linked landscape attributes to water quality in various regions (Tran et al., 2010), a significant research gap remains—particularly in the context of India's ecologically sensitive and topographically complex regions, such as the Himalayan foothills. One key gap is the limited focus on natural landscape drivers within India. Most existing research emphasizes anthropogenic stressors, leaving a dearth of studies that quantitatively assess the role of natural landscape factors, beyond broad LULC classifications, especially in smaller order streams within hilly catchments.

Another critical gap involves the underestimation of topographical and hydrological influences. The synergistic role of detailed topographic attributes (such as slope, aspect, and elevation) alongside catchment hydrology (including drainage density, stream proximity, and flow paths), in combination with LULC patterns, is not well-quantified in these regions. For instance, the way steep slopes exacerbate erosion and nutrient runoff

(Wasson et al., 2002), or how riparian zone integrity affects pollutant retention (Naiman & Décamps, 1997), requires more localized, terrain-specific investigation.

Furthermore, there is a lack of integrated assessments that examine how LULC, topography, and hydrological characteristics collectively interact to influence river water quality in hilly watersheds—areas that are particularly vulnerable to ecological degradation. Addressing these gaps by investigating the relationship between diverse landscape characteristics (quantified as metrics) and river water quality in such terrains is essential for generating nuanced, data-driven insights that can guide more effective and sustainable watershed management strategies.

1.3 Aim and Objectives

Aim

To analyse the impact of changes in landscape characteristics on river water quality in hilly regions and propose interventions and strategies.

Objectives

1. To study the relationship between landscape characteristics and river water quality.
2. To select a suitable hilly study area and identify key influencing parameters.
3. To analyse the impact of hilly landscape characteristics on river water quality.
4. To provide planning strategies or recommendations based on the findings.

1.4 Research Design

The study begins with a thorough examination of the foundational literature, focusing on the interplay between landscape characteristics and river water quality. This initial phase focuses on a comprehensive review of global case studies, emphasizing the role of land use/land cover patterns, topography, and hydrological connectivity in shaping water quality dynamics. The analysis reveals recurring gaps in existing research, particularly the underutilized integration of landscape metrics to quantify spatial or landscape characteristics. The findings from the literature review inform the study's theoretical framework, which prioritizes landscape metrics as actionable tools for analysing water quality. This foundation not only clarifies the relationship between spatial configurations and hydrological processes but also sets the stage for the next objective: analysing hilly region dynamics. By isolating key landscape characteristics, the study advances a methodologically grounded approach to address the unique challenges of hilly regions, where steep gradients and fragmented land use amplify pollutant interactions.

The study shifts focus to selecting a suitable hilly study area, prioritizing regions that fill existing research gaps while highlighting natural landscape dynamics. A case study in the Northeast Himalayan hills of India is chosen due to the region's under-explored status, ecological sensitivity, and critical role in local water security. The selected river, a primary drinking water source for Aizawl, serves as an ideal focal point, as it integrates agricultural runoff, urban waste inputs, and steep topography, creating a complex interplay of natural and anthropogenic stressors. The methodology employs GIS-based tools to delineate micro study zones, starting with pour points at water monitoring stations to define contributing watersheds. Zones are established, each representing distinct pollution profiles to ensures spatial variability, enabling comparative analysis of landscape-water quality interactions. Final landscape metrics and water quality parameters are selected based on data availability and relevance to hilly terrains. This structured approach bridges theoretical insights from the literature review with empirical analysis, ensuring the third objective

The third objective employs multi-year temporal and spatial analyses to unravel the impact of landscape characteristics on river water quality in hilly terrains. The study initiates with intensity analysis of land use/land cover (LULC) changes over the years. This analysis quantifies gains and losses within and between LULC classes and gives us insights on the expansion of other classes. Temporal trends in water quality parameters are then examined through time-series analysis across the study zones, distinguishing zone-specific variations (linked to local land use patterns) from broad, system-wide degradation like climate-driven shifts or unregulated anthropogenic activities. Relationship analysis follows, leveraging correlation tests to identify which landscape metrics most strongly influence individual water quality parameters. Network visualization maps these interactions, highlighting key drivers of pollutant dynamics.

Finally, degree of impact analysis is conducted via linear regression, quantifying the magnitude of influence each landscape metric exerts on water quality. These findings are synthesized into a fishbone diagram, integrating landscape-water quality linkages with LULC change trends to illustrate how topography, land use, and hydrological connectivity collectively shape river health. This multi-faceted approach not only identifies statistical relationships but also provides a holistic framework for diagnosing and addressing water quality challenges in hilly regions, which could help in providing strategies or recommendations.

The fourth objective builds upon the analytical insights to formulate strategic recommendations aimed at mitigating water quality degradation in hilly terrains. Emphasis is placed on nature-based and land-centric approaches. These strategies prioritize adaptability to the unique physiographic constraints of hilly regions while maintaining

ecological integrity and supporting water security. Translating these broad strategies into actionable interventions, the study proposes space-specific spatial planning measures tailored to the study area. Each measure ensures localized, evidence-driven planning responses.

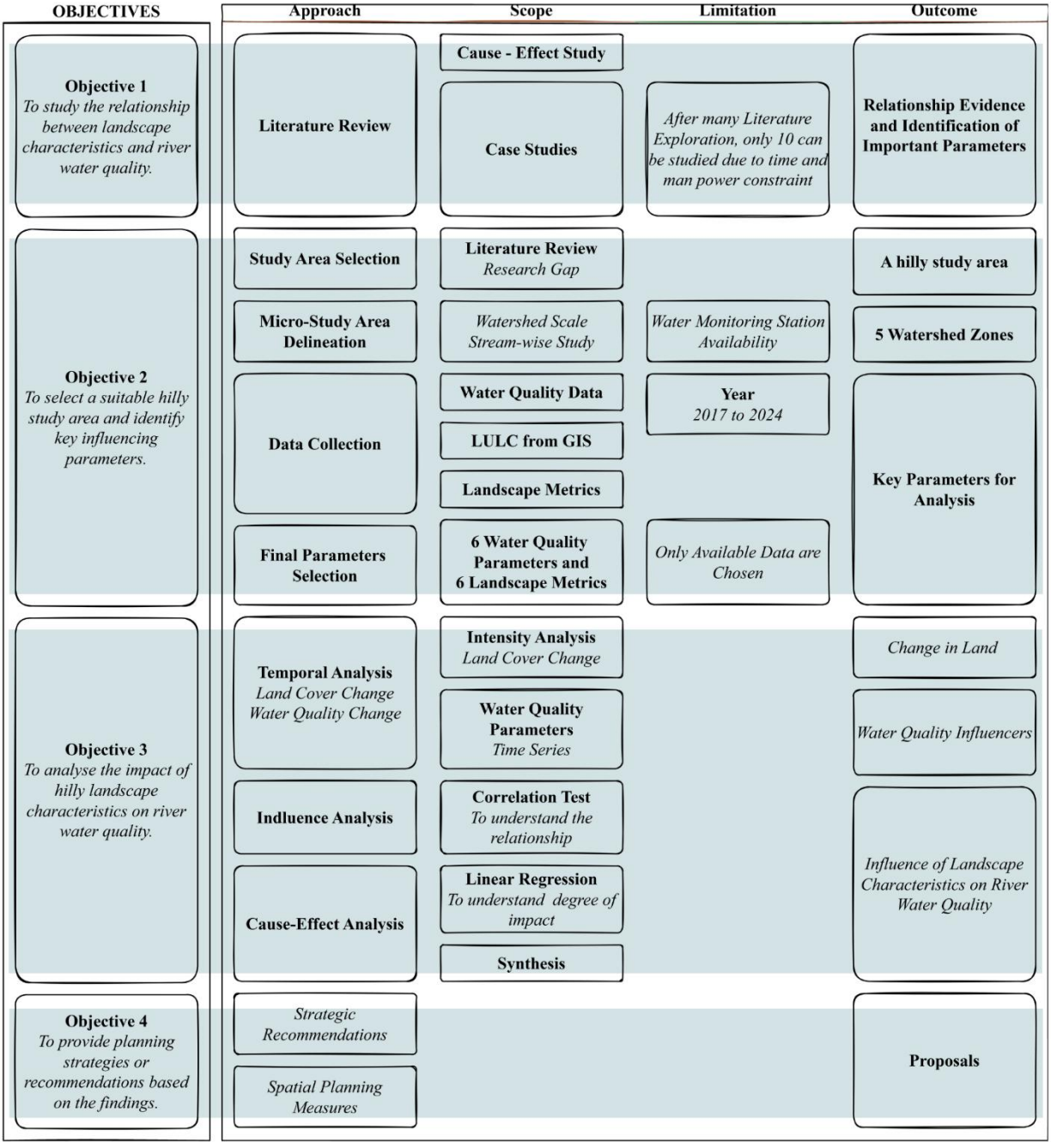

Figure 2 Methodology

2 Chapter II: Literature Review

2.1 Riverine System

Rivers, critical lifelines for ecosystems and human civilizations, face unprecedented threats from global environmental challenges including pollution, climate change, and habitat fragmentation. Worldwide, studies highlight the degradation of river water quality due to anthropogenic pressures such as industrial discharge, agricultural runoff, and urbanization(Akhtar et al., 2021; Meybeck, 2003). For instance, the European Water Framework Directive acknowledges the crucial interplay between land use and river health, mandating integrated management strategies (European Parliament and Council, 2000). Similarly, in North American watersheds, research demonstrates how sedimentation and nutrient loading, often exacerbated by deforestation and intensive farming, can lead to eutrophication, thereby threatening biodiversity and water usability (Bennett et al., 2001; J. D. Allan, 2004). These global insights underscore an urgent need to contextualize such findings within regions possessing unique geomorphological and socio-economic dynamics, like India's hilly terrains.

Figure 3 Riverine Environment

In India, riverine systems are both ecologically and culturally pivotal, yet they experience acute stress from unplanned urbanization, deforestation, and agricultural intensification. Major basins, such as the Ganges and Brahmaputra, exhibit deteriorating water quality, largely attributed to unchecked point and non-point source pollution (Matta et al., 2022; CPCB, 2018). While research on lowland river systems is relatively abundant, hilly regions—characterized by steep gradients, high seasonal flow variability, and fragile ecosystems—remain significantly understudied. This disparity persists despite their critical role in regulating downstream water quantity and quality, and it mirrors a broader academic tendency to prioritize large-scale watershed analyses over localized, topographically nuanced investigations (Shen et al., 2015; G. Q. Wang et al., 2014).

Existing academic approaches to river water quality often employ scale-specific frameworks. These include riparian buffer zone assessments, which analyze the immediate land-water interface, or watershed-level modelling to understand broader land-use impacts (Mander et al., 2005; Shen et al., 2015). Temporal analyses further refine these insights by evaluating seasonal pollutant shifts or long-term impacts of climate variables (e.g., precipitation, temperature) on hydrological cycles and water quality (Delia

et al., 2021; Van Vliet et al., 2013). Hierarchical stream studies also contribute by differentiating impacts on low-order streams, which are sensitive to localized disturbances, versus high-order rivers that reflect cumulative basin-scale stressors (Ding et al., 2016). While these diverse approaches provide foundational knowledge, they often do not sufficiently integrate the interactive effects of multiple landscape characteristics—such as slope, aspect, soil type, and detailed vegetation patterns—in modulating water quality outcomes, particularly within complex hilly terrains.

The cumulative effects of anthropogenic activities interacting with landscape features manifest in altered nutrient dynamics, sediment transport, and microbial contamination, all directly influencing river health. For example, deforestation in catchments can escalate surface runoff, increasing turbidity and potentially mobilizing contaminants like heavy metals within stream networks (Ríos-Villamizar et al., 2017) . Concurrently, agricultural intensification, especially on vulnerable slopes in foothill regions, often elevates nitrate and phosphate levels, risking eutrophication and oxygen depletion (Heathwaite et al., 1996; Wurtsbaugh et al., 2019) .

However, a persistent research gap lies in robustly distinguishing anthropogenic drivers from the baseline influence of natural landscape variability. While many studies attribute water quality shifts primarily to human activities, the inherent role of topography (e.g., slope, elevation), geology, natural vegetation gradients, and hydrological connectivity in shaping baseline water quality, and in mediating pollution impacts, is often not explicitly isolated or quantified. This distinction is especially critical for hilly regions, where specific landscape characteristics can either significantly amplify pollution risks (e.g., steep slopes accelerating runoff from agricultural land) or provide natural mitigation (e.g., dense forest cover on certain aspects reducing erosion). Understanding these complex interactions is vital for developing effective, targeted management strategies.

2.2 Case Studies

Ten cases have been reviewed collectively to establish a robust empirical foundation for understanding the interplay between landscape characteristics and river water quality across diverse geographical and temporal contexts. Spanning nearly three decades (1997–2023), these investigations encompass regions such as the Midwestern United States, Japan, China, Malaysia, Iran, and the Caspian Sea Basin, underscoring the universality of landscape-water quality linkages while highlighting context-specific nuances. The overarching objective across these studies, which is quantifying how land use patterns, spatial configurations, and landscape connectivity influence riverine systems, aligns with the broader discourse on sustainable watershed management. By synthesizing their methodologies and findings, this case study delineates critical themes, methodological advancements, and implications for hilly regions.

Table 1 Cases Studies of Landscape Characteristics with Water Quality

Sl.No.	Study Area	Citation
1	Midwestern United States (various stream ecosystems)	(Johnson et al., 1997)
2	Chugoku District, Japan (river systems)	(Amiri & Nakane, 2009)
3	China (multiple river systems at different spatial scales)	(Wang et al., 2014)
4	Dongjiang River Basin, China (low-order streams)	(Ding et al., 2016)
5	Northeast China (trans-boundary river basin)	(Cheng et al., 2018)
6	China (multiple watersheds across different scales)	(Zhang et al., 2018)
7	Czech Republic (headwater catchments)	(Staponites et al., 2019)
8	Bentong, Malaysia (urbanized watershed)	(Shehab et al., 2021)
9	Southern Caspian Sea Basin, Iran	(Masteali et al., 2023)
10	Caspian Sea Basin, Iran	(Aalipour et al., 2023)

Methodological and Statistical Techniques

Methodologically, the studies employ a spectrum of statistical and GIS-based tools to quantify landscape-water quality linkages. Making a rasterised Land Use/ Land Cover map or image is a common and necessary approach. Ding et al. (2016) and Wang et al. (2014) leveraged GIS-based spatial analysis to map pollutant hotspots in agricultural catchments, emphasizing the role of remote sensing in identifying erosion-prone areas. While some papers use unique methods for analysis like graph theory (Masteali et al., 2023), Partial Least Square Regression(Cheng et al., 2018), Factor Analysis (Shehab et al., 2021), etc., the most common analysis method is to use correlation test and multivariate regression. Multivariate regression has multiple independent variables that predicts one common dependent variable, it's base is a linear regression. This thesis will use linear regression for to understand the impact of each landscape metrics with each water quality parameters, to understand the nuances and complications.

Spatial Scale Dependency

A critical revelation across studies is the scale-dependent influence of land use on water quality. Wang et al. (2014) and Ding et al. (2016) demonstrated that agricultural impacts on nutrient loading are most pronounced at the catchment scale, where cumulative runoff dominates, but weaken at the riparian scale due to localized retention processes. Zhang et al. (2018) further clarified that urban-derived pollutants (e.g., BOD, EC) exhibit stronger correlations at finer spatial scales (e.g., 100–300 m riparian buffers), whereas forest cover

effects are most significant at watershed scales. This scale dependency necessitates multi-scalar management frameworks, as interventions effective at one scale may fail at another. Cheng et al. (2018) advocated for eco-functional regionalization in transboundary basins, aligning conservation zones with hydrologically coherent sub-basins to optimize pollution mitigation. This thesis will use watershed scale of low order streams, to understand the direct influence of the landscape characteristics without much other influence.

Land Use and Water Quality Correlation

A recurring theme across studies is the strong correlation between land use patterns and water quality degradation or improvement. (Johnson et al.1997) pioneered early efforts to link agricultural and urban land use in Midwestern U.S. catchments to elevated nutrient concentrations (nitrate, phosphate) and organic pollution (BOD), demonstrating that agricultural intensification increases sedimentation and nutrient loading, while forested areas act as natural filters. Wang et al. (2014) expanded this framework in China, revealing that agricultural expansion at the expense of forests exacerbates nitrogen and phosphorus fluxes, particularly in low-order streams with minimal riparian buffers. Similarly, Ding et al. (2016) emphasized the scale-dependent impact of agricultural land use in the Dongjiang River Basin, where fragmented crop fields amplify pollutant export during monsoonal rains. Conversely, forested landscapes consistently emerge as critical buffers, reducing erosion, enhancing infiltration, and sequestering nutrients, as evidenced by Cheng et al. (2018) in Northeast China. These findings reinforce the dual role of land use as both a stressor and a mitigant, necessitating land-use planning to prioritize riparian and hillslope forest conservation in vulnerable terrains.

Hydrological and Topographic Influences

Topography emerges as a critical modulator of landscape-water quality interactions. Amiri & Nakane (2009) integrated terrain variables (e.g., slope, Topographic Wetness Index [TWI]) in Japan, revealing that steep slopes amplify surface runoff, increasing sediment and nutrient export from agricultural zones. Cheng et al. (2018) linked hydrological distance metrics, such as proximity to streams, to pollutant dispersion in Northeast China, where hillslope-to-channel connectivity governs sediment yield and nutrient loading. Shehab et al. (2021) further emphasized that rainfall intensity interacts with topography to magnify urban runoff impacts in Malaysia's mountainous watersheds. These studies collectively advocate for integrating terrain-specific parameters into water quality models, particularly in hilly regions where slope and flow pathways dictate pollutant routing.

2.3 Landscape Characteristics

Landscape characteristics encompass the intrinsic physical, ecological, and climatic attributes of a region that collectively shape its environmental dynamics. In riverine systems, these characteristics, such as **Land cover, Land use, Land management, Atmospheric deposition, Geology/soil type, Climate, Topography, Catchment hydrology** , act as foundational drivers of hydrological processes and water quality outcomes (Lintern et al., 2018). Hilly terrains amplify hydrological connectivity through steep slopes, accelerating erosion and nutrient transport, while forest-dominated landscapes mediate pollutant filtration via root networks and organic matter accumulation (McLachlan & Horstmann, 1998; Stieglitz et al., 2003). These natural parameters, distinct from anthropogenic influences, form the basis for understanding baseline water quality conditions and predicting vulnerabilities in river systems.

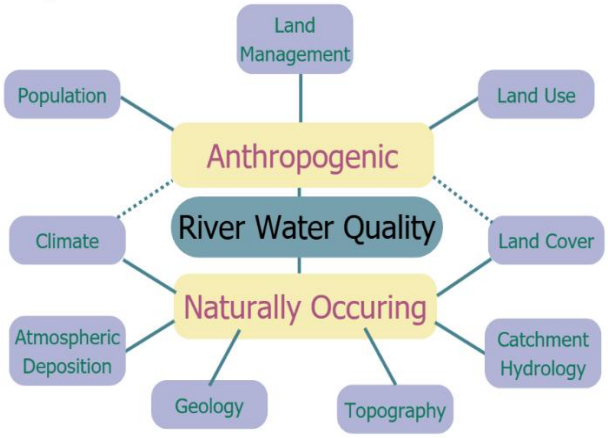

Figure 4 Landscape Characteristics

The interplay between landscape characteristics and river water quality is rooted in their spatial variability. Land cover, whether forested, agricultural, or urbanized, dictates surface runoff patterns and pollutant retention, while land use practices, such as fertilizer application or deforestation, alter nutrient loading and sedimentation rates (Somura et al., 2012). Similarly, geological formations influence groundwater recharge and mineral dissolution (S. Wang & Jaffe, 2004), affecting parameters like hardness and alkalinity, whereas soil properties determine infiltration capacity and contaminant adsorption (S. Wang & Jaffe, 2004). Climate variables, including precipitation intensity and temperature, further modulate these interactions by altering flow regimes and biogeochemical cycles (Bolstad & Swank, 1997; Van Vliet et al., 2013). Together, these factors create a mosaic of water quality conditions, where spatial heterogeneity emerges not merely from human activities but from the inherent structure of the landscape itself.

This spatial variability underscores the need for a holistic framework to quantify landscape characteristics beyond isolated parameters. Traditional approaches often compartmentalize factors like slope gradients or vegetation density, neglecting their synergistic effects on riverine health. A steep, deforested hillside may exhibit high erosion rates due to the combined influence of topography and land cover loss, whereas a gently sloping, forested catchment could stabilize sediment fluxes despite heavy rainfall (Stieglitz et al., 2003; G. Q. Wang et al., 2014). To address this complexity, the

concept of landscape metrics is introduced—a multidimensional tool to systematically evaluate the spatial arrangement, composition, and configuration of landscape elements. Unlike conventional landscape architecture frameworks focused on design aesthetics, these metrics prioritize quantitative, scale-invariant measurements (e.g., patch density, edge density, fractal dimensions) to capture the nuanced interactions between land surface and terrain features with water quality dynamics(Uuemaa et al., 2007; Amiri & Nakane, 2009; Wu et al., 2012).

2.3.1 Landscape Metrics

Landscape metrics are standardized quantitative indices designed to characterize the spatial structure, composition, and connectivity of landscape elements. These metrics operationalize complex terrain features into measurable parameters, enabling systematic analysis of ecological and hydrological processes. A patch, defined as a contiguous area of homogeneous land cover, serves as a fundamental unit for assessing spatial heterogeneity. The edges delineating boundaries between patches act as transitional zones influencing material fluxes, such as sediment or nutrient transport. Classes categorize patches into distinct land use or land cover types, providing a framework to evaluate their spatial distribution and ecological interactions (Kedron & Frazier, 2019).

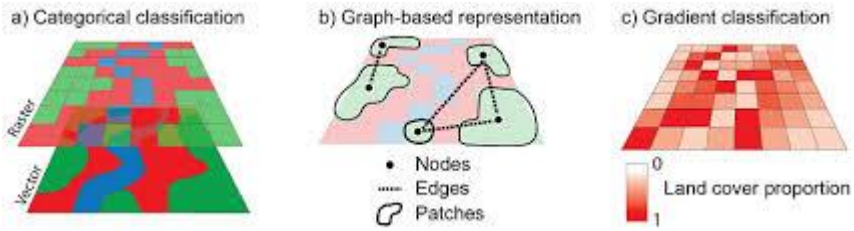

Figure 5 Landscape Metrics Terminology

The utility of landscape metrics lies in their capacity to quantify spatial patterns and their cascading effects on river water quality. Patch size and connectivity modulate hydrological retention and pollutant filtration, with larger, contiguous forest patches demonstrating enhanced erosion control (Strayer et al., 2003; Aalipour et al., 2023; Stieglitz et al., 2003). Edge density metrics correlate with the intensity of land-water interactions, where high edge density in riparian zones amplifies pollutant infiltration from adjacent land uses (Uuemaa et al., 2007; Cheng et al., 2018). Similarly, the proportion of land use classes within a watershed determines nutrient loading rates, with agricultural dominance often leading to elevated nitrogen and phosphorus concentrations in river systems (Johnson et al., 1997; Matta et al., 2022). These metrics collectively capture the interplay between spatial configurations and hydrological outcomes, transcending isolated parameter analysis.

The cause-effect relationships inherent to landscape metrics underscore their relevance in river water quality studies. In hilly terrains, steep slopes combined with fragmented vegetation patterns, quantified by patch fragmentation indices, exacerbate surface runoff and sediment yield, degrading water clarity and increasing contaminant transport (Aalipour et al., 2022). Conversely, well-connected riparian buffers, evidenced by high patch cohesion values, mitigate erosion and filter pollutants, preserving water quality. The spatial arrangement of land use classes, such as clustered urban zones versus dispersed agricultural plots, further modulates pollutant accumulation hotspots and hydrological connectivity (D. Allan et al., 1997; BASNYAT et al., 1999). These interactions highlight that water quality variability is not merely a function of individual landscape characteristics but emerges from their synergistic spatial configuration, which landscape metrics uniquely codify. Tlawng. By integrating these metrics, this thesis advances a methodology to isolate the natural geomorphological drivers of water quality from anthropogenic influences.

Based on the synthesis of the ten case studies, the most prevalent and critical landscape metrics indices are identified. Detailed definitions, mathematical formulations, and interpretations of these metrics are provided below to elucidate their ecological significance, probable value ranges, and implications for river water quality dynamics.

Table 2 Important Landscape Metrics Supported by Case Studies

Landscape Metrics Index	Formula	Citation
Patch Density (PD)	$(n / A) \times 100$	1, 2, 3, 4, 6, 8
Largest Patch Index (LPI)	$(A_{i_{max}} / A) \times 100$	3, 5, 6, 7
Edge Density (ED)	$(E / A) \times 100$	2, 3, 4, 5, 6, 7
Landscape Shape Index (LSI)	$(0.25 \times \Sigma P_i) / \sqrt{(A)}$,	4, 6, 7, 10
Aggregation Index (AI)	$(g_{ij} / g_{ij_{max}}) \times 100$	3, 4, 5, 9
Shannon's Diversity Index (SHDI)	$-\Sigma(p_i \ln p_i)$	3, 5, 6, 7
Shannon's Evenness Index (SHEI)	SHDI / log(n)	6, 7
Slope Percentage (S%)	$(\Delta h / d) \times 100$	3, 7
Stream Proximity (SP)	$\sqrt{((x - x\_stream)^2 + (y - y\_stream)^2)}$	5, 7

Patch Density (PD) quantifies the number of discrete landscape patches per unit area, calculated as:

$PD = (n / A) \times 100$,

where n is the total number of patches and A is the total landscape area (in km² or ha).

PD reflects landscape fragmentation, with higher values indicating greater fragmentation and lower values signifying fewer, larger patches (Uuemaa et al., 2009). Probable ranges vary by scale: urban landscapes may exceed PD > 50 patches/km², while forested regions typically exhibit PD < 10 patches/km². In hilly regions, steep slopes and erosional processes often fragment vegetation patches, increasing PD and influencing hydrological connectivity by altering surface runoff pathways.

Largest Patch Index (LPI) measures the proportional dominance of the largest patch in the landscape, calculated as:
$LPI = (A_{max} / A) \times 100$,
where A_{max} is the area of the largest patch and A is the total landscape area. LPI ranges from 0% (no dominant patch) to 100% (entire landscape as a single patch), with higher values indicating landscape homogenization and lower values reflecting heterogeneity (Uuemaa et al., 2009). LPI is critical for assessing riparian buffer integrity: low LPI values in forested zones may signal deforestation or habitat fragmentation, exacerbating erosion and sediment transport into rivers.

Edge Density (ED) quantifies the total length of patch edges per unit area, calculated as:
$ED = (E / A) \times 100$,
where E is the total edge length (in meters or kilometers) and A is the total landscape area. ED serves as a proxy for landscape complexity, with higher values indicating increased edge-to-area ratios and lower values reflecting simplicity (Uuemaa et al., 2009). Typical ranges span ED < 100 m/ha for homogeneous forests to ED > 500 m/ha for urbanized catchments. In hilly regions, ED correlates with hydrological connectivity: steep slopes and intersecting land use types amplify surface runoff and pollutant fluxes along high-density edges.

Landscape Shape Index (LSI) evaluates the geometric complexity of patches, calculated as:$LSI = (0.25 \times \Sigma P_i) / \sqrt{(A)}$,
where ΣP_i is the total perimeter of all patches and A is the total landscape area. LSI compares observed perimeter-to-area ratios against a theoretical minimum (a square landscape). Values > 1 indicate irregularly shaped patches, while ≈ 1 signifies compact shapes. In hilly regions, LSI is particularly relevant for riparian zones: high LSI values (e.g., LSI > 2) may reflect sinuous stream channels with complex edges, enhancing pollutant retention but also increasing sediment mobilization during high flows.

Aggregation Index (AI) measures the degree of patch clustering, calculated as:
$AI = (g_{ij} / g_{ij_{max}}) \times 100$,
where g_{ij} is the observed number of adjacent patch-type pairs and $g_{ij_{max}}$ is the maximum possible adjacency. AI ranges from 0% (maximally disaggregated patches) to 100% (perfectly aggregated patches), with higher values indicating clustered land use types)

and lower values denoting scattered patterns (Uuemaa et al., 2009). In hilly regions, AI aids in assessing buffer zone effectiveness: high AI in riparian forests suggests contiguous vegetation, reducing sediment and nutrient loading into rivers, whereas low AI implies fragmented buffers, increasing pollutant transport.

Shannon's Diversity Index (SHDI) quantifies landscape heterogeneity, calculated as:
$SHDI = -\Sigma(p_i \ln p_i)$,
where p_i is the proportion of landscape occupied by class i. SHDI increases with both the number of land use classes and their evenness, ranging from 0 (single-class dominance) to log(n) (maximal diversity) (Uuemaa et al., 2009) . For example, a hilly catchment with mixed forests, agriculture, and urban areas may exhibit SHDI > 1.5, whereas monoculture plantations yield SHDI < 0.5. High SHDI values in riparian zones correlate with reduced nutrient loading, as diverse land uses create varied hydrological barriers to pollutant transport.

Shannon's Evenness Index (SHEI) assesses the uniformity of class distribution, calculated as:
$SHEI = SHDI / \log(n)$,
where n is the number of land use classes. SHEI ranges from 0 (uneven class distribution) to 1 (perfectly even distribution) (Uuemaa et al., 2009). SHEI informs erosion management: values > 0.7 indicate balanced vegetation cover, reducing slope instability, while lower values suggest uneven land use (e.g., deforested slopes), amplifying runoff and sediment yield.

Slope Percentage (S%) quantifies topographic steepness, calculated as:
$S\% = (\Delta h / d) \times 100$,
where Δh is elevation change, and d is horizontal distance. S% ranges from 0% (flat) to > 100% (vertical cliffs), with higher values intensifying erosion and runoff velocity. Slopes > 30% are critical zones for water quality, as they accelerate sediment transport and pollutant fluxes into rivers.

Stream Proximity (SP) measures distance from landscape elements to the nearest stream, calculated as:
$SP = \sqrt{((x - x\_stream)^2 + (y - y\_stream)^2)}$,
where x, y are landscape coordinates. SP ranges from 0 (adjacent to streams) to > 1000 m (remote uplands). SP < 100 m signifies high vulnerability to pollutant loading, as proximity facilitates rapid runoff and contaminant infiltration. This metric is critical for buffer zone delineation, prioritizing conservation within SP < 300 m to mitigate slope-induced erosion impacts.

2.4 Water Quality

River water quality represents a critical indicator of aquatic ecosystem health, reflecting the interplay between natural processes and human activities. Globally, water quality trends reveal widespread degradation, driven by nutrient enrichment, sedimentation, pathogen contamination, and chemical pollutants (Udeigwe et al., 2011). In hilly regions, these challenges are compounded by terrain-specific dynamics, such as slope-induced erosion and variable hydrological connectivity, which amplify pollutant transport and alter biogeochemical cycles(Stieglitz et al., 2003). Traditional assessment methods, including in-situ monitoring and laboratory-based physicochemical analysis, remain foundational, but advancements in remote sensing, machine learning models, and spatially distributed sensors now enable high-resolution, real-time evaluations (Chen et al., 2023).

A persistent challenge lies in isolating the influence of landscape characteristics from anthropogenic stressors, as both shape water quality outcomes synergistically. This necessitates a framework that differentiates natural variability from human-driven impacts, a gap this thesis addresses through landscape metrics.

2.4.1 Water Quality Parameters

River water quality is assessed through a comprehensive suite of physicochemical and biological indicators, each reflecting distinct environmental processes, anthropogenic stressors, and natural variability. These parameters are critical for diagnosing aquatic ecosystem health, identifying pollution sources, and guiding management strategies. In hilly regions, where topography, geology, and LULC interact dynamically, the spatial and temporal variability of these parameters is amplified, necessitating a nuanced classification of their sources, behaviours, and ecological implications.

Oxygen-Related Parameters

Dissolved Oxygen (DO) and Biological Oxygen Demand (BOD) are foundational indicators of aquatic ecosystem health, reflecting the balance between oxygen supply and consumption. DO quantifies the amount of oxygen dissolved in water, essential for sustaining aquatic organisms. Steep slopes and rapid flow velocities enhance aeration, often maintaining high DO levels (>6 mg/L) in pristine, forested catchments (Bolstad & Swank, 1997). However, anthropogenic activities such as urban wastewater discharge, agricultural runoff, and deforestation introduce organic matter into river systems, stimulating microbial degradation processes that consume oxygen and elevate BOD. BOD, a measure of oxygen consumed by microorganisms to decompose organic pollutants, inversely correlates with DO. Seasonal monsoon rains exacerbate soil erosion and organic matter transport, temporarily increasing BOD and reducing DO, particularly in deforested or agricultural zones (Bolstad & Swank, 1997). Prolonged hypoxia (<2 mg/L)

can lead to fish kills and shifts in aquatic biodiversity, underscoring the need to monitor these parameters in topographically dynamic regions.

Hydrogen Ion Concentration (pH)

pH, a logarithmic measure of hydrogen ion activity, is a master variable influencing chemical speciation and biological processes in aquatic systems. While natural pH typically ranges from 6.5 to 8.5, optimal for most aquatic life, significant deviations often indicate pollution or distinct geological influences (Wetzel, 2001). Acidic conditions (pH < 6.0) can result from acid mine drainage (AMD), where sulphide mineral oxidation generates sulphuric acid (Akcil & Koldas, 2006), acid precipitation, or the leaching of organic acids from peatlands. Such acidification can mobilize toxic metals like aluminum, harming aquatic organisms (Nordstrom, 2011). Conversely, alkaline pH (> 9.0) may be associated with certain industrial effluents or naturally occur in catchments rich in carbonate minerals (e.g., limestone), which buffer against pH changes and can maintain stability..

Nutrient Parameters

Nitrogen (N) and phosphorus (P) are essential nutrients regulating primary productivity, but they become critical pollutants when their concentrations exceed natural ecological thresholds, leading to eutrophication (Carpenter et al., 1998).Nitrogen exists in various forms, including nitrate ($N\text{-}NO_3^-$), nitrite ($N\text{-}NO_2^-$), and ammonia ($N\text{-}NH_3$). Nitrate ($N\text{-}NO_3^-$) is highly mobile and often the dominant inorganic nitrogen form. Primary sources include agricultural fertilizers, livestock waste, sewage, and atmospheric deposition. Nitrite ($N\text{-}NO_2^-$) is a transient intermediate in nitrification and denitrification. Elevated levels are uncommon in well-oxygenated waters but can indicate pollution. Ammonia ($N\text{-}NH_3/NH_4^+$) results from organic matter decomposition and direct inputs from wastewater or agricultural waste. Its toxicity to aquatic life is pH and temperature-dependent, with the un-ionized form (NH_3) being particularly harmful, especially in neutral to alkaline waters (Randall & Tsui, 2002; USEPA, 2013). Phosphorus (SRP, largely PO_4^{3-}) and Total Phosphorus (TP), Phosphorus often acts as the limiting nutrient in freshwater systems. Major sources include agricultural runoff (fertilizers and animal manures), wastewater discharges (detergents, sewage), and natural weathering of phosphate-bearing rocks.

Hardness and Ionic Parameters

Hardness, defined as the concentration of calcium (Ca^{2+}) and magnesium (Mg^{2+}) ions, influences water usability and aquatic life adaptation. These ions derive from the chemical weathering of carbonate rocks and silicate minerals, which is induced by erosion. They also come from construction materials. Hardness indirectly affects aquatic organisms by modulating the bioavailability of heavy metals; for instance, high calcium concentrations

reduce the toxicity of lead and cadmium by competing for binding sites on biological membranes (J. D. Allan et al., 2021).

Electrical Conductivity (EC), a measure of water's ability to conduct an electric current, serves as a proxy for total dissolved solids (TDS). EC values are influenced by geology, evaporative concentration, and anthropogenic inputs such as industrial discharges, agricultural irrigation return flows, and road salt runoff. Mineral-rich soils contribute to natural EC elevations (500–1000 µS/cm), while mining activities can spike EC to >1500 µS/cm due to acid mine drainage releasing sulphates and heavy metals (Olías et al., 2004). High EC reduces water usability for irrigation, as elevated salinity impairs plant nutrient uptake and soil structure.

Solid Particulates

Solid particulates, including Total Solids (TS), Total Dissolved Solids (TDS), Total Suspended Solids (TSS), and turbidity, reflect the physical state of river water. Total Solids (TS) is the sum of all dissolved and suspended solids.

Total Dissolved Solids (TDS) comprises dissolved inorganic salts (e.g., calcium, magnesium, potassium, sodium, bicarbonates, chlorides, sulphates) and small amounts of organic matter. TDS is primarily influenced by catchment geology (weathering of rocks and soils) and evaporative concentration (Chapman, 1996).

Primary sources are soil erosion from agricultural lands, forests (especially after disturbances like logging or fire), construction sites, and urban stormwater runoff. In hilly regions, steep slopes, vulnerable soils, and high-intensity rainfall events significantly accelerate erosion processes, often leading to high TSS concentrations (e.g., >50 mg/L) (Waters, 1995; Owens et al., 2005).

Elevated TSS also contributes to sedimentation, which can degrade spawning habitats and alter channel morphology

2.5 Relationship of Hills and River

Synthesis of the ten case studies identifies the most prevalent and ecologically responsive water quality parameters, alongside their mechanistic linkages to landscape metrics. These relationships are further explicated through cause, emphasizing how spatial configurations shape pollutant transport and biogeochemical processes in hilly catchments.

Table 3 Cases of Hilly Landscape Characteristics and Water Quality Study

Citation	Water Quality Parameters	Takeaways
(Cheng et al., 2018)	pH, EC, DO, COD, COD-MN, NH3, NO3, TN, TP, F-, CL-, SO4	pH correlates with SHEI and Land parcel. EC with PLAND, SHDI, CONTAG, AI. NH3 with SHEI, PD, ED, PLAND, AI Total Nitrogen with SHDI, PLAND. Total Phosphorus with ED, PLAND, CONTAG.
(Staponites et al., 2019)	Ca, EC, NO3, NO2, pH, TSS, PO4, TP	Ca, EC and Total Phosphorus are very significantly correlated with stream proximity and slope. TSS, NO3 and Phosphate is moderately significant. NO2 and pH are not significant.
(Zhang et al., 2023)	pH, EC, TP, TN	It doesn't focus on WQP but on the predictive power of landscape metrics for river water quality, especially topographic relief. Steep slopes have high predictability.

From the case studies, relevant parameters in hilly regions could be identified.

Table 4 Important Water Quality Parameters Supported by Case Studies

Water Quality Parameters	Unit of Measurement	Standard	Recommending Agency	Citation
Dissolved Oxygen (DO)	mg/L	5	ICMR/BIS	(Cheng et al., 2018)
pH		6.5 - 8.5	ICMR/BIS	(Cheng et al., 2018; Staponites et al., 2019; Zhang et al., 2018)
Electrical Conductivity (EC)	µS/cm	300	ICMR	Cheng et al., 2018; Staponites et al., 2019; Zhang et al., 2018)
Nitrite (NO_2^-)	mg/L	1	BIS	(Staponites et al., 2019)
Ammonia (NH_3)	mg/L	0.5	BIS	(Cheng et al., 2018)
Calcium (Ca^{2+})	mg/L	75	BIS	(Staponites et al., 2019)
Phosphate (PO_4^{3-})	mg/L	0.1	USPH	(Staponites et al., 2019)
Total Suspended Solids (TSS)	mg/L	500	ICMR	(Staponites et al., 2019)

Dissolved Oxygen (DO)

Dissolved oxygen (DO) levels exhibit a strong positive correlation with Aggregation Index (AI) and Forest Cover (%), as demonstrated by studies analysing Midwestern U.S. catchments (Johnson et al., 1997) and agricultural-dominated regions in China (Wang et al., 2014; Ding et al., 2016; Cheng et al., 2018). High AI values, indicating clustered vegetation patches, enhance groundwater recharge and organic matter retention, which sustains microbial oxygen consumption and promotes oxygen diffusion into streams (Johnson et al., 1997; Cheng et al., 2018). In hilly regions, contiguous forested zones (high AI) stabilize slopes, reducing sedimentation that could otherwise deplete DO through organic matter decomposition (Staponites et al., 2019). This underscores the critical role of aggregated forest patches in maintaining aerobic conditions essential for aquatic life.

pH

pH variability is significantly influenced by Edge Density (ED) and Patch Density (PD), as evidenced by research in Japan (Amiri et al., 2009) and urbanized watersheds in Malaysia (Shehab et al., 2021). High ED (e.g., fragmented land use edges) increases pollutant influx from adjacent urban or agricultural zones, introducing acidifying agents (e.g., nitrates, sulfates) or alkaline materials (e.g., limestone quarry runoff) (Amiri et al., 2009; Shehab et al., 2021). Similarly, elevated PD in hilly catchments correlates with pH instability due to rapid runoff from small, dispersed patches, which amplifies pollutant connectivity and alters buffering capacity (Wang et al., 2014; Cheng et al., 2018). These findings highlight the necessity of minimizing land use fragmentation to stabilize pH in topographically dynamic regions.

Electrical Conductivity (EC)

EC levels are strongly modulated by Patch Density (PD) and Built-Up (%), with studies in urbanized Chinese basins (Ding et al., 2016; Shehab et al., 2021) and the Caspian Sea Basin (Aalipour et al., 2023) documenting this relationship. Fragmented urban zones (high PD) increase pollutant connectivity through impervious surfaces, transporting dissolved ions (e.g., chlorides, sulfates) into streams (Ding et al., 2016; Shehab et al., 2021). In hilly regions, steep slopes exacerbate this effect, accelerating runoff from built-up areas (high Built-Up (%)) and concentrating ion sources (Aalipour et al., 2023). These dynamics underscore the need for compact urban planning to mitigate salinity-driven water quality degradation in topographically complex terrains.

Nitrite (NO_2^-)

NO_2^- levels are governed by Edge Density (ED) and Shannon's Diversity Index (SHDI), with research in agricultural catchments (Johnson et al., 1997; Wang et al., 2014) and riparian zones (Zhang et al., 2018) demonstrating this linkage. High ED increases pollutant transfer from agricultural/urban edges to streams, while low SHDI (low land use

diversity) in monoculture-dominated regions exacerbates nitrite accumulation due to synthetic fertilizer use (Wang et al., 2014; Zhang et al., 2018). In contrast, mixed land use (high SHDI) enhances biogeochemical processing, reducing NO_2^- through microbial uptake and denitrification (Staponites et al., 2019). These mechanisms highlight the importance of diverse riparian buffers for nitrite mitigation in hilly catchments.

Ammonia (NH_3)

NH_3 concentrations are influenced by Landscape Shape Index (LSI), as shown by studies in China (Cheng et al., 2018) and Japan (Amiri et al., 2009). Irregular riparian patch shapes (high LSI) increase water-soil contact time, promoting nitrification and reducing ammonia via microbial uptake (Cheng et al., 2018). Conversely, compact land use (low LSI) accelerates runoff, limiting nutrient processing and elevating NH_3 (Amiri et al., 2009). In hilly regions, dendritic riparian buffers (high LSI) are critical for mitigating ammonia toxicity, particularly in areas with steep slopes and rapid hydrological connectivity.

Calcium (Ca^{2+})

Calcium concentrations are linked to Landscape Shape Index (LSI) and Patch Density (PD), as evidenced by studies in karstic terrains (Masteali et al., 2023) and forested slopes (Aalipour et al., 2023). High LSI in limestone-rich hilly regions increases surface water-rock contact, dissolving Ca^{2+} from exposed bedrock (Masteali et al., 2023). Conversely, high PD in forested zones reduces Ca^{2+} mobilization by stabilizing soil and limiting erosion (Aalipour et al., 2023). These findings emphasize the dual role of topography and vegetation in regulating calcium dynamics in sensitive geological contexts.

Phosphate (PO_4^{3-})

Phosphate levels are shaped by Largest Patch Index (LPI) and Shannon's Diversity Index (SHDI), with studies in agricultural catchments (Johnson et al., 1997; Wang et al., 2014) and riparian zones (Zhang et al., 2018) documenting this relationship. Large contiguous forest patches (high LPI) reduce phosphate loading by intercepting runoff and enhancing soil retention (Johnson et al., 1997; Wang et al., 2014). Conversely, low LPI (fragmented forests) and low SHDI (monoculture agriculture) elevate PO_4^{3-} due to fertilizer runoff and reduced biogeochemical filtering (Zhang et al., 2018). In hilly regions, diverse vegetation (high SHDI) enhances nutrient uptake, mitigating phosphate losses through root absorption and microbial immobilization.

Total Suspended Solids (TSS)

TSS concentrations are governed by Slope (%) and Stream Proximity (SP), as shown by studies in steep terrains (Johnson et al., 1997) and urbanized watersheds (Shehab et al., 2021). Slopes >30% increase sediment yield, while proximity to streams (<100 m)

facilitates unimpeded sediment transport to channels (Johnson et al., 1997; Shehab et al., 2021). In hilly catchments, forested buffers within 300 m of streams (low SP) mitigate TSS by trapping sediments, whereas deforested slopes (<100 m SP) exacerbate turbidity (Shehab et al., 2021). These dynamics underscore the importance of riparian buffer preservation in steep, erosion-prone landscapes.

Table 5 Relationship between Water Quality Parameters and Landscape Metrics

Water Quality Parameters	Contributor	Influencing Landscape Metrics
Dissolved Oxygen (DO)	Urban wastewater, agriculture runoff, deforestation	Aggregation Index (AI), Forest Cover (%)
pH	Fertilizer runoff, erosion	Edge Density (ED), Patch Density (PD)
Electrical Conductivity (EC)	Road salt runoff, agriculture runoff	Patch Density (PD), Built Up (%)
Nitrite (NO_2^-)	Domestic sewage, Fertilizer runoff	Edge Density (ED), Shannon's Diversity Index (SHDI)
Ammonia (NH_3)	Fertilizer runoff, sewage	Landscape Shape Index (LSI)
Calcium (Ca^{2+})	Erosion, urbanisation	Landscape Shape Index (LSI), Patch Density (PD)
Phosphate (PO_4^{3-})	Construction runoff, agriculture runoff	Largest Patch Index (LPI), Shannon Diversity Index (SHDI)
Total Suspended Solids (TSS)	Erosion, stormwater	Slope (%), Stream Proximity (SP)

2.6 Methods and Techniques

2.6.1 Intensity Analysis

Intensity Analysis is a quantitative framework used to analyse and understand land use/land cover changes over time. It is a systematic approach that compares observed intensities of changes to uniform intensities, helping to identify patterns and trends in the data. The primary objective of Intensity Analysis is to provide insights into the dynamics of land use/land cover changes, which is crucial for environmental monitoring, urban planning, and resource management (Aldwaik & Pontius, 2012).

The Intensity Analysis framework involves analysing changes at different levels, typically starting with the category level. At this level, it examines the overall intensity of change for each land cover category. The total change intensity (S) is calculated as a percentage of the total area under consideration (Pontius et al., 2013). This value represents the overall rate of change across all categories.

$$\text{Total change} = S = \frac{\sum_{j=1}^{J}\left\{\left(\sum_{i=1}^{J} C_{ij}\right) - C_{jj}\right\} 100\%}{\sum_{j=1}^{J}\sum_{i=1}^{J} C_{ij}}$$

The Total Gains and Loss are calculated by:

$$G_j = \frac{\{\text{area of gain of } j\}100\%}{\text{area of } j \text{ at final time}} = \frac{\left\{\left(\sum_{i=1}^{J} C_{ij}\right) - C_{jj}\right\}100\%}{\sum_{i=1}^{J} C_{ij}}$$

$$L_i = \frac{\{\text{area of loss of } i\}100\%}{\text{area of } i \text{ at initial time}} = \frac{\left\{\left(\sum_{j=1}^{J} C_{ij}\right) - C_{ii}\right\}100\%}{\sum_{j=1}^{J} C_{ij}}$$

Intensity Analysis then compares the observed intensity of gain and loss for each category to the total change intensity (S). If a category's gain or loss intensity is greater than S, it is considered an "active" gainer or loser, respectively. Conversely, if the intensity is less than S, the category is deemed "dormant." This comparison helps identify categories that are experiencing more significant changes relative to their size.

Beyond the category level, Intensity Analysis examines the intensity of transitions between specific categories. This involves calculating the intensity of transition from one category to another and comparing it to a uniform intensity. The uniform intensity represents the expected intensity of transition if the change were to occur uniformly across all categories. By comparing observed transition intensities to uniform intensities, Intensity Analysis identifies whether certain transitions are targeted or avoided.

The framework further extends to analysing the intensity of transitions at the transition level. Here, it assesses the intensity of transitions from a particular losing category to different gaining categories and vice versa. This analysis helps to understand the specific patterns of change and whether certain transitions are systematically targeted or avoided(Aldwaik & Pontius, 2012).

Intensity Analysis is a powerful tool for understanding the complex dynamics of land use/land cover changes. By providing a detailed and quantitative analysis of the patterns and trends in the data, it enables researchers and policymakers to gain a deeper understanding of the processes driving these changes. This knowledge is essential for developing effective strategies for managing landscapes, mitigating the impacts of undesirable changes, and promoting sustainable land use practices (Pontius et al., 2013).

One of the key strengths of Intensity Analysis is its ability to distinguish between systematic and random patterns of change. By comparing observed intensities to uniform intensities, it identifies whether certain transitions are more or less intense than expected

by chance. This information is critical for understanding the drivers of land use/land cover changes and for developing targeted interventions.

In conclusion, Intensity Analysis is a valuable framework for analysing land use/land cover changes. Its systematic approach and quantitative methods provide a comprehensive understanding of the dynamics involved in these changes. By identifying patterns and trends in the data, Intensity Analysis informs strategies for managing landscapes and promoting sustainable land use practices.

2.6.2 Correlation Test and P-value

The Pearson correlation coefficient (r) is a statistical measure used to assess the strength and direction of the linear relationship between two continuous variables. This test is widely used in research to determine how one variable changes in relation to another. The Pearson correlation is particularly useful when trying to understand whether an increase in one variable leads to an increase (or decrease) in the other and to what extent this relationship is linear (Sedgwick, 2012).

Key Features of Pearson Correlation

The Pearson correlation coefficient ranges from -1 to 1, where the direction and strength of the relationship between two variables can be interpreted as follows:

r = 1 represents a perfect positive correlation, meaning both variables move together in the same direction.

r = -1 represents a perfect negative correlation, meaning as one variable increases, the other decreases.

r = 0 indicates no linear correlation between the two variables.

Values closer to 1 or -1 indicate stronger relationships, while values closer to 0 suggest weaker correlations. The Pearson correlation only captures linear relationships, so if the relationship between two variables is non-linear, Pearson's r may not adequately represent the strength of their association.

p-Value in Pearson Correlation

A crucial aspect of interpreting the Pearson correlation is determining whether the observed correlation is statistically significant. This is achieved through the p-value, which accompanies the correlation coefficient.

The p-value helps you understand whether the relationship you observe is likely due to random chance(Greenland et al., 2016). It tests the following hypotheses: Null Hypothesis (H_0): There is no correlation between the two variables (r=0).

Alternative Hypothesis (H_1): A correlation exists between the two variables ($r \neq 0$).

If the p-value is below a certain threshold, typically 0.05, it suggests that the observed correlation is statistically significant, and we can reject the null hypothesis. A p-value

above 0.05, on the other hand, implies that the observed correlation could be due to chance, meaning the correlation is not statistically significant.

A low p-value (< 0.05) indicates strong evidence against the null hypothesis, supporting the conclusion that a relationship exists between the two variables. Conversely, a high p-value (> 0.05) suggests weak evidence against the null hypothesis, indicating that any observed correlation may be due to random variation.

2.6.3 Regression Analysis

Regression analysis is a statistical technique used to examine the relationship between two or more variables. Linear regression is the simplest form, used to explore the linear relationship between a dependent variable (the outcome we want to predict) and one or more independent variables (the predictors)(Zou et al., 2003).

In simple linear regression, the relationship between the variables is modeled using the equation:

$y = \beta_0 + \beta_1 x + \varepsilon$

Here:

- y is the dependent variable.
- x is the independent variable.
- β_0 is the intercept, indicating the expected value of y when x = 0.
- β_1 is the slope or regression coefficient, showing how much y changes with a one-unit increase in x.
- ε is the error term, accounting for variation not explained by the model.

The intercept (β_0) represents the baseline level of the dependent variable, and the coefficient (β_1) reflects the strength and direction of the relationship. A positive β_1 means y increases with x, while a negative β_1 means y decreases as x increases.

In multiple linear regression, where there are multiple independent variables (x_1, x_2, ..., x_n), the model becomes:

$y = \beta_0 + \beta_1 x_1 + \beta_2 x_2 + ... + \beta_n x_n + \varepsilon$

Regression is a powerful tool for cause-effect analysis. While it does not prove causality, it helps identify and quantify potential relationships. For example, in environmental studies, one might use regression to assess how water pollution (y) is influenced by nearby land use (x). In economics, it might show how income (y) depends on education level (x).

By estimating the coefficients, researchers can interpret the influence of each predictor and forecast outcomes under different conditions, making regression a cornerstone method in decision-making, policy analysis, and forecasting.

3 Chapter III: Study Area

3.1 Introduction to the River

The Tlawng River stands out as a compelling case study for investigating the influence of hilly landscape characteristics on river water quality, filling critical gaps in existing research and policy frameworks.

Figure 6 Tlawng River

The Tlawng River's steep topography, elongated watershed, and connection to the Eastern Himalayan biodiversity hotspot distinguish it from India's predominantly lowland river studies. Unlike the Ganges or Brahmaputra, which dominate hydrological research, the Tlawng's narrow, high-gradient basin amplifies hydrological connectivity, sediment transport, and slope-induced erosion, offering a natural laboratory to isolate geomorphological effects on water quality. Its dense tropical forests and seasonal monsoon-driven flows further enrich the interplay between natural landscape metrics and pollutant dynamics.

As a tributary of the Barak River, the Tlawng contributes to the Ganga-Brahmaputra-Meghna system, a transboundary lifeline for India, Bangladesh, and Bhutan. However, the Barak's hydrology remains understudied compared to the Ganges, despite its critical role in northeast India's water security (Paszkowski et al., 2021). The Tlawng's role as a primary water source for Aizawl, combined with its downstream connectivity to the Barak and Meghna, positions it as a strategic node for understanding upstream-downstream water quality linkages in politically sensitive, ecologically fragile regions.

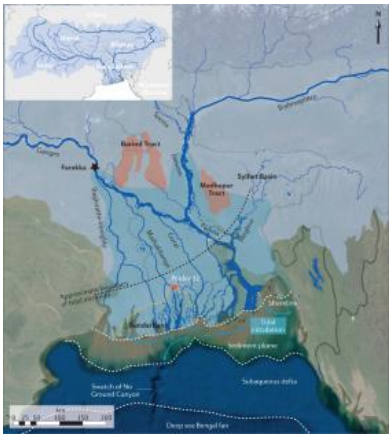

Figure 7 Ganga-Brahmaputra-Meghna system

Most Indian River studies focus on lowland, floodplain-dominated systems (e.g., Ganges, Yamuna), neglecting the hilly catchments that contribute disproportionately to sediment and nutrient loading. The Tlawng's steep gradients and monsoon-driven flows exemplify the unaddressed challenges of slope-induced erosion, fragmented riparian buffers, and urbanization on fragile hillslopes. These issues critical for sustainable watershed management in the Eastern Himalayas.

The Tlawng River is safeguarded by uniquely stringent legal frameworks, including the 800-meter green belt under the Mizo District (Forest) Act and the 15-meter buffer zones in Aizawl's Master Plan 2030. Yet, these protections conflict with intensive anthropogenic pressures, such as unregulated waste dumping and urban sprawl. This juxtaposition of policy ambition and implementation gaps offers a rare opportunity to study the disconnect between legal mandates and on-ground realities in hilly regions.

The Save the Riparian Project, a community-driven initiative to clean Tlawng's gorges, exemplifies grassroots efforts to combat pollution in hilly regions. However, its impact is hindered by poor waste management practices and lack of government infrastructure (e.g., garbage traps). Studying this project provides insights into community-based river management, a growing research frontier in India's ecologically sensitive zones.

Figure 8 Save the Riparian Movement

3.1.1 Tlawng River Profile

The Tlawng River, a defining hydrological feature of Mizoram, emerges as a critical lifeline for the region's ecological and socio-economic systems. Originating from Zobawk in Lunglei District, this northward-flowing river traverses Aizawl and Lunglei districts, carving through steep, densely forested valleys before discharging into the Barak Valley in Cachar, Assam. With a total length of 157.38 km and a watershed area of 170,145 hectares, the Tlawng stands as Mizoram's longest and most voluminous river. Its elongated, narrow basin—a product of tectonic activity and intense monsoon-driven erosion—creates a dynamic gradient of ecological and hydrological processes, positioning the river as a pivotal case study for analyzing landscape-water quality interactions in hilly terrains.

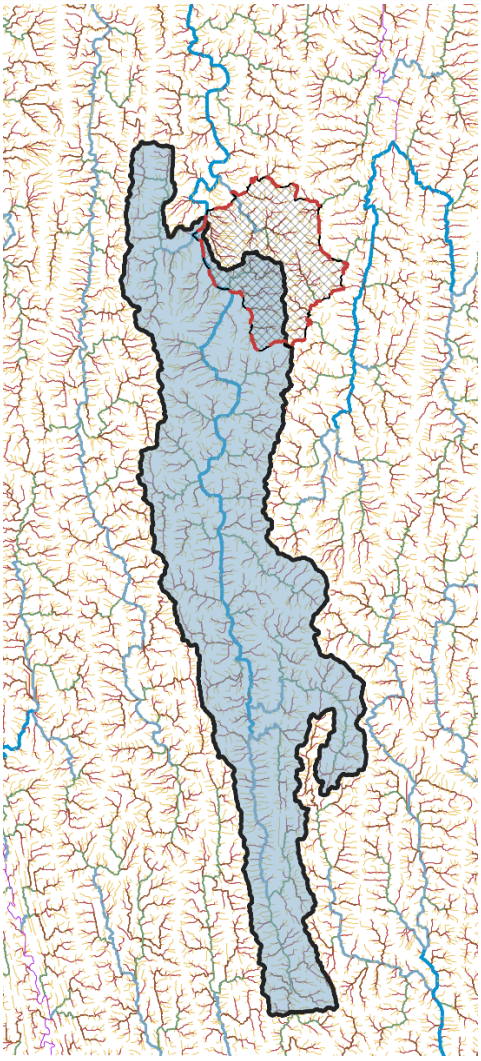

Figure 9 Watershed of Tlawng Riverr taken from Water Treatment Plant

The Tlawng River serves as the primary water source for Aizawl, a city flanked by the river to the west and the Tuirial River to the east. Its western drainage system channels runoff into the Tlawng, which supplies 90% of Aizawl's potable water through the Greater Aizawl Water Supply Scheme (GAWSS). This infrastructure highlights the Tlawng's role as an ecological and infrastructural linchpin, sustaining a population of over 400,000 residents with 55 liters per capita per day (LPCD) of water (Master Plan for Aizawl: Vision 2040).

The Tlawng River's ecological integrity is safeguarded by the Mizo District (Forest) Act, 1955, which mandates an 800-meter green belt on either side of the river to preserve its riparian ecosystems. Complementing this, the Master Plan for Aizawl (Vision 2030) recommends a 15-meter green buffer along major drainage channels, recognizing the river's role in mitigating erosion and maintaining water quality. These legal frameworks underscore the Tlawng's status as a biodiversity corridor and a natural regulator of sediment and nutrient fluxes, particularly in the Eastern Himalayan biodiversity hotspot. Despite its legal protections and infrastructural importance, the Tlawng River faces acute anthropogenic pressures. Seasonal flooding, exacerbated by steep slopes and intense monsoon rainfall, accelerates erosion and sediment transport, degrading water quality.

The Tlawng River's unique interplay of steep topography, legal protections, and socio-economic dependencies makes it an ideal case study for assessing landscape-water quality linkages. Its role as Aizawl's critical water source, yet vulnerability to slope-induced erosion, urban pollution, and climate variability, highlights the urgency of distinguishing natural geomorphological influences (e.g., slope-driven sedimentation) from anthropogenic degradation. By analysing landscape metrics alongside water quality parameters, this study aims to inform targeted interventions to preserve the Tlawng's ecological integrity while sustaining its socio-economic functions.
Criteria for selecting the area, which is watershed area, basemap, lulc 2018 map for every zone. why those area, zone wise description, name, land use, main polluters, etc.

3.2 Introduction to the Study Area

Mizoram, a state nestled in India's northeast, epitomizes the ecological and cultural diversity of the Eastern Himalayan region. As the fifth smallest state in India, Mizoram's population of 1.09 million (2011 Census)—with a density of 52.05 persons/km²—is predominantly rural (47.89%) but increasingly urbanized, with approximately 30% of residents concentrated in Aizawl. Bordered by Myanmar and Bangladesh to the south and Assam, Manipur, and Tripura to the north, Mizoram spans 21,081 km² of rolling hills, deep valleys, and forested watersheds, with elevations ranging from 592 m to over 2,000 m in the southern ranges. Mizoram's climate is mild but increasingly erratic, shaping the Tlawng River's hydrology. With an average annual temperature of 24.75°C and 1,289 mm of rainfall over 173 rainy days, the region experiences intense monsoon-driven flows (July–September), contributing to seasonal flooding and slope instability.

3.2.1 Aizawl City Profile

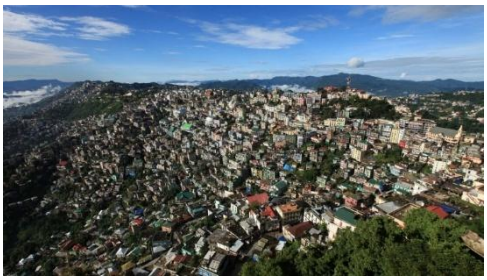

Aizawl, the capital of Mizoram, is a city defined by its terrain. Its landscape is characterized by steep slopes, narrow valleys and is sculpted by its rugged topography and ecological sensitivity. Nestled in the north-central hills of the state, the city's elevation ranges from 60 m to 1,440 m above mean sea level. Aizawl, the political and economic heart of Mizoram, houses 310,891 residents, approximately 30% of Mizoram's population. This population is projected to be approximately 400,000 by 2025 Despite its small geographic footprint, Aizawl faces rapid urbanization, with most of its population concentrated in its steep, fragmented terrain.

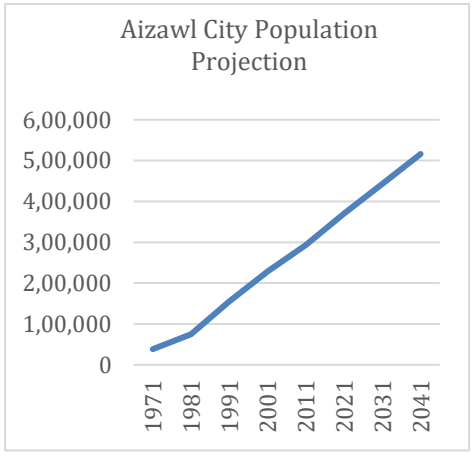

Aizawl's landscape is defined by steep slopes (up to 89°). The terrain is highly dissected, with 60.23% of the area classified as moderately sloped (10°–30°) and 25.99% as high-gradient (30°–45°) . This

rugged topography complicates infrastructure development, amplifies erosion risks, and shapes the city's drainage dynamics. The Tlawng River, Aizawl's primary water source, flows along the city's western edge, channeling monsoon-driven runoff through a network of gorges and valleys. Aizawl experiences a mild subtropical climate, with mean annual temperatures of 24.75°C and annual rainfall of 1,289 mm, concentrated over 173 rainy days. However, climate change has intensified weather extremes, including violent April–May storms and increased landslide risks.

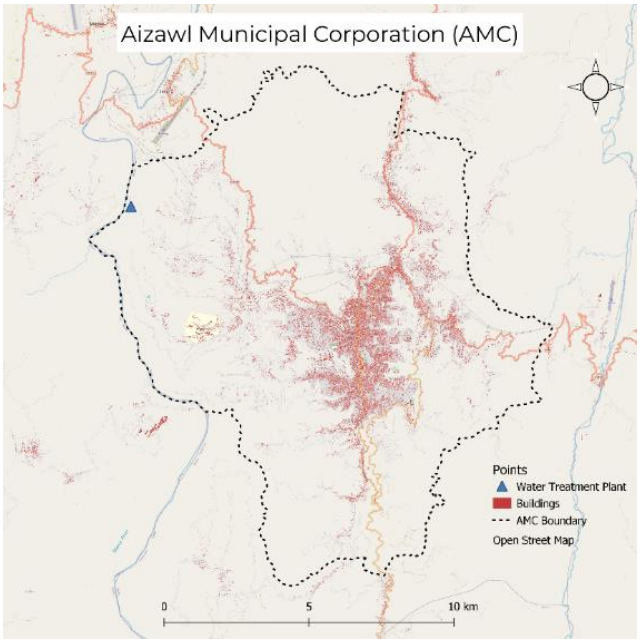

Figure 11 Building Footprint Map of AMC

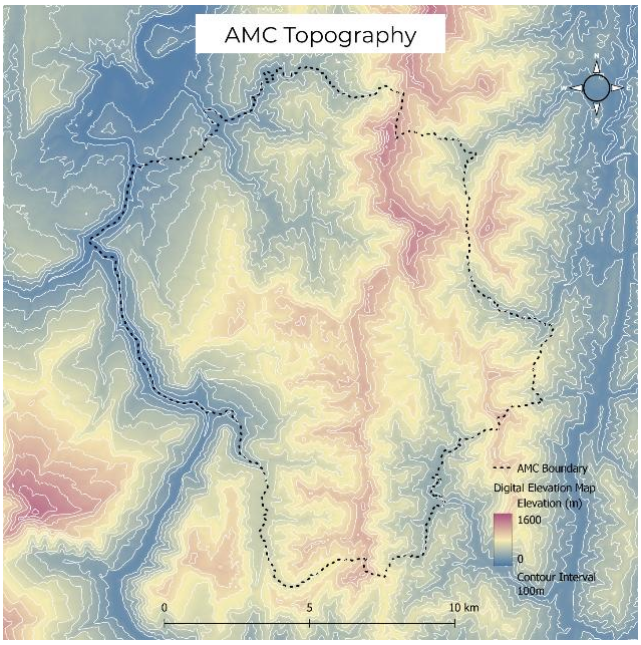

Figure 10 Topography Map of AMC

The GIS-Based Master Plan for Aizawl (Vision 2040) delineates Aizawl City (AMC) including several neighbouring towns as its Aizawl Planning Area . It also highlights the city's land use patterns, a stark contrast between developed and underdeveloped areas.

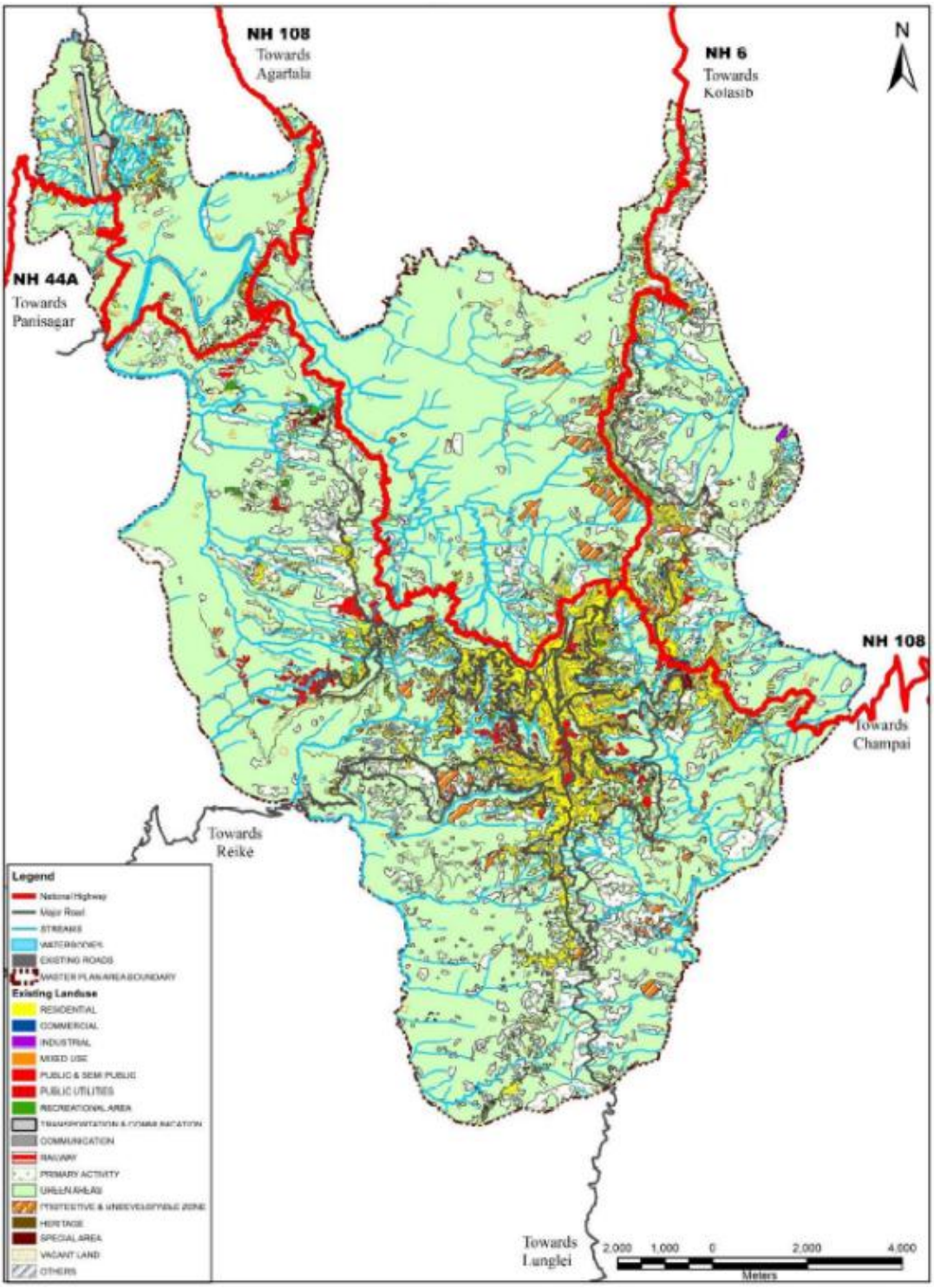

Figure 12 Existing Land Use Map of Aizawl Urban Area, Masterplan 2040

Only 12.21% of the planning area (24.8 km²) is developed, with 71.4% of this classified as residential. Residential zones sprawl along highways, old town cores, and agricultural fringes, often intermixed with commercial uses (e.g., roadside shops with residential upper floors) . Commercial land use occupies a mere 0.02% (0.04 km²), while industrial areas account for 0.03% (0.06 km²) .

The remaining 87.79% of the area is underdeveloped, dominated by forests (40.1%), scrublands (25.99%), and protective zones (72.65%) such as steep slopes and rocky outcrops . Waterbodies, including the Tlawng River and its tributaries, cover 1.58% (3.2 km²) of the area, while agricultural land (25.06 km²) supports horticulture, plantations, and small-scale farming .

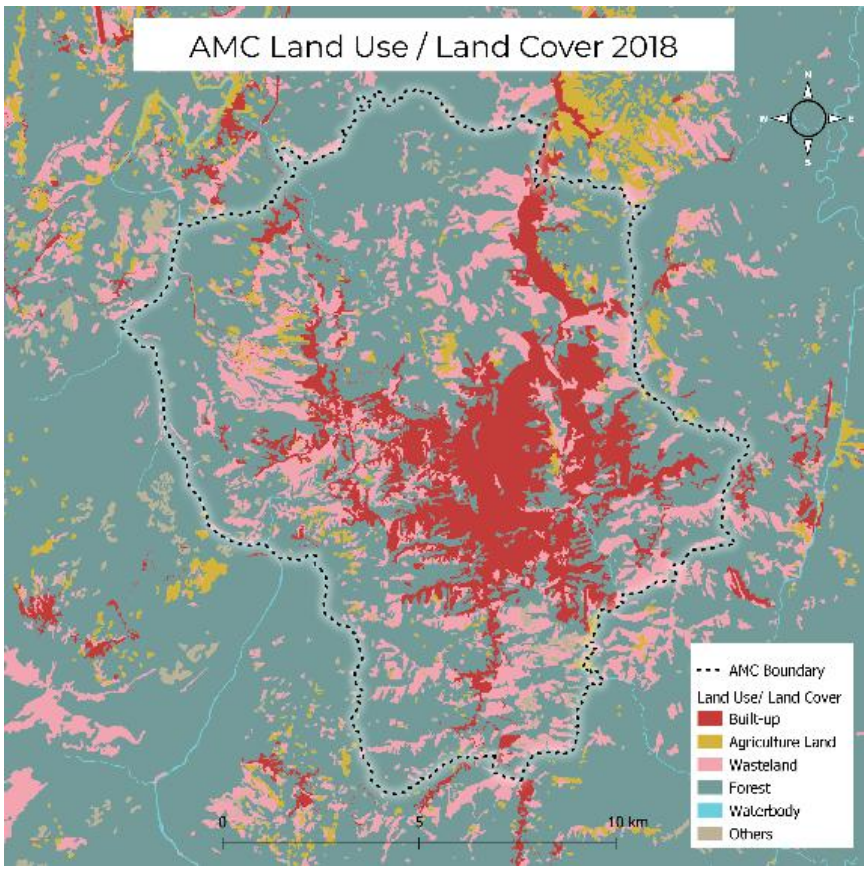

Figure 13 LULC Map of AMC, 2018 *(Source: MIRSC)*

Transportation infrastructure occupies 17.03% (4.22 km²) of the developed area, with 3.7 km² dedicated to roads and 0.53 km² to parking/medians . Public and semi-public spaces (e.g., schools, hospitals) cover 9.27% (2.3 km²) of developed land, while recreational areas (parks, playgrounds) occupy 1.47% (0.36 km²) . However, urban expansion into steep slopes and forested zones threatens ecological stability, as 87.79% of the planning area remains vulnerable to unplanned development .

Aizawl's water supply, managed by the Public Health and Engineering Department (PHED), relies entirely on surface water from the Tlawng River, as groundwater is inaccessible due to the region's steep terrain. The city's water supply system, designed as a dead-end network to accommodate steep gradients, pumps raw water from the Tlawng River through the gawss

Commissioned in two phases (10.8 MLD in 1988 and 24 MLD in 2007), GAWSS currently provides 55 liters per capita per day (LPCD) to Aizawl's 310,891 residents (2011 Census), divided into 48 supply zones under the Aizawl Municipal Corporation (AMC). However, this supply falls short of projected demand, with a 11.52 MLD deficit as of 2011, driven by rapid urbanization and infrastructure demands. The city's rapid urbanization, driven by in-migration and infrastructure development, has intensified pressure on its natural resources, particularly water. With 72% of households receiving piped water supply as of 2015 (AMRUT Mission baseline), the state aims to achieve 100% piped water access, a goal contingent on the health of the Tlawng River .

According to CPHEEO norms, Aizawl's domestic water demand is estimated at 135 LPCD for households with sewerage and 70 LPCD for villages, while a 10% floating population (e.g., migrants, tourists) requires 45 LPCD. Non-domestic demand (commercial, institutional) adds another 45 LPCD, and fire-fighting requirements are calculated per CPHEEO standards. Based on these metrics, the 2040 horizon year demand for Aizawl's growing population is projected to surge to 102.60 MLD, nearly doubling the current supply capacity of 34.8 MLD (Master Plan Aizawl 2040). This stark disparity underscores the urgency of optimizing Tlawng River management to prevent critical shortages.

The Tlawng River's role as Aizawl's singular water source necessitates urgent interventions to address current deficits and future demand. Climate variability, urban encroachment, and pollution already strain the river's capacity, with unregulated waste dumping in gorges and slope-induced sedimentation degrading water quality. The Save the Riparian Project (2024) highlights grassroots efforts to mitigate pollution, yet systemic challenges persist, including inadequate garbage traps and fragmented land use policies. Without robust management, the Tlawng's ability to meet escalating demand will collapse, jeopardizing Aizawl's ecological and socio-economic stability..

3.2.2 Micro- Study Area

The micro study areas were strategically selected based on monitored stream locations equipped with water quality monitoring stations. At each sampling site, a pour point was established to delineate the contributing watershed, capturing all upstream natural springs, surface flows, and anthropogenic inputs within the defined boundary. This approach ensures a comprehensive assessment of hydrological connectivity by integrating natural processes (e.g., spring-fed flows, slope-driven runoff) and human-induced stressors (e.g., land use impacts, pollutant pathways).

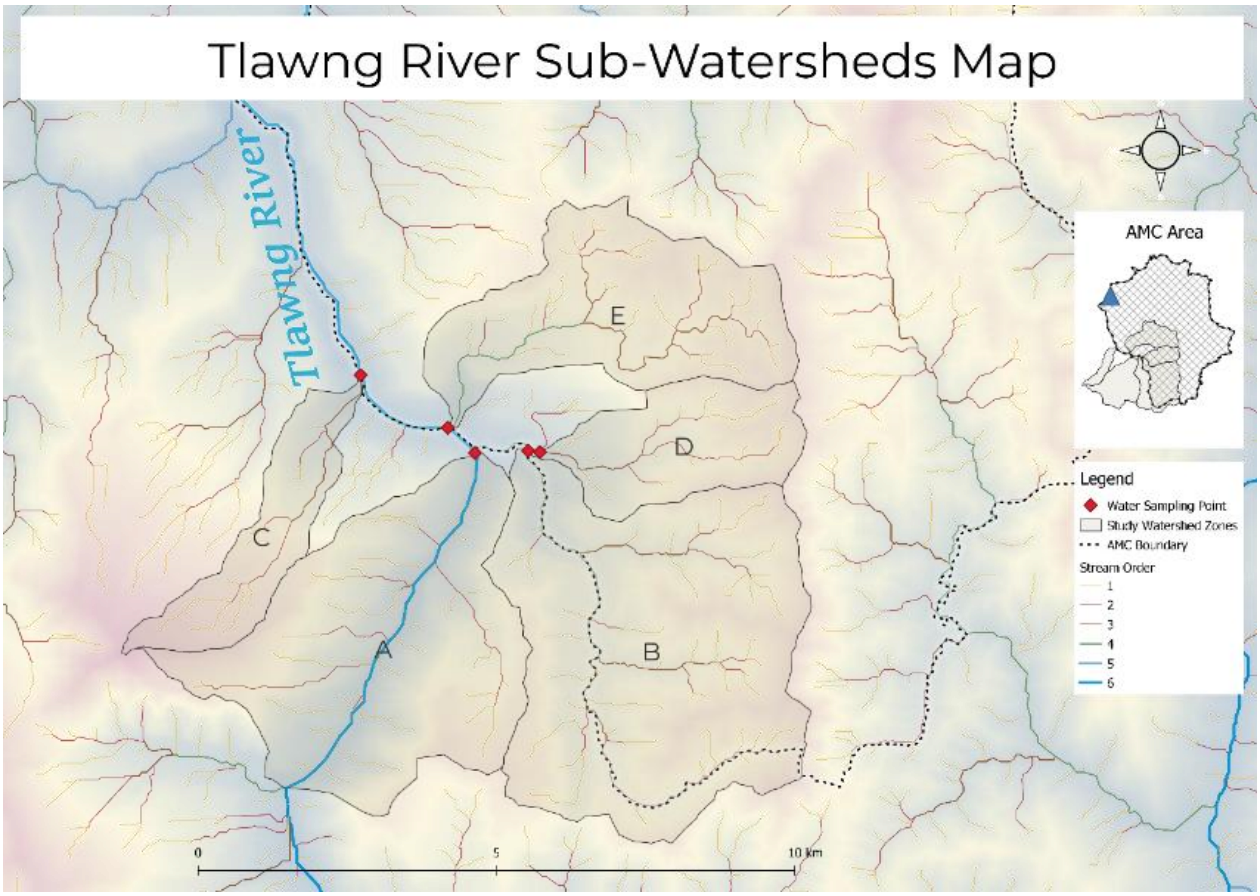

Figure 14 Stream Network Map of Micro-Study Area

Five distinct watersheds were identified, each representing unique pollution dynamics and landscape interactions. These zones are as follows:
Zone A - Tlawng Upper Stream: Dominated by agricultural activities
Zone B - Serlui Stream: A mixed stressor zone where agricultural practices and sediment runoff from deforested slopes
Zone C - Vaipuanpho Stream: Primarily impacted by agricultural land use
Zone D - Tuikual Stream: Experiencing municipal waste discharge
Zone E - Sakhisih Stream: Another municipal waste-affected zone

The selection of these zones reflects a gradient of anthropogenic pressures superimposed on hilly landscape characteristics. Zones A, B, and C emphasize agriculture-driven degradation, critical in understanding how slope-agriculture interactions amplify pollutant transport. Zones D and E focus on urbanization-induced stressors, highlighting the interplay between steep topography and municipal waste management challenges. By isolating these zones, the study systematically distinguishes landscape-driven variability from human-induced pollution, aligning with the thesis's objective of proposing landscape-sensitive interventions. The inclusion of

both natural hydrological flows (via spring-fed streams) and anthropogenic inputs (agricultural, municipal) enables a nuanced evaluation of cause-effect relationships between landscape metrics and water quality parameters.

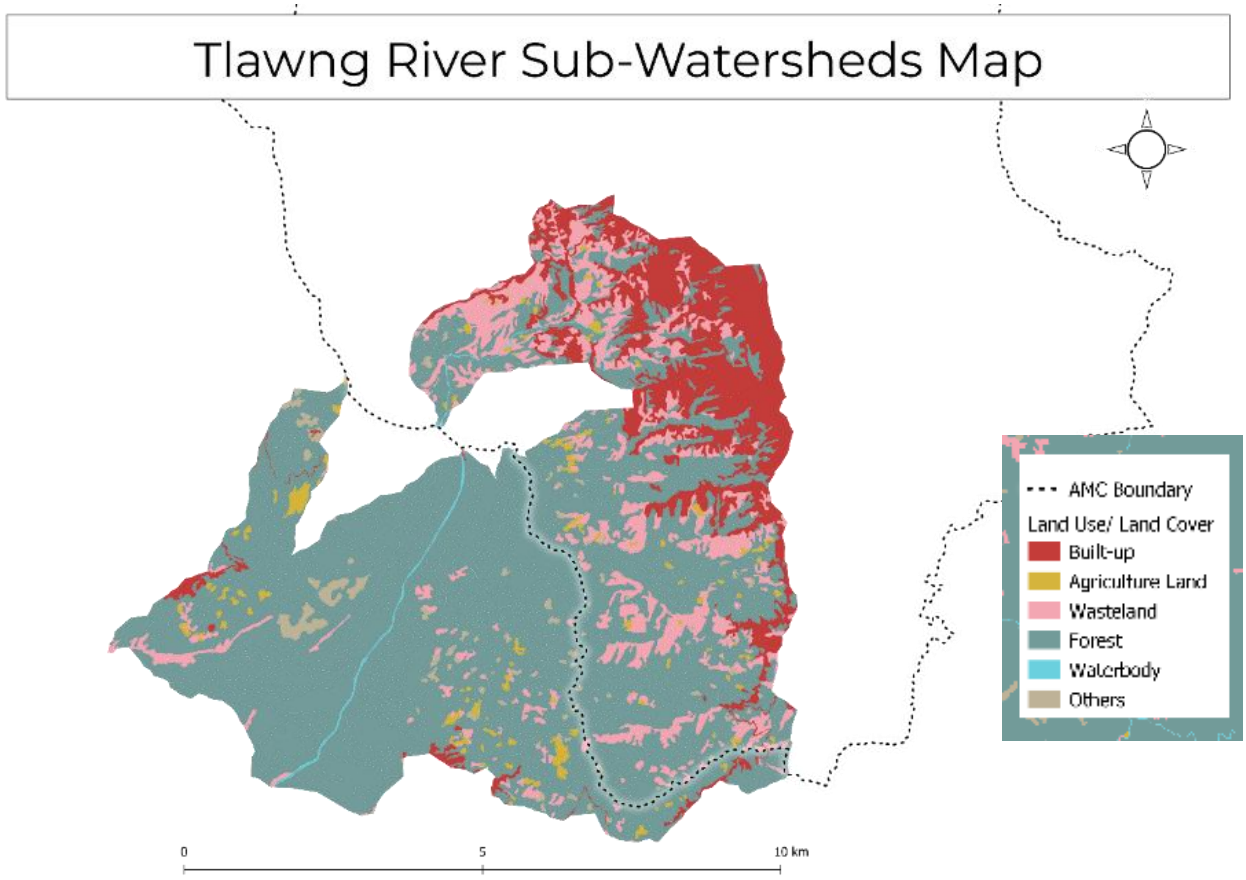

Figure 15 LULC Map of Micro Study Area (Source: MIRSC, 2018)

3.3 Key Parameters

After data collection from the selected micro-study area, unavailable data were discarded from the important Landscape Metrics and Water Quality Parameters observed from the Literature Reviews.

Table 6 Key Landscape Metrics

Landscape Metrics	Chosen Parameter	Defence for Choice
Patch Density (PD)	Yes	An important and popular characteristic for study
Largest Patch Index (LPI)	No	Mostly determined by the type of land use
Edge Density (ED)	Yes	Studies proved that it has great influence
Percentage of Land (PLAND)	Yes	To understand the influence by each land uses
Landscape Shape Index (LSI)	No	Studies shows irregular influence
Aggregation Index (AI)	Yes	Land use quantity study for better planning
Shannon's Diversity Index (SHDI)	Yes	Watershed landscape level understanding
Shannon's Evenness Index (SHEI)	Yes	Characteristics of whole watershed patches
Slope Percentage (S%)	Yes	To understand topographical influence
Stream Proximity (SP)	Yes	To understand catchment hydrology

Table 7 Key Water Quality Parameters

Water Quality Parameters	Chosen Parameter	Defence for Choice
Dissolved Oxygen (DO)	No	Is not Influential enough from studies
pH	Yes	Captures diversified influence
Electrical Conductivity (EC)	Yes	Studies proved that it has great influence
Nitrite (NO_2^-)	No	No data
Ammonia (NH_3)	Yes	Captures all other nutrient related parameters
Calcium (Ca^{2+})	Yes	An important parameter to measure hardness
Phosphate (PO_4^{3-})	Yes	To diversify the study with its agriculture connection
Total Suspended Solids (TSS)	Yes	Erosion related, linking to topographical study

Sample Size

LULC Data was taken from ESRI LULC from 2017 to 2024. The LULC classes consist of Forest, Rangeland and Built-up. Since, there are 5 watershed zones, LULC for 8 years for each of them was taken. And from this LULC, 4 Landscape Metrics are derived through Fragstats software (Mcgarigal & Ene, 2023). The sample size is as follows.

Table 8 Sample Size of Landscape Metrics

Classes Distribution	No. of Watershed Zones	No. of Years	No. of Samples per Landscape Metrics Index	No. of Landscape Metrics Indices	Total Samples per Class
Forest	5	8	40	6	240
Rangland	5	8	40	6	240
Built-up	5	8	40	6	240
Landscape	5	8	40	2	80

Water Quality Data was taken from Mizoram Pollution Control Board. It is a secondary data collected through their website. Water Quality Parameters Value were collected for every year from 2017 to 2024.

Table 9 Sample Size of Water Quality Parameters

No. of Water Quality Parameters	No. of Watershed Zones	No. of Years	No. of Samples per Water Quality Parameter	Total Samples
6	5	8	40	240

4 Chapter IV: Analysis

4.1 Temporal Analysis

Just Introduction, types of analysis used and for what type of outcome, 4 to 5 lines Two types of temporal analysis is done, Land Cover Change Analysis through Intensity Analysis and Water Quality Parameters through Time Series.

4.1.1 Land Cover Change

Intensity analysis compares observed gains and losses of each land-use/land-cover (LULC) class against the uniform change intensity (*S*=5.93%),

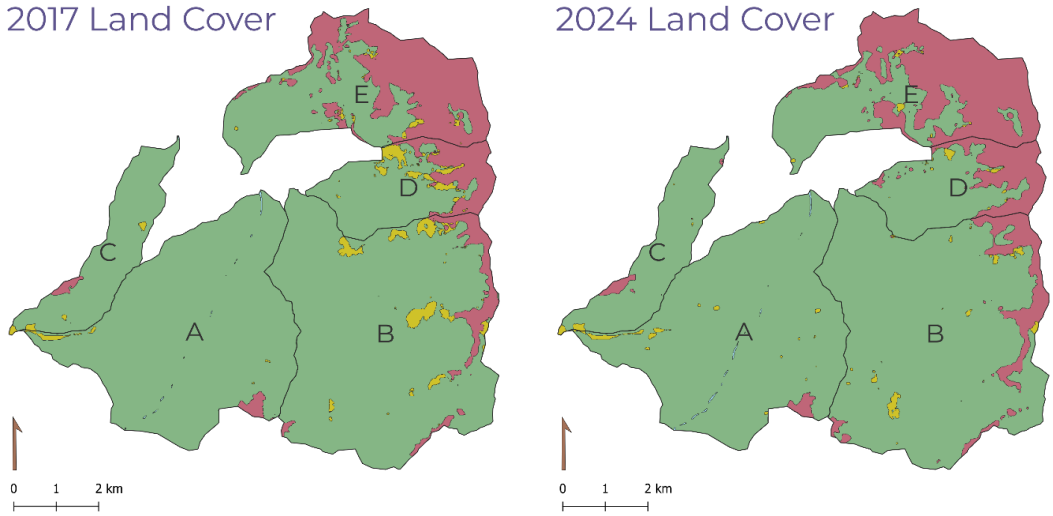

Figure 16 Map showing ESRI Land Cover

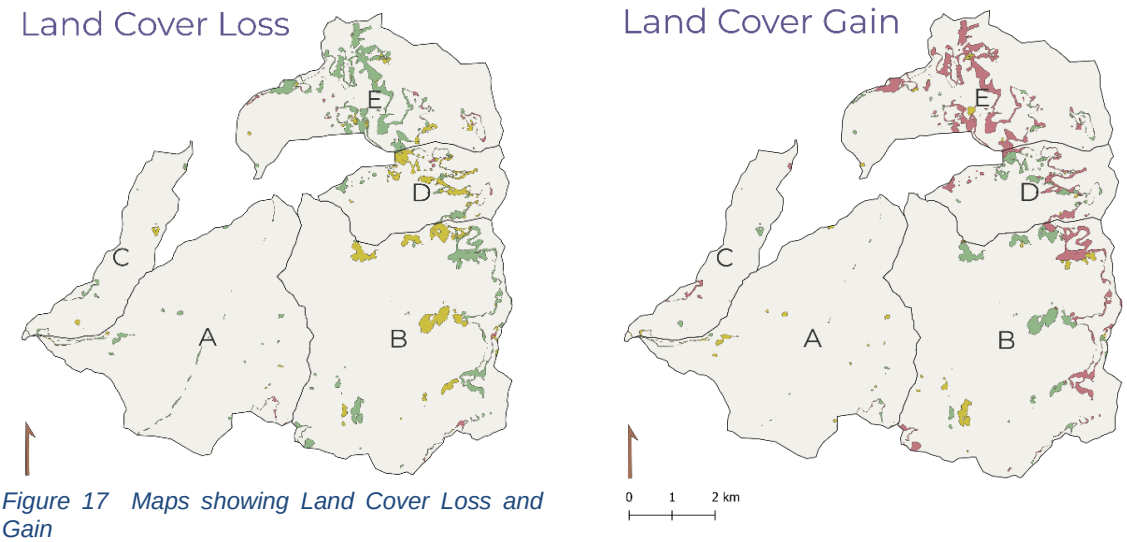

Figure 17 Maps showing Land Cover Loss and Gain

which represents the hypothetical rate of change if transitions were evenly distributed across all categories. Categories with gains or losses exceeding *S* are classified as **"active"** (non-random, targeted change), while those below S*S* are deemed **"dormant"** (random or minimal change).

Table 10 Land Cover Transition from 2017 to 2024

From	To	Area (km²)
Forest	Forest	57871
	Rangeland	414.8
	Built-up	2143.4
Rangeland	Forest	1036.9
	Rangeland	268.5
	Built-up	359.9
Built-up	Forest	172.1
	Rangeland	6.6
	Built-up	9797.1

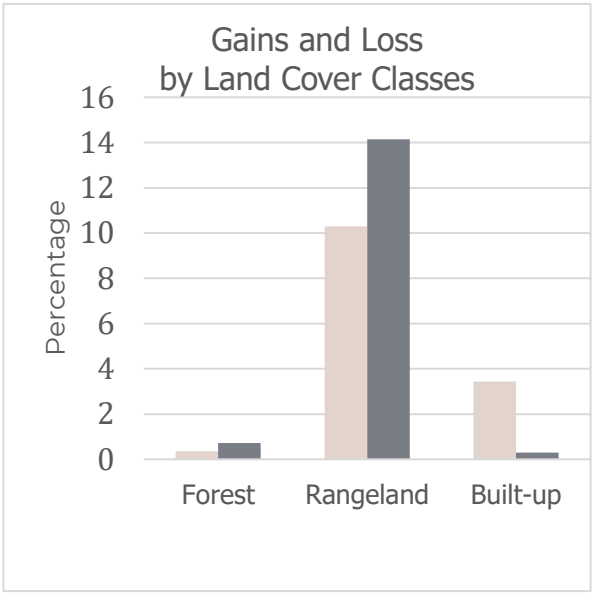

The gains of Forest fall below the uniform intensity threshold (*S*=5.93%), classifying Forest as a **dormant** category. Despite the large absolute area lost by Forest (2143.4 km²), the percentage loss (0.72%) remains below *S*, suggesting Forest dynamics are relatively stable compared to other categories. Rangeland gains are primarily from **Forest** (414.8 km²), highlighting deforestation for grazing or pastoral use. This exceeds the uniform intensity threshold, marking Rangeland as the **most active** category. Its losses also exceed *S*, reinforcing Rangeland's dynamic role.

While the gains of Built-up exceed losses (0.3%), they fall below the uniform intensity threshold (*S*=5.93%), classifying Built-up as **dormant**. This suggests urbanization is concentrated in specific areas rather than widespread. The near-complete avoidance of losses (-0.96 to Forest, -0.04 to Rangeland) underscores the irreversible nature of urban expansion.

Transition

The transition matrix quantifies the **magnitude and directionality** of changes between LULC classes, revealing dominant processes driving land transformation.

Forest

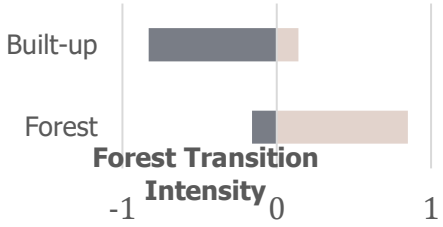

Forest experienced the largest loss to Built-up (2143.4 km²), indicating significant urban expansion into forested areas. This aligns with targeted transition intensity (+0.86), confirming urbanization as a dominant driver. Forest also lost 414.8 km² to Rangeland, reflecting deforestation for grazing or agricultural conversion. This corresponds to the high transition intensity (+0.98) from Forest to Rangeland. Forest gained 1036.9 km² from Rangeland, suggesting natural regeneration or reforestation efforts in degraded rangelands (targeted intensity: +0.85). Its minimal gains from Built-up (172.1 km², +0.14) imply limited reforestation in previously urbanized areas.

Rangeland

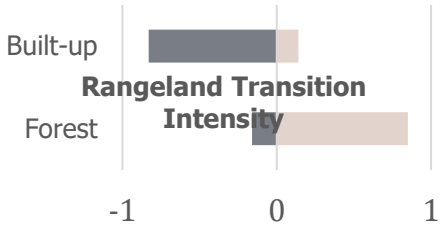

Rangeland lost 1036.9 km² to Forest, indicating ecological recovery in rangeland areas (avoided loss intensity: -0.74). This suggests either active reforestation or abandonment of marginal grazing lands. It also lost 359.9 km² to Built-up, though this represents a smaller proportion of its total area and aligns with the avoided loss intensity (-0.26), implying resistance to urban encroachment. Rangeland gained 414.8 km² from Forest, reinforcing the trend of deforestation for pastoral use (targeted intensity: +0.98).

It has marginal gains from Built-up (6.6 km², +0.02) suggest rare cases of urban abandonment or land-use shifts.

Built-up

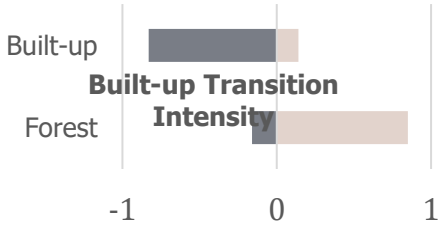

Built-up areas lost only 172.1 km² to Forest and 6.6 km² to Rangeland, reflecting the permanence of urban infrastructure (avoided loss intensities: -0.96 and -0.04). This underscores the irreversible nature of urbanization. It gained 2143.4 km² from Forest, the largest single transition in the matrix, highlighting urban sprawl into forested ecosystems. It also gains from Rangeland (359.9 km²) indicate secondary urban expansion into semi-natural landscapes.

The massive conversion of Forest and Rangeland to Built-up underscores rapid urban expansion. Forest loss to Rangeland highlights ongoing pressure from agricultural or pastoral land use, driven by population growth or economic demands. Rangeland-to-Forest gains indicate ecological recovery. Rangeland acts as a transitional zone, absorbing losses from Forest while also regenerating.

4.1.2 Water Quality Parameters

pH

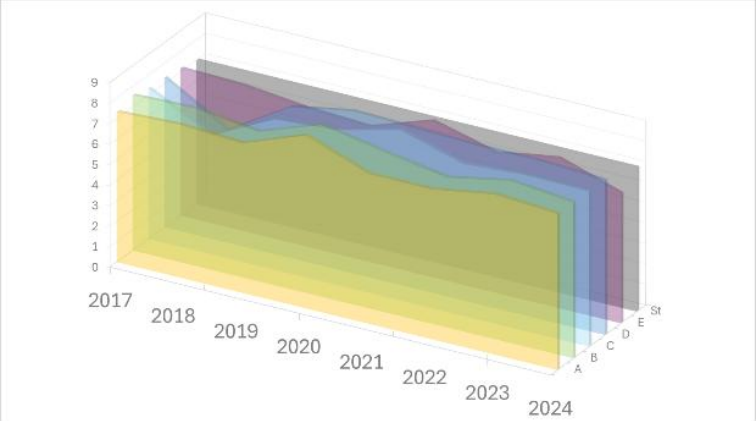

Figure 18 pH Time Series

The pH data across Zones A–E from 2017 to 2024 reveals notable deviations from the ICMR/BIS standard range (6.5–8.5), indicating potential influences from environmental and anthropogenic factors. Sharp declines in pH, such as the acidic values of 5.78 (Zone C, 2018) and 5.48 (Zone D, 2018), suggest episodic inputs of acidic substances, likely linked to organic acid release from soil erosion. These anomalies coincide with seasonal or regional precipitation patterns, as heavy rainfall can mobilize acidic runoff from urbanized or deforested areas, lowering pH temporarily. Similarly, the 2024 drop to 6.3 in Zone E may reflect cumulative effects of land-use changes, such as urban sprawl or agricultural intensification, which increase exposure to acidic pollutants or alter natural buffering capacities.

Conversely, alkaline spikes like 8.43 (Zone A, 2020) and 8.3 (Zone C, 2021) hint at nutrient enrichment from agricultural runoff (e.g., fertilizers) or reduced dilution during dry periods, concentrating alkaline compounds. Urbanization likely exacerbates these trends, as impervious surfaces enhance runoff carrying detergents, industrial effluents, or concrete leachates. Zones which have higher forest percentage (e.g., Zones A and B) show relatively stable pH but occasional alkalinity. Meanwhile, Zones C and D, potentially in agricultural or eroded landscapes, exhibit extreme fluctuations, underscoring vulnerability to land-use practices and soil degradation.

Overall, the pH variability reflects a interplay of precipitation-driven erosion, urbanization-induced pollution, and agricultural runoff. Acidic events correlate with high-intensity rainfall mobilizing pollutants, while alkalinity spikes align with droughts or nutrient loading. Human activities, such as deforestation, construction, and fertilizer use, likely amplify these natural processes, reducing the system’s resilience to pH shifts.

Electrical Conductivity (EC)

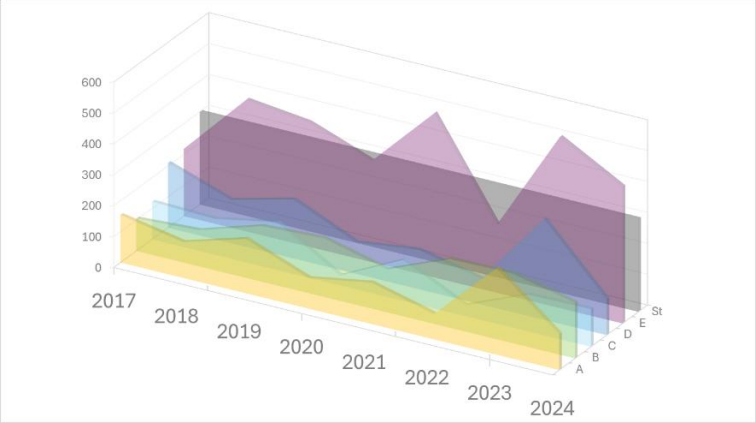

Figure 19 EC Time Series

EC data across Zones A–E (2017–2024) reveals significant deviations from the ICMR standard of 300 µS/cm, with values ranging from extremely low (32 µS/cm in Zone C, 2020) to highly elevated (554 µS/cm in Zone E, 2023). Zones A, D, and E exhibit alarming spikes, such as Zone E's 554 μS/cm (2023) and Zone D's 327 μS/cm (2023), far exceeding the standard. These zones likely drain urbanized or industrialized areas, where runoff from impervious surfaces (e.g., roads, factories) introduces dissolved salts, heavy metals, and organic pollutants. Urban stormwater, laden with road salts, sewage leaks, or construction sediments, likely contributes to elevated EC.

Zone C's erratic EC values—such as 32 µS/cm (2020) and 119 µS/cm (2024)—indicate agricultural influences. Low EC in 2020 may reflect dilution from heavy rainfall or reduced fertilizer use during a fallow period, while higher values in later years could signal seasonal nutrient runoff (e.g., nitrates, phosphates) post-application. Similarly, Zone B's moderate increase to 222 µS/cm (2022) and 180 µS/cm (2024) may correlate with agricultural intensification near its watershed. Zones A and D show marked fluctuations (e.g., Zone A: 280 µS/cm in 2023; Zone D: 327 µS/cm in 2023), potentially linked to soil erosion from deforestation, construction, or overgrazing.

Extreme EC drops, like Zone A's 82 μS/cm (2022) and Zone C's 32 μS/cm (2020), likely reflect dilution from prolonged or intense rainfall, which flushes ions from the watershed. Conversely, droughts or low-flow periods (e.g., 2021–2023) concentrate dissolved solids, exacerbating EC spikes in Zones D and E. For example, Zone E's 532 μS/cm (2021) aligns with reduced dilution during dry conditions, amplifying pollutant concentrations.

The EC trends underscore a mix of urban-industrial pollution, agricultural runoff, precipitation variability, and erosion as primary drivers. Zones E and D face acute stress from anthropogenic inputs. Zones A and C highlight vulnerability to seasonal dynamics and land-use practices.

Ammonia (NH_3)

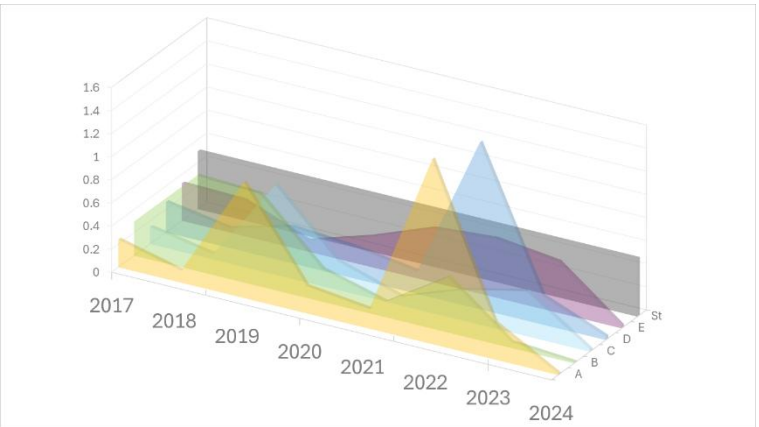

Figure 20 NH_3 Time Series

The ammonia (NH_3) data across Zones A–E (2017–2024) reveals widespread exceedances of the BIS standard of 0.5 mg/L, with values peaking at 1.6 mg/L (Zone A, 2022) and 1.444 mg/L (Zone D, 2022). These spikes, alongside notable variations during the Covid-19 pandemic (2020–2021), highlight the interplay of anthropogenic pressures, seasonal activities, and environmental drivers. Ammonia levels are strongly tied to human activities. Zones A and D exhibit extreme values, such as Zone D's 1.444 mg/L (2022) and Zone A's 1.6 mg/L (2022), likely reflecting concentrated agricultural runoff (e.g., fertilizer use, livestock waste) or industrial discharges. Zone B's 0.825 mg/L (2018) and Zone E's 0.509 mg/L (2022) suggest sewage or domestic effluent contamination, particularly in urbanized watersheds. Seasonal patterns, such as Zone C's 0.775 mg/L (2019) and Zone A's 1.003 mg/L (2019), align with agricultural cycles (e.g., fertilizer application periods).

The lockdowns in 2020–2021 due to the pandemic temporarily reduced NH_3 levels in many zones, underscoring human activity's role. Zone B's value dropped from 0.802 mg/L (2019) to 0.281 mg/L (2020), Zone C from 0.775 mg/L (2019) to 0.247 mg/L (2020).. However, Zone D's 2021 increase to 0.194 mg/L (from 0.315 mg/L in 2019) suggests localized persistence of pollution sources. By 2022, NH_3 surged in Zones A, D, and E, indicating resumed or intensified activities. Zone A's 1.6 mg/L (2022) and Zone D's 1.444 mg/L (2022) may reflect post-lockdown recovery and agricultural intensification. Additionally, low precipitation or drought conditions could have concentrated pollutants, compounding the rebound effect.

NH_3 trends underscore the dominance of agricultural runoff, industrial effluents, and sewage in driving pollution, with Covid-19 lockdowns temporarily mitigating these pressures. Post-2021 rebounds suggest rapid re-establishment of anthropogenic stressors.

Calcium (Ca^{2+})

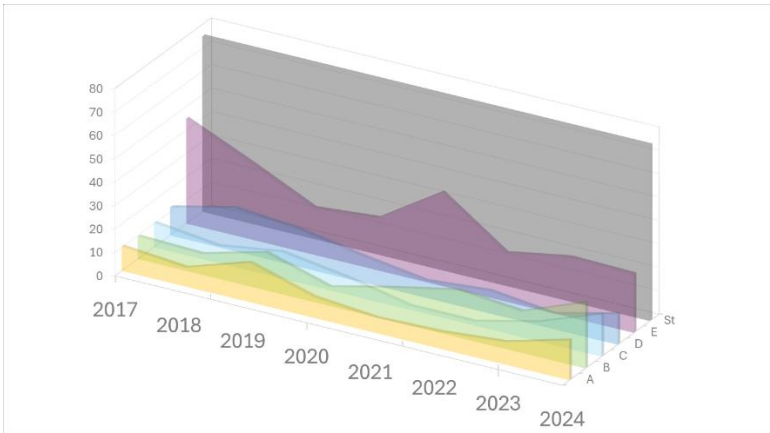

Figure 21 Ca^{2+} Time Series

The calcium (*Ca^{2+}*) concentrations across Zones A–E (2017–2024) remain well below the BIS standard of 75 mg/L, indicating no direct health risks from excess calcium. However, spatial and temporal variations reveal insights into geological, hydrological, and anthropogenic influences, with notable shifts during the Covid-19 pandemic (2020–2021).

Zones with consistently higher Ca levels (e.g., Zone E: 20–44.8 mg/L) likely drain areas rich in calcium-bearing minerals (e.g., limestone, gypsum), where natural weathering contributes to baseline concentrations. Zone E's elevated values (e.g., 44.8 mg/L in 2017, 40 mg/L in 2021) align with carbonate-rich geology, while Zones A–D (mostly <20 mg/L) may have less calcareous parent material. Seasonal fluctuations (e.g., Zone B: 28 mg/L in 2024) also reflect groundwater interactions, as dry periods enhance mineral dissolution.

Zone A's 2024 rise to 17 mg/L (after 2023's 9.6 mg/L) could reflect agricultural activities and fertilizer runoff. Zone D's 2017 value (12 mg/L) dropping to 6.4 mg/L in 2023 suggests reduced erosion or land-use changes. Zone C's 2020–2021 drop to 1.6 mg/L (lowest in dataset) likely reflects agricultural and anthropogenic activities. Zone E's 2020 decline to 22.4 mg/L (from 32.8 mg/L in 2018) may indicate reduced urban runoff pandemic disruptions. These patterns underscore the role of anthropogenic activity in modulating calcium levels, even for a naturally abundant ion.

Calcium trends highlight a mix of natural geology and anthropogenic drivers (urbanization, agriculture) shaping water quality. Tut overall, the trends shows that human inactivity (eg: pandemic), have made changes in patterns but not too abrupt or significant. The zone wise difference in patterns indicate the role of land changes in the parameter's increase and decrease.

Phosphate (PO_4^{3-})

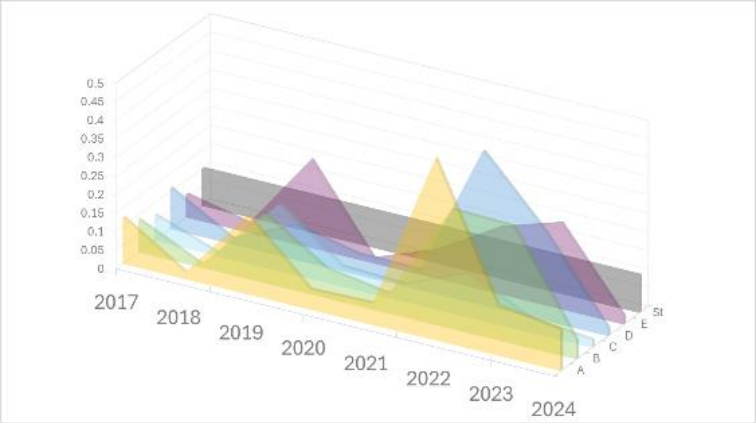

Figure 22 PO_4^{3-} Time Series

The phosphate (*PO_4^{3-}*) data across Zones A–E (2017–2024) reveals frequent exceedances of the USPH standard of 0.1 mg/L, with values peaking at 0.489 mg/L (Zone A, 2022) and 0.416 mg/L (Zone D, 2022). These fluctuations highlight the interplay of agricultural practices, urbanization, pandemic-induced activity shifts, and hydrological drivers. Phosphate spikes, such as Zone A's 0.489 mg/L (2022) and Zone B's 0.316 mg/L (2023), strongly correlate with agricultural intensification and urban effluents. Zone E's 0.238 mg/L (2019) and 0.231 mg/L (2023) suggest mixed agricultural-urban influences, while Zones C and D exhibit lower but variable inputs, likely from diffuse sources like soil erosion or low-density farming.

Lockdowns in 2020–2021 significantly reduced anthropogenic activity, leading to sharp declines in phosphate levels. Zone A's value dropped from 0.213 mg/L (2019) to 0.054 mg/L (2020) and Zone B from 0.188 mg/L (2019) to 0.079 mg/L (2020), also Zone D from 0.093 mg/L (2019) to 0.056 mg/L (2020). These reductions underscore the impact of halted industrial operations, reduced fertilizer application, and decreased urban runoff during the pandemic, demonstrating the system's responsiveness to human activity changes. By 2022, phosphate levels surged in Zones A, B, and D, exceeding the standard by 2–4 times. Zone A's 0.489 mg/L (2022) and Zone D's 0.416 mg/L (2022) likely reflect resumed agricultural practices, intensified urbanization, and potential wastewater infrastructure failures post-lockdown. The rebound aligns with global trends of heightened nutrient pollution following pandemic recovery periods.

Phosphate trends underscore the dominance of agricultural runoff, urbanization, and pandemic-driven activity shifts in shaping water quality. The 2022 rebound highlights the vulnerability of aquatic systems to resumed anthropogenic pressures post-crisis, while 2024's compliance suggests actionable success in pollution control.

Total Suspended Solids (TSS)

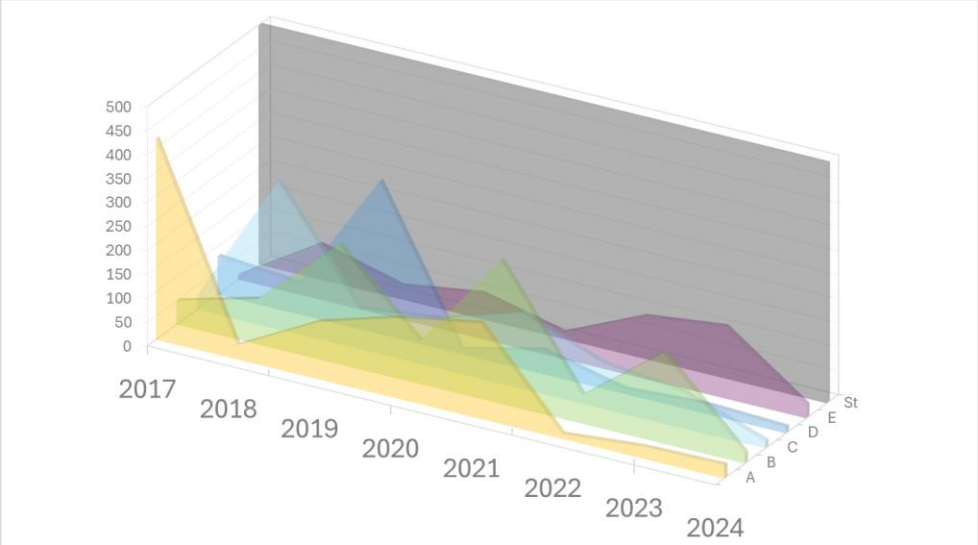

Figure 23 TSS Time Series

The Total Suspended Solids (TSS) data across Zones A–E (2017–2024) reveals significant spatial and temporal variability, with values peaking at 320 mg/L (Zone D, 2019) and 300 mg/L (Zone B, 2021) but remaining below the ICMR standard of 500 mg/L. These trends reflect the influence of erosion and urbanization with notable improvements observed by 2024.

High TSS values in Zones B, C, and D (e.g., Zone D: 320 mg/L in 2019, Zone B: 300 mg/L in 2021) suggest erosion from deforestation, construction sites, or agricultural fields. Zone C's 310 mg/L (2018) and 160 mg/L (2021) align with seasonal soil disturbance, while Zone D's 2019 spike likely reflects heavy rainfall or land clearing. Zones A and E, with generally lower TSS (e.g., Zone A: 420 mg/L in 2017, dropping to 28 mg/L in 2024), may experience less intensive land-use pressures. Urbanized zones (A and B) show sporadic spikes, such as Zone A's 420 mg/L (2017) and Zone B's 300 mg/L (2021), indicative of stormwater carrying sediments from impervious surfaces. Zone B's elevated values in 2021–2023 (220–300 mg/L) may link to post-pandemic infrastructure projects or inadequate erosion control.

Extreme rainfall or droughts can also modulate TSS levels. Zone D's 2019 spike (320 mg/L) and Zone B's 2021 peak (300 mg/L) may correlate with intense storms eroding unprotected soils. Zone A's 2020–2024 decline (from 170 mg/L to 28 mg/L) could reflect improved vegetation cover or reduced runoff due to altered rainfall patterns post-2020.
TSS trends underscore the dominance of erosion from agriculture, urban runoff, and construction. The 2024 compliance highlights potential successes in watershed management, though the abruptness of the decline warrants validation.

Conclusion

Based on the analysis, distinct patterns emerged for each water quality parameter in relation to landscape characteristics and external influences.

Table 11 Observation of Water Quality Parameters Time Series

Water Quality Parameters	Observations	Potential Polluters
pH	Potentially many influencers	Fertilizer runoff, erosion
Electrical Conductivity (EC)	Zone wise variability, landscape characteristics influenced	Road salt runoff, agriculture runoff
Ammonia (NH_3)	Pandemic effect seen, human activity influenced	Fertilizer runoff, sewage
Calcium (Ca^{2+})	Zone wise variability, landscape characteristics influenced	Erosion, urbanisation
Phosphate (PO_4^{3-})	Pandemic effect seen, human activity influenced	Construction runoff, agriculture runoff
Total Suspended Solids (TSS)	Patterns unrecognised much, potential precipitation influenced	Erosion, stormwater

pH levels appeared to be influenced by multiple, potentially overlapping factors, making it difficult to isolate a single cause. Electrical Conductivity (EC) and Calcium (Ca^{2+}) showed zone-wise variability, indicating a strong influence from surrounding landscape features. In contrast, Ammonia (NH_3) and Phosphate (PO_4^{3-}) levels reflected changes linked to human activity, particularly during the pandemic period, highlighting the impact of anthropogenic factors. Total Suspended Solids (TSS) did not exhibit clear patterns, though precipitation may play a role in its fluctuations. These observations underscore the complex interplay between natural landscape characteristics, human activities, and climatic factors in shaping river water quality. Understanding these dynamics is essential for developing targeted and effective watershed management strategies.

4.2 Correlation Analysis

Forest

Pearson Correlation Test is done to examine the relationships between forest landscape metrics (**F_PLAND, F_AI, F_PD, F_ED, F_Slope, F_SP**) and water quality parameters (**pH, EC, NH_3, Ca^{2+}, PO_4^{3-}, TSS**) using correlation coefficients (*r*) and statistical significance (*p*-values). The analysis distinguishes landscape-driven patterns from external anthropogenic influences.

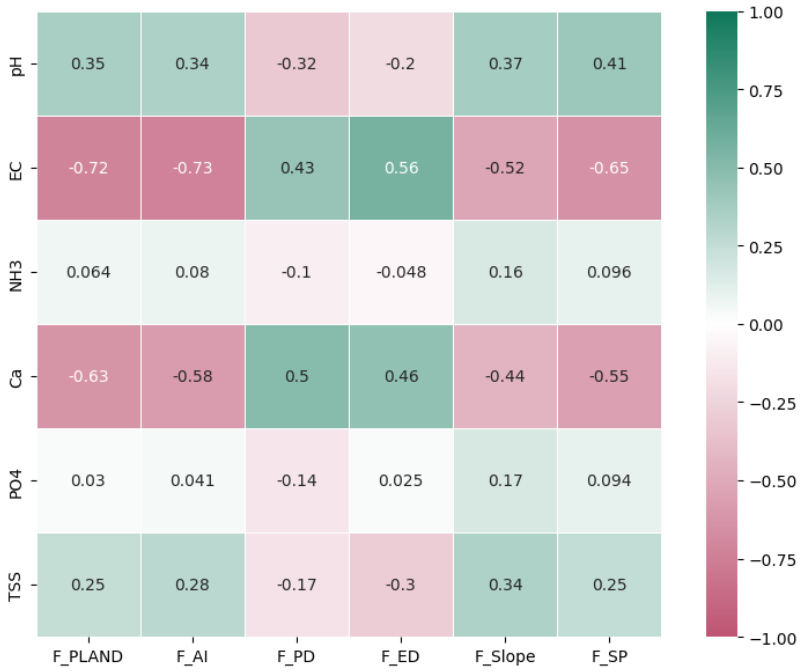

Figure 24 Correlation Heatmap of Water Quality Parameters and Forest Metrics

Results

EC and **Ca^{2+}** were strongly influenced by all metrics ($p < 0.01$ for EC with F_PLAND/F_AI/F_SP; $p < 0.05$ for Ca^{2+}), reflecting forest cover's role in regulating ionic balance. **pH** was moderately sensitive ($p < 0.05$ for F_PLAND/F_Slope/F_SP), with forests buffering acidity through canopy interception and mineral weathering. **TSS** emerged as a marginally landscape-sensitive parameter due to its moderate correlation with F_Slope ($r = 0.34$, $p = 0.04$), potentially linked to slope-driven erosion in forested areas. **NH_3** and **PO_4^{3-}** showed no significant correlations with any metric ($p > 0.05$), indicating these pollutants are driven by external sources (e.g., sewage, agriculture) rather than forest configuration. Weak positive trends (e.g., F_PLAND-PO_4^{3-}, $r = 0.03$, $p = 0.85$) further support the lack of consistent landscape-driven patterns.

Rangeland

Pearson Correlation Test is done to examine the relationships between rangeland landscape metrics (**F_PLAND, F_AI, F_PD, F_ED, F_Slope, F_SP**) and water quality parameters (**pH, EC, NH_3, Ca^{2+}, PO_4^{3-}, TSS**) using correlation coefficients (*r*) and statistical significance (*p*-values). The analysis distinguishes landscape-driven patterns from external anthropogenic influences.

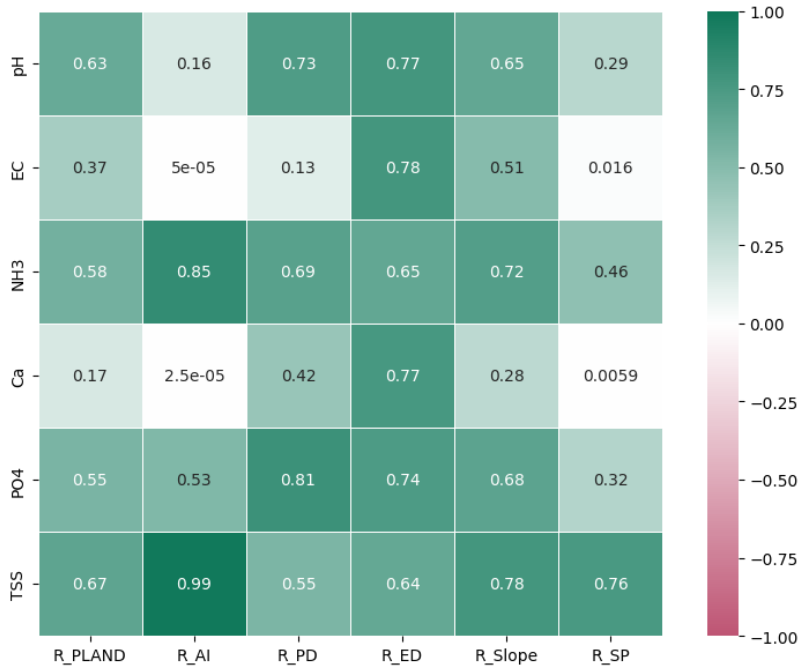

Figure 25 Correlation Heatmap of Water Quality Parameters and Rangeland Metrics

Result

EC and **Ca^{2+}** emerged as the most sensitive to rangeland metrics, particularly **R_AI** and **R_SP** ($p < 0.01$). Aggregated rangelands (R_AI) reduced EC and Ca^{2+}, likely through organic acid inputs or soil stabilization, while stream-proximate rangelands (R_SP) further filtered ions. These findings align with forest results, where connectivity and riparian buffers regulate ionic balance, though rangelands exhibit weaker buffering effects compared to forests. **pH, NH_3, PO_4^{3-}**, and **TSS** showed no significant correlations with any rangeland metric ($p > 0.05$), mirroring forest results for NH_3 and PO_4^{3-}. This suggests these parameters are driven by external factors (e.g., agricultural runoff, livestock waste) rather than rangeland configuration. Weak positive trends (e.g., R_PLAND-Ca^{2+}, r = -0.22) further support the lack of consistent landscape-driven patterns.

Built-up

Pearson Correlation Test is done to examine the relationships between rangeland landscape metrics (**F_PLAND, F_AI, F_PD, F_ED, F_Slope, F_SP**) and water quality parameters (**pH, EC, NH_3, Ca^{2+}, PO_4^{3-}, TSS**) using correlation coefficients (*r*) and statistical significance (*p*-values). The analysis distinguishes landscape-driven patterns from external anthropogenic influences.

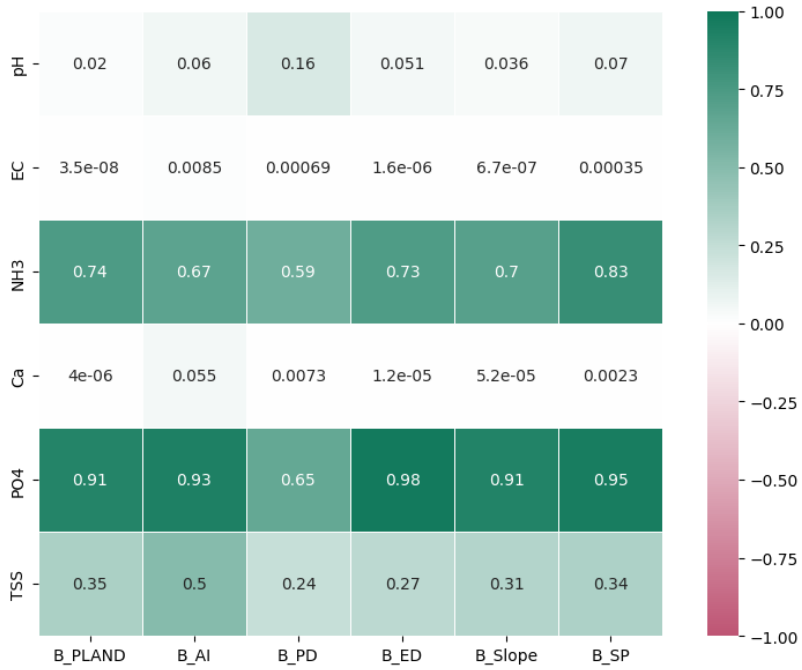

Figure 26 Correlation Heatmap of Water Quality Parameters and Built-up Metrics

Result

EC and **Ca^{2+}** were the most sensitive to built-up metrics, with significant correlations across all metrics ($p < 0.01$ for EC with B_PLAND/B_ED/B_Slope; $p < 0.05$ for Ca^{2+} with B_PLAND/B_Slope/B_SP). Urbanization amplifies ionic and calcium inputs through impervious surfaces, slope-driven runoff, and stream-proximate development. **pH** showed moderate sensitivity, with significant negative correlations for B_PLAND (r = -0.37, p = 0.02) and B_Slope (r = -0.33, p = 0.04), indicating urban acidification via atmospheric deposition and acidic materials. **NH_3, PO_4^{3-}**, and **TSS** showed no significant correlations with any built-up metric ($p > 0.05$), reinforcing their dependence on external sources (e.g., sewage, agriculture). Weak trends (e.g., B_PLAND-TSS, r = -0.24, p = 0.35) suggest urbanization may reduce TSS via paved surfaces limiting sediment input, though this relationship is not statistically robust.

Landscape

Pearson Correlation Test is done to examine the relationships between landscape-level metrics Shannon's Diversity Index (SHDI), Shannon's Evenness Index (SHEI) and water quality parameters (**pH, EC, NH_3, Ca^{2+}, PO_4^{3-}, TSS**) using correlation coefficients (*r*) and statistical significance (*p*-values). The analysis distinguishes landscape-driven patterns from external anthropogenic influences.

Figure 27 Correlation Heatmap of Water Quality Parameters and Landscape Metrics

SHDI (Shannon's Diversity Index) showed significant positive correlations with EC ($r = 0.50$, $p < 0.001$) and Ca^{2+} ($r = 0.44$, $p = 0.004$), indicating that higher landscape diversity amplifies ionic and calcium leaching, likely due to mixed land-use interactions (e.g., urban patches, fragmented forests). SHEI (Shannon's Evenness Index) mirrored these results, with significant positive correlations for EC ($r = 0.48$, $p < 0.001$) and Ca^{2+} ($r = 0.43$, $p = 0.005$), reinforcing that balanced land-use distributions exacerbate ionic pollution. pH exhibited weak negative correlations with both metrics ($r = -0.25$ for SHDI; $r = -0.24$ for SHEI), non-significant ($p > 0.12$), suggesting minimal buffering effects.

NH_3, PO_4^{3-}, and TSS showed no significant relationships with SHDI/SHEI ($p > 0.65$), underscoring their dominance by external drivers (e.g., agriculture, sewage). Notably, TSS correlated negatively with SHDI/SHEI ($r = -0.27$ to -0.26, $p > 0.28$), implying diverse landscapes may reduce particulate matter via vegetation filtering, though not statistically significant. Landscape diversity and evenness strongly regulate EC and Ca^{2+} but have no meaningful influence on NH_3, PO_4^{3-}, or TSS, necessitating targeted pollution control for these parameters.

Inference

The comparative analysis of forest, rangeland, and built-up landscapes reveals distinct patterns in their influence on water quality parameters, driven by interactions between landscape metrics and anthropogenic factors

Table 12 Influence of Landscape Metrics on Water Quality Parameters

Water Quality Parameters	Forest Metrics	Rangeland Metrics	Built-up Metrics	Landscape-Level Metrics
pH	F_PLAND (↑),R_AI (↑), R_SP (↑) F_AI (↑), F_Slope (↑)		B_PLAND (↓), B_ED (↓), B_AI (↓)	SHDI (↓), SHEI (↓)
EC	F_PLAND (↓),R_PLAND (↓), R_AI (↑), F_AI (↓), F_PD(↓), R_PD (↑), (↑), F_ED (↑),R_Slope (↑), R_SP F_Slope (↑),(↓) F_SP (↓)		B_PLAND (↑), B_PD (↑), B_ED (↑), B_AI (↑), B_Slope (↑), B_SP (↑)	SHDI (↑), SHEI (↑)
NH_3	None (p > 0.05)	None (p > 0.05)	None (p > 0.05)	None (p > 0.05)
Ca^{2+}	F_PLAND (↓),R_PLAND (↓), R_AI (↑), F_AI (↓), F_PD(↓), R_PD (↑), (↑), F_ED (↑),R_Slope (↑), R_SP F_Slope (↑),(↓) F_SP (↓)		B_PLAND (↑), B_PD (↑), B_ED (↑), B_AI (↑), B_Slope (↑), B_SP (↑)	SHDI (↑), SHEI (↑)
PO_4^{3-}	None (p > 0.05)	None (p > 0.05)	None (p > 0.05)	None (p > 0.05)
TSS	F_AI (↑),R_PLAND (↓), F_Slope (↑) R_PD (↓), R_Slope (↓), R_SP (↓)		B_PLAND (↓), B_SP (↓)	SHDI (↓), SHEI (↓)

. **Forests** and **rangelands** exhibit strong regulation of **electrical conductivity (EC)** and **calcium (Ca^{2+})**, mediated by vegetation connectivity, stream proximity, and slope. In contrast, **built-up areas** amplify ionic and calcium pollution through impervious surfaces, fragmentation, and slope-driven runoff. **pH** shows moderate sensitivity to all three land-use types, while **NH_3**, **PO_4^{3-}**, and **TSS** are universally dominated by anthropogenic inputs, with minimal landscape-driven patterns.

Forests demonstrate the strongest buffering capacity, with aggregated patches (F_AI) and stream-proximate vegetation (F_SP) reducing EC and Ca^{2+} significantly ($p < 0.001$ for both metrics). Fragmentation (F_PD, F_ED) counteracts this by increasing ionic leaching, highlighting the dual role of forest structure in stabilizing or destabilizing water chemistry. **Rangelands** share similarities, with aggregated vegetation (R_AI) and riparian connectivity (R_SP) lowering EC and Ca^{2+}, though their weaker correlations (r = -0.60 to

-0.61) suggest reduced buffering compared to forests. **Built-up areas** exhibit the opposite trend: urban cover (B_PLAND), edge density (B_ED), and steep slopes (B_Slope) strongly elevate EC and Ca^{2+} (r = 0.63–0.69), reflecting pollution from concrete, road dust, and slope-driven runoff. Stream-proximate urban development (B_SP) further exacerbates these effects, underscoring the direct pollution pathway from built-up areas to waterways.

pH reveals contrasting responses across land-use types. **Forests** buffer acidity through canopy interception and mineral weathering (F_PLAND: r = 0.35, p = 0.02; F_Slope: r = 0.37, p = 0.02), while **built-up areas** acidify streams via industrial effluents and impervious surfaces (B_PLAND: r = -0.37, p = 0.02; B_Slope: r = -0.33, p = 0.04). **Rangelands** show no significant pH trends, likely due to lower vegetation density and grazing-induced soil disturbance. **TSS** exhibits marginal sensitivity to forest slope (r = 0.34, p = 0.04) and weak negative correlations in built-up areas (r = -0.24, p = 0.35), suggesting natural vegetation mobilizes organic particulates seasonally, while urban paving limits sediment input. However, these relationships are secondary to anthropogenic drivers for TSS.

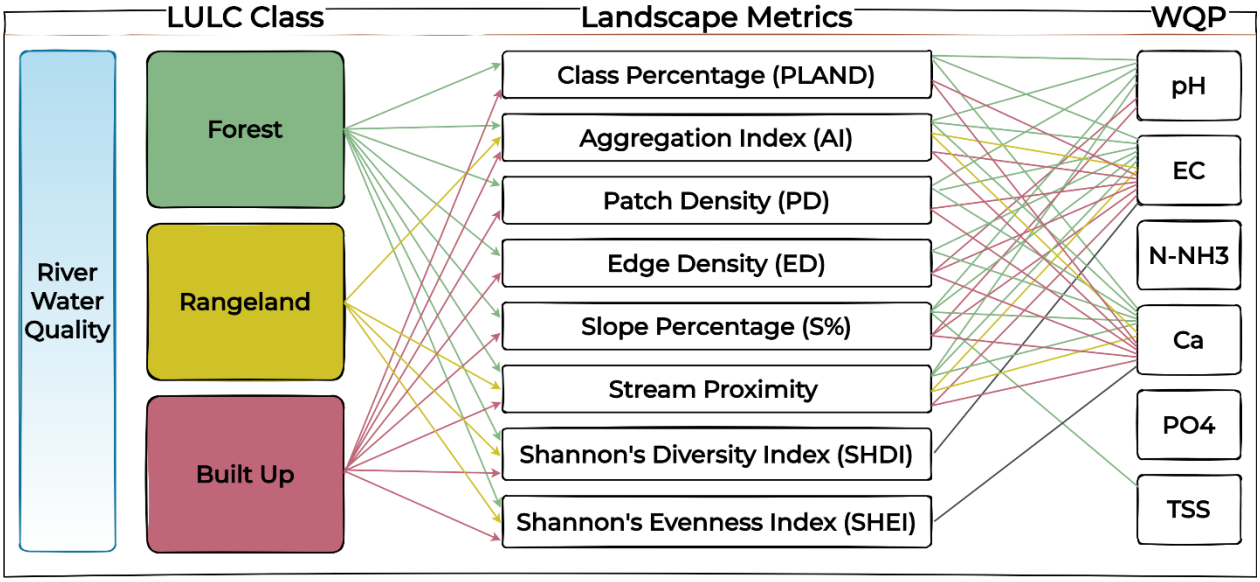

Figure 28 Land Cover Influence Network Diagram

Network of Interactions

The interplay between landscape metrics creates synergistic or antagonistic effects on water quality, varying by land-use type. In **forests**, aggregation (F_AI) and stream proximity (F_SP) synergistically reduce EC and Ca^{2+}, while fragmentation metrics (F_PD, F_ED) introduce trade-offs by increasing ionic leaching. For example, edge density (F_ED) correlates positively with EC (r = 0.56, p < 0.001), counteracting the buffering effects of contiguous forests. **Slope** interacts with forest cover to amplify buffering

capacity (r = 0.37, p = 0.02), though it also marginally increases TSS (r = 0.34, p = 0.04), highlighting seasonal organic debris inputs.

In **rangelands**, aggregation (R_AI) and stream proximity (R_SP) synergistically lower EC and Ca^{2+}, but fragmentation metrics (R_PD, R_ED) show no significant relationships, indicating limited edge-driven effects. Grazing pressure may disrupt metric interactions, as evidenced by weaker correlations compared to forests. **Slope** in rangelands shows no significant impact on TSS (r = -0.07, p = 0.78), suggesting vegetation mitigates erosion even on steep terrain.

Built-up areas exhibit the strongest metric synergies, with slope (B_Slope), edge density (B_ED), and urban cover (B_PLAND) compounding ionic pollution. For instance, high B_Slope (r = 0.69, p < 0.001) and B_ED (r = 0.68, p < 0.001) amplify EC through rapid runoff and edge-zone pollution, while stream-proximate development (B_SP) ensures direct pollutant discharge to waterways. However, these metrics also create trade-offs, such as reduced TSS in urbanized areas (r = -0.24, p = 0.35) due to paved surfaces limiting sediment input.

4.3 Regression Analysis

To assess the degree of impact that landscape characteristics have on water quality parameters, linear regression analysis was performed. Regression models were developed for each land cover class—forest, rangeland, built-up—and at the overall landscape level. For clearer visual interpretation, all landscape metric values were scaled from 1 to 100 using the Min-Max scaling method. This approach simplified comparisons and enhanced the readability of the results.

Forest

pH

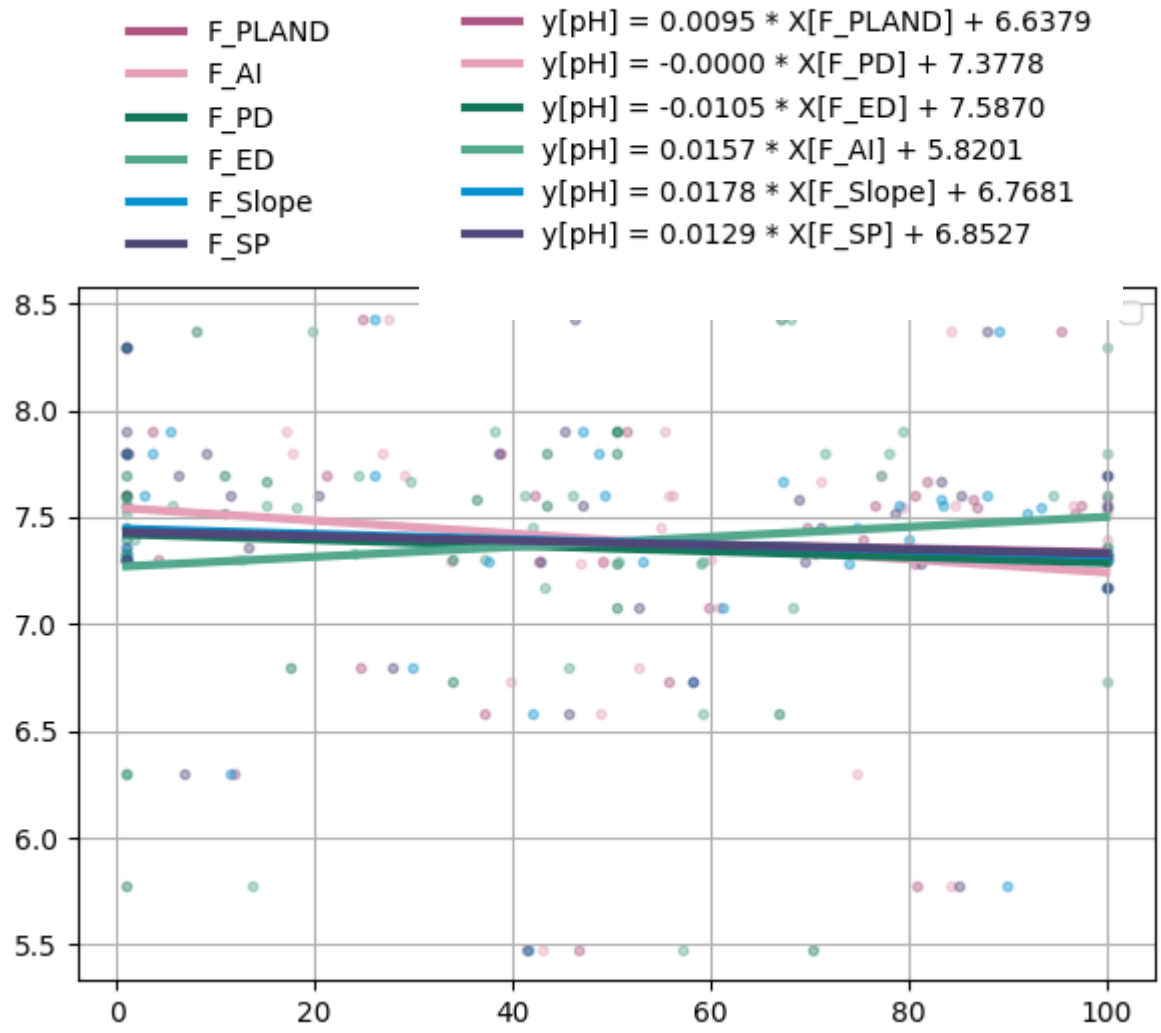

Figure 29 Regression Plot between pH and Forest Metrics

The regression analysis shows that forest cover (F_PLAND) and aggregation (F_AI) exert minor positive influences on pH, with slopes of 0.0095 and 0.0157, respectively. The equation y[pH] = 0.0095X + 6.6379 for F_PLAND indicates that a 10% increase in forest cover raises pH by ~0.095 units, reflecting slight acid buffering (e.g., from organic acids in litter). Similarly, the aggregated forest metric (y = 0.0157X + 5.8201) suggests that contiguous patches enhance buffering capacity, though effects remain marginal. In contrast, fragmentation (F_PD, F_ED) and slope (F_Slope) exhibit near-zero slopes, indicating negligible impacts. Stream proximity (F_SP) shows a weak positive slope (y = 0.0129X + 6.8527), reinforcing that forests near waterways provide minimal pH stabilization. These results align with correlation findings, underscoring forests' limited role in regulating acidity unless cover or aggregation is extensive.

Electrical Conductivity (EC)

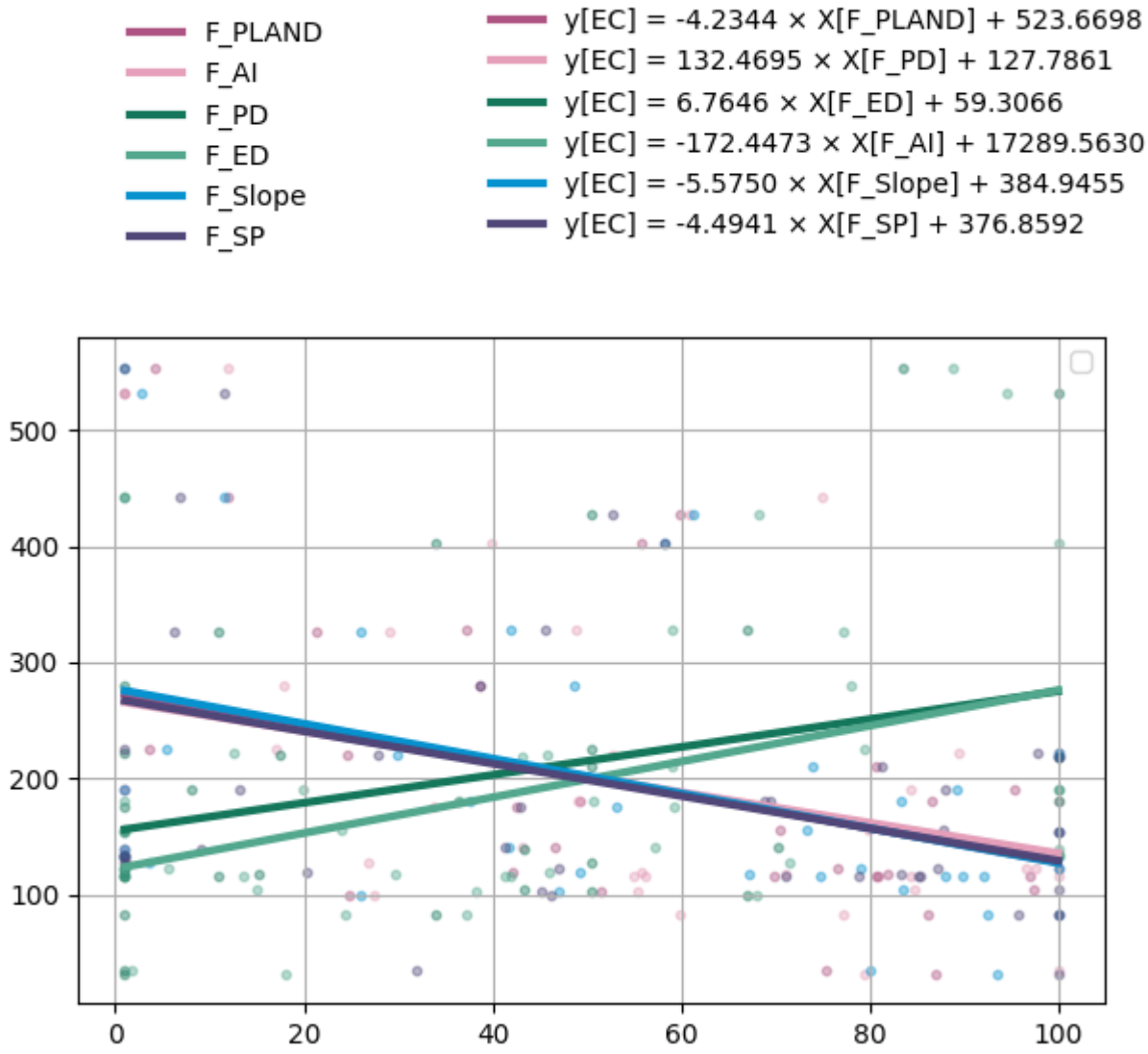

Figure 30 Regression Plot between EC and Forest Metrics

Forest metrics strongly regulate EC, with F_PLAND and F_AI showing steep negative slopes. The equation for F_PLAND indicates that a 10% increase in forest cover reduces EC by ~42 µS/cm, likely due to reduced runoff and ionic retention in soils. F_AI (aggregation) exhibits an even steeper slope, highlighting that contiguous forests drastically lower EC by stabilizing soils and promoting organic acid inputs. In contrast, fragmentation metrics (F_PD, F_ED) amplify EC, with F_PD showing a 1-unit increase in patch density raises EC by 132 µS/cm and F_ED reflecting edge-driven nutrient leaching. Stream proximity (F_SP) further mitigates EC, underscoring riparian buffers' role in filtering ions. These results emphasize that preserving aggregated, stream-proximate forests and limiting fragmentation is critical for reducing ionic pollution.

Nitrogen Ammonia (NH_3)

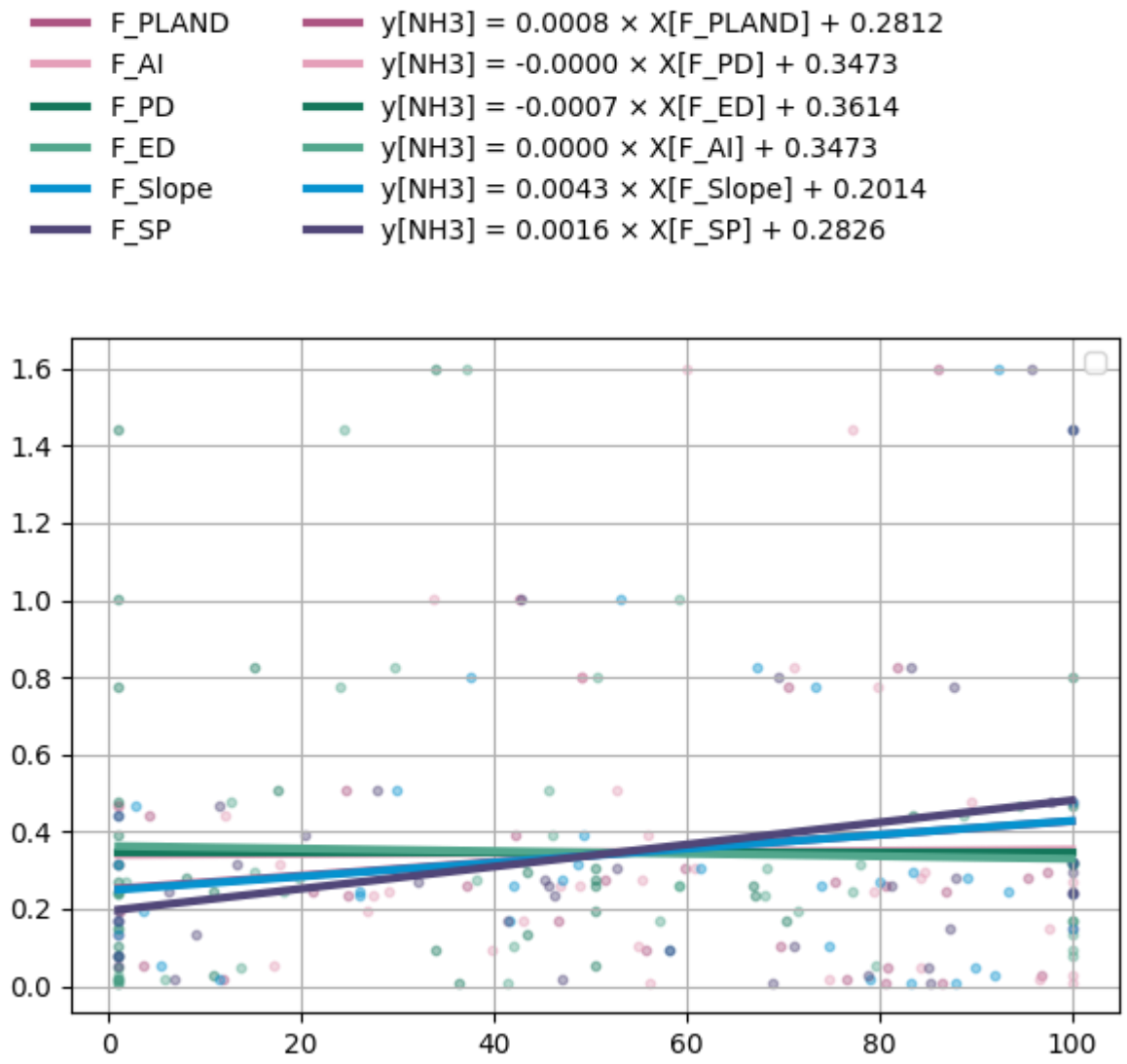

Figure 31 Regression Plot between NH_3 and Forest Metrics

All forest metrics exhibit near-zero slopes for NH_3, confirming no meaningful influence of forest structure on this pollutant. For example, F_PLAND (y = 0.0008X + 0.2812) shows a 10% increase in forest cover raises NH_3 by only 0.008 mg/L, a negligible effect. Similarly, fragmentation (F_PD, F_ED) and stream proximity (F_SP) yield flat slopes (y = -0.0000X + 0.3473 to y = 0.0016X + 0.2826), indicating external sources (e.g., sewage, livestock waste) dominate NH_3 concentrations. Baseline NH_3 levels (~0.28–0.36 mg/L) remain stable regardless of forest configuration, reinforcing that forest management alone cannot mitigate this pollutant.

Calcium (Ca^{2+})

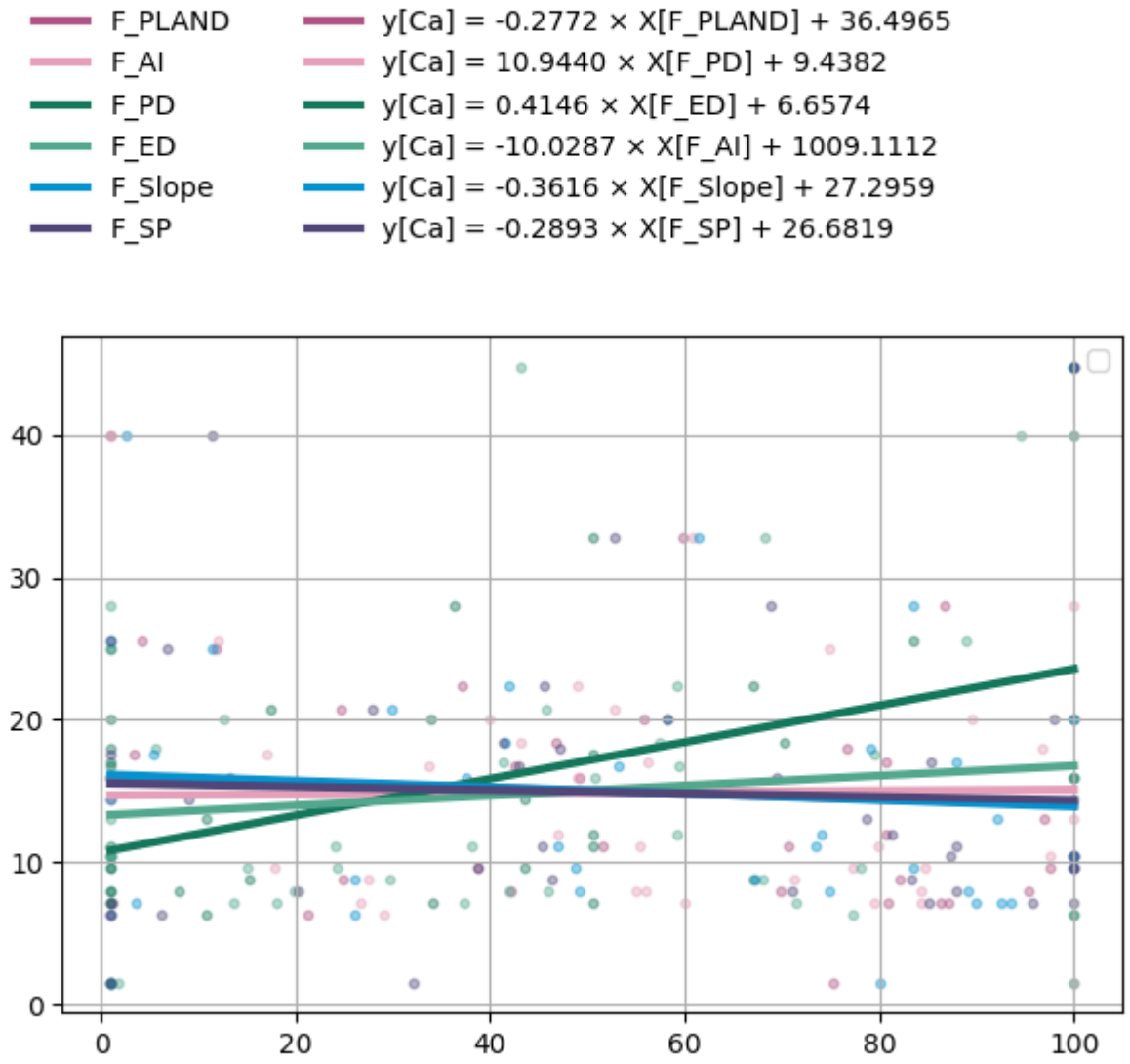

Figure 32 Regression Plot between Ca^{2+} and Forest Metrics

Forest metrics demonstrate robust regulation of Ca^{2+}, with F_PLAND and F_AI showing pronounced negative slopes. The equation y[Ca] = -0.2772X + 36.4965 indicates that a 10% increase in forest cover reduces calcium leaching by ~2.77 mg/L, likely due to soil stabilization. F_AI (aggregation) exhibits an even steeper slope (y = -10.03X + 1009.11), reflecting that contiguous forests reduce Ca^{2+} by ~10 mg/L per unit increase in aggregation. Conversely, fragmentation metrics (F_PD, F_ED) amplify Ca^{2+} leaching, with F_PD (y = 10.94X + 9.44) showing a 1-unit increase in patch density raises calcium by ~10.94 mg/L. Stream proximity (F_SP) further mitigates Ca^{2+} (y = -0.2893X + 26.68), underscoring riparian vegetation's role in filtering calcium. These results reinforce that preserving aggregated forests and riparian buffers, while limiting fragmentation, is key to reducing calcium pollution.

Phosphate (PO_4^{3-})

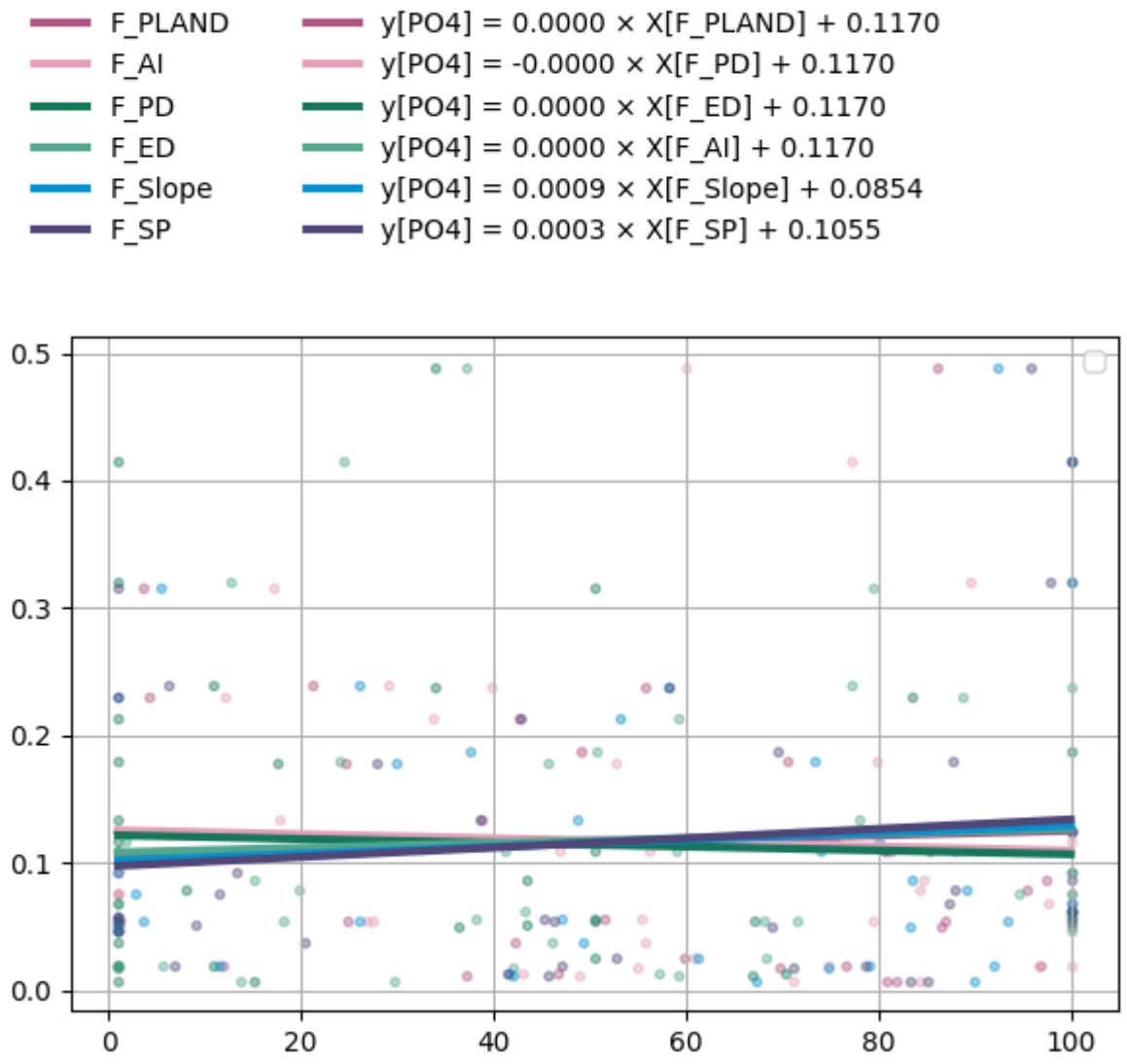

Figure 33 Regression Plot between PO_4^{3-} and Forest Metrics

All forest metrics exhibit near-zero slopes for PO_4^{3-}, indicating forests have no meaningful influence on phosphate levels. For instance, F_PLAND (y = 0.0000X + 0.1170) and F_PD (y = -0.0000X + 0.1170) show baseline PO_4^{3-} (~0.08–0.11 mg/L) remains stable regardless of forest structure. Similarly, F_Slope (y = 0.0009X + 0.0854) and F_SP (y = 0.0003X + 0.1055) yield negligible increases in phosphate with slope or stream proximity. These findings align with correlation results, confirming that external factors dominate phosphate concentrations, and forest management alone cannot mitigate this pollutant.

Total Suspended Solids (TSS)

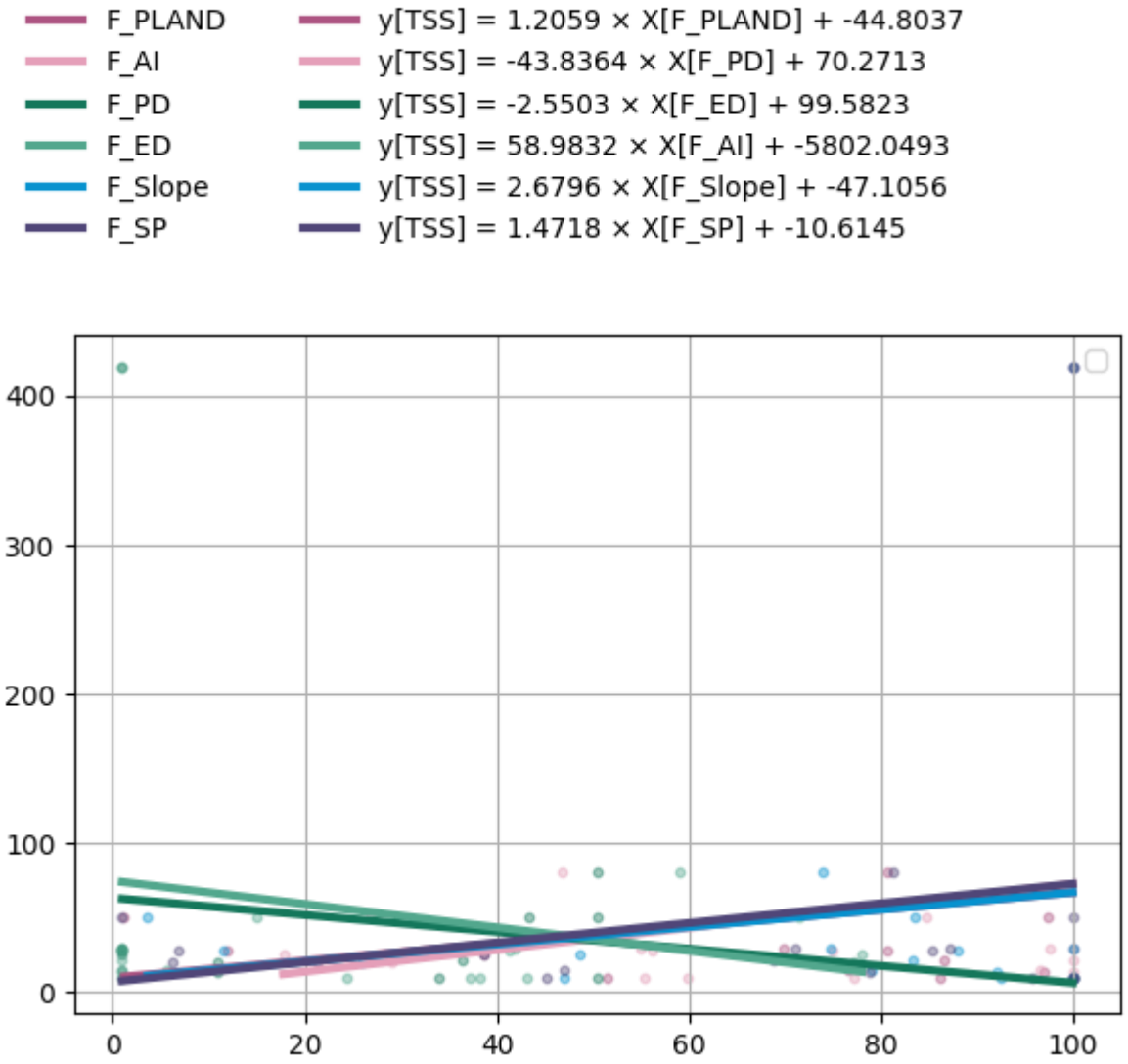

Figure 34 Regression Plot between TSS and Forest Metrics

Forest metrics exhibit dual roles in influencing TSS. F_PLAND shows a positive slope (y = 1.206X - 44.80), indicating higher forest cover marginally increases TSS by 1.2 mg/L per 1% increase, likely due to organic matter inputs (e.g., leaf litter). F_AI (aggregation) has a steep positive slope (y = 58.98X - 5802.05), suggesting contiguous forests elevate TSS significantly, reinforcing seasonal organic debris contributions. Conversely, fragmentation (F_PD) shows a strong negative slope (y = -43.84X + 70.27), implying fragmented forests reduce TSS. F_Slope exhibits a moderate positive slope (y = 2.68X - 47.11), indicating steep slopes in forests increase TSS (2.68 mg/L per unit slope) due to erosion, though the negative intercept (-47.11) suggests minimal impact at low slopes.

Rangeland

pH

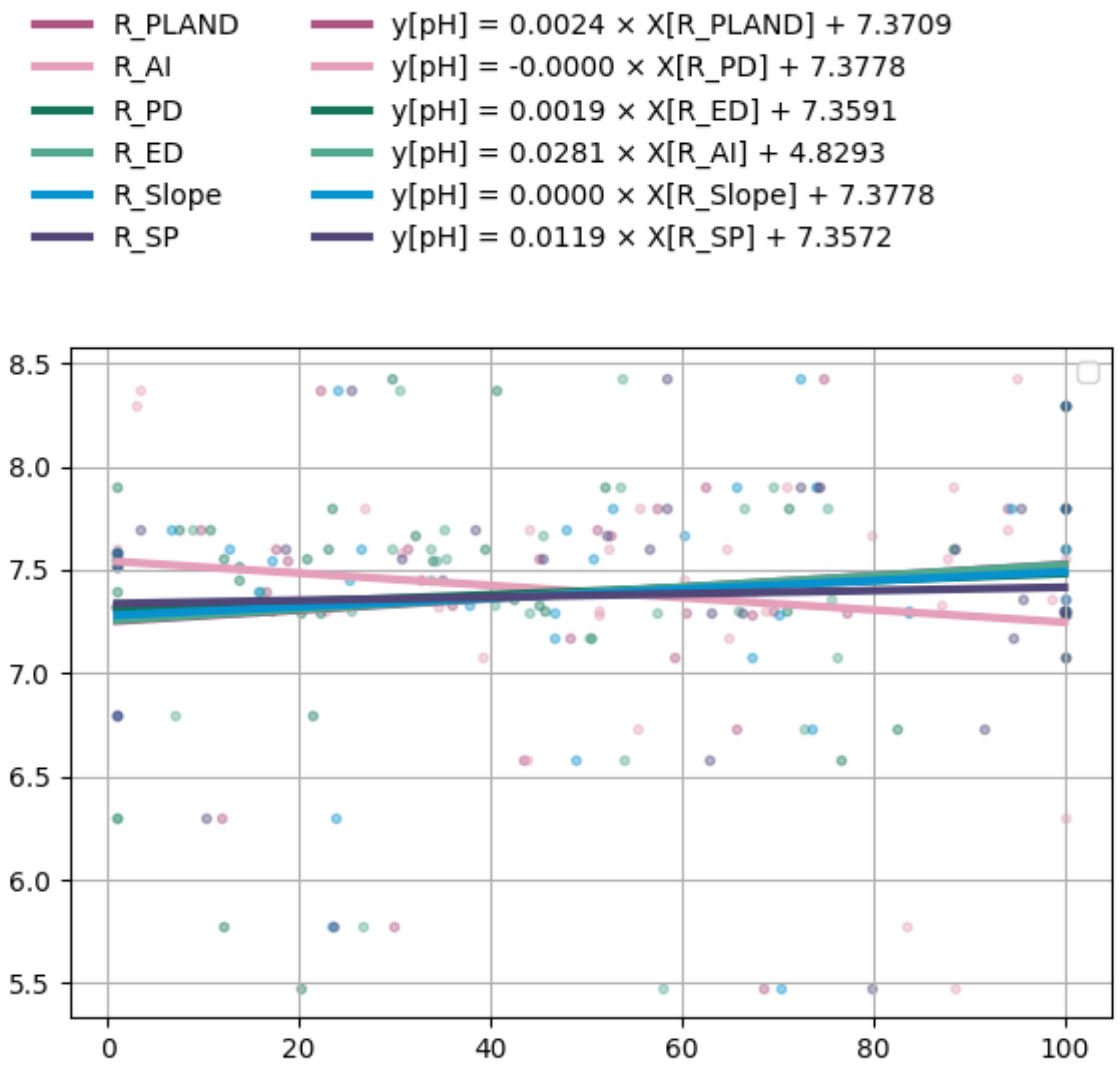

Figure 35 Regression Plot between pH and Rangeland Metrics

The regression equations for **pH** show negligible effects of rangeland metrics, with slopes close to zero across all variables. **R_PLAND** (rangeland cover) has a slope of 0.0024 (*y[pH] = 0.0024X + 7.3709*), indicating that a 10% increase in rangeland cover raises pH by only 0.024 units, a marginal effect. **Aggregation (R_AI)** exhibits a slightly steeper slope, suggesting contiguous rangelands may buffer acidity better than fragmented ones. However, **fragmentation metrics** (R_PD, R_ED) and **slope** show near-zero slopes, reinforcing that rangeland structure has minimal impact on pH. **Stream proximity (R_SP)** also has a weak positive slope (0.0119, *y = 0.0119X + 7.3572*), implying rangelands near streams provide slight buffering. These results align with correlation findings, underscoring that rangeland weakly influence pH compared to forests.

Electrical Conductivity (EC)

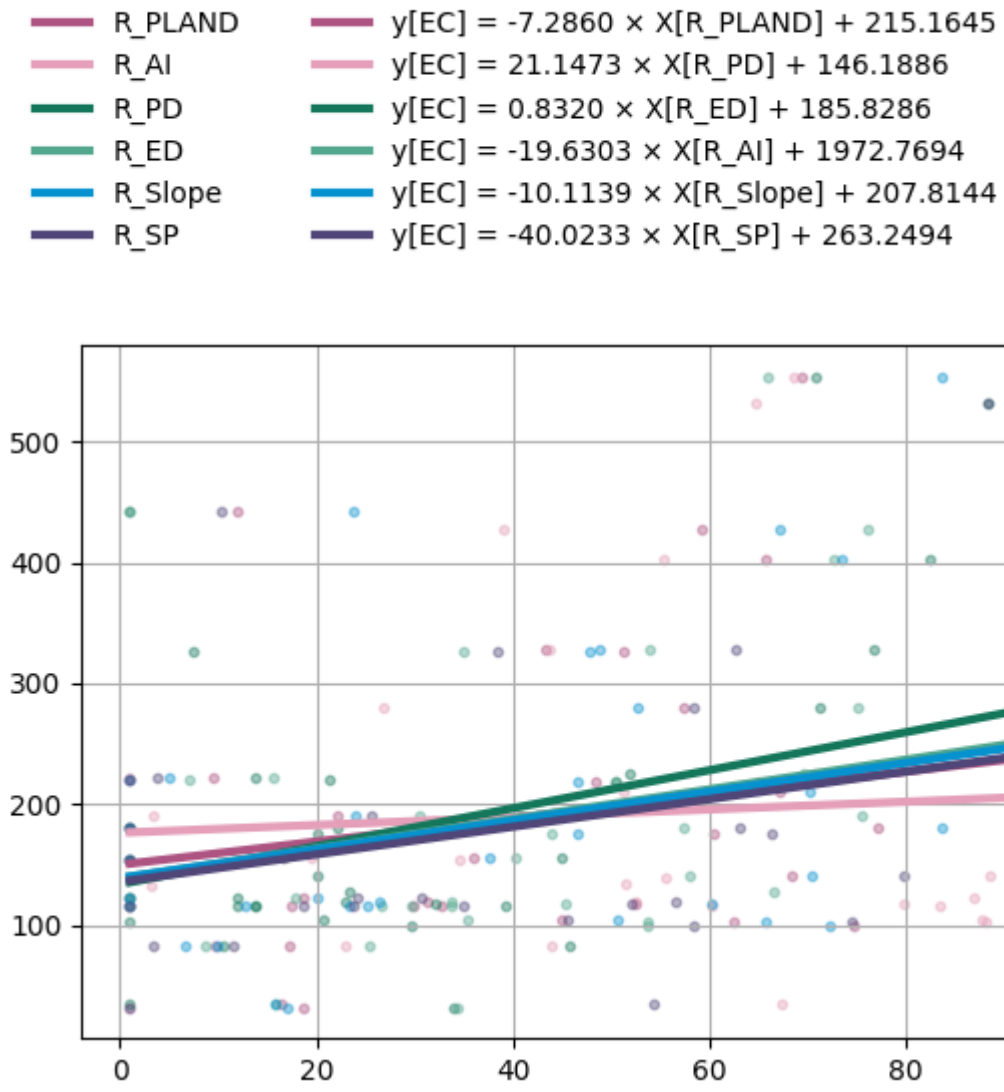

Figure 36 Regression Plot between EC and Rangeland Metrics

Rangeland metrics demonstrate robust regulation of **EC**, with **R_PLAND** and **R_AI** showing steep slopes. The equation for R_PLAND indicates that a 10% increase in rangeland cover reduces EC by ~73 µS/cm, likely due to vegetation stabilizing soils and filtering ions. **R_AI** (aggregation) exhibits an even steeper slope, showing that contiguous rangelands reduce EC by ~19.6 µS/cm per unit increase in aggregation. Conversely, **fragmentation (R_PD)** amplifies EC, indicating a 1-unit increase in patch density raises EC by 21.15 µS/cm. **Stream proximity (R_SP)** further mitigates EC, underscoring that rangeland near streams filter ions effectively. **Slope (R_Slope)** also shows a moderate negative slope, suggesting steeper gradients in rangelands may enhance infiltration and reduce runoff.

Nitrogen Ammonia (NH_3)

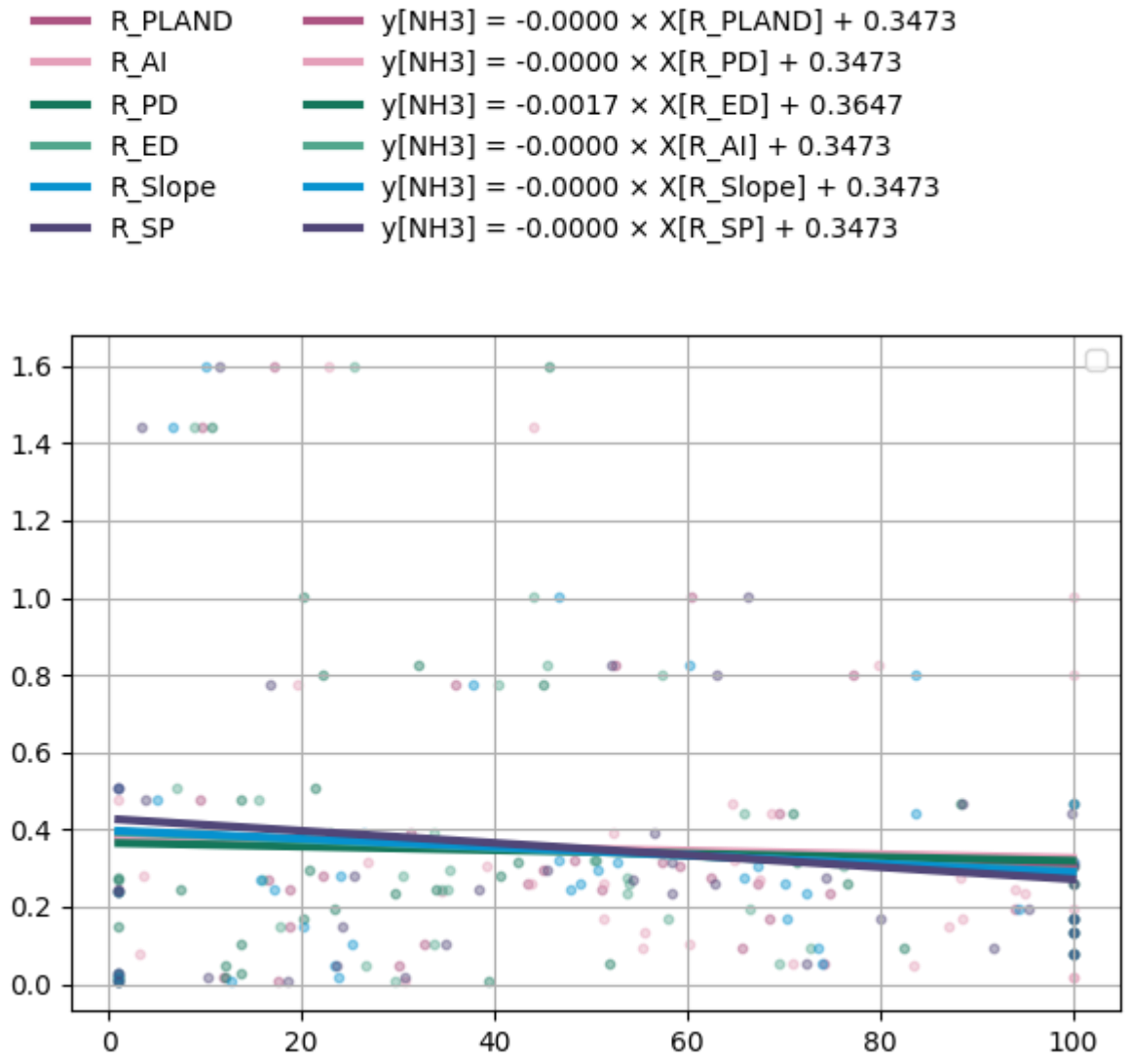

*Figure 37 Regression Plot between **NH_3** and Rangeland Metrics*

All rangeland metrics exhibit near-zero slopes for **NH_3**, confirming no meaningful influence of rangeland structure on this pollutant. For example, **R_PLAND** (*y = -0.0000X + 0.3473*) and **R_SP** (*y = -0.0000X + 0.3473*) show baseline NH_3 levels (~0.35 mg/L) remain stable regardless of rangeland configuration. Similarly, **fragmentation metrics** (R_PD, R_ED) and **slope** yield flat slopes, reinforcing that external factor (e.g., livestock waste, agricultural runoff) dominate NH_3 concentrations. These findings align with correlation results, emphasizing that rangeland management alone cannot mitigate NH_3 pollution.

Calcium (Ca^{2+})

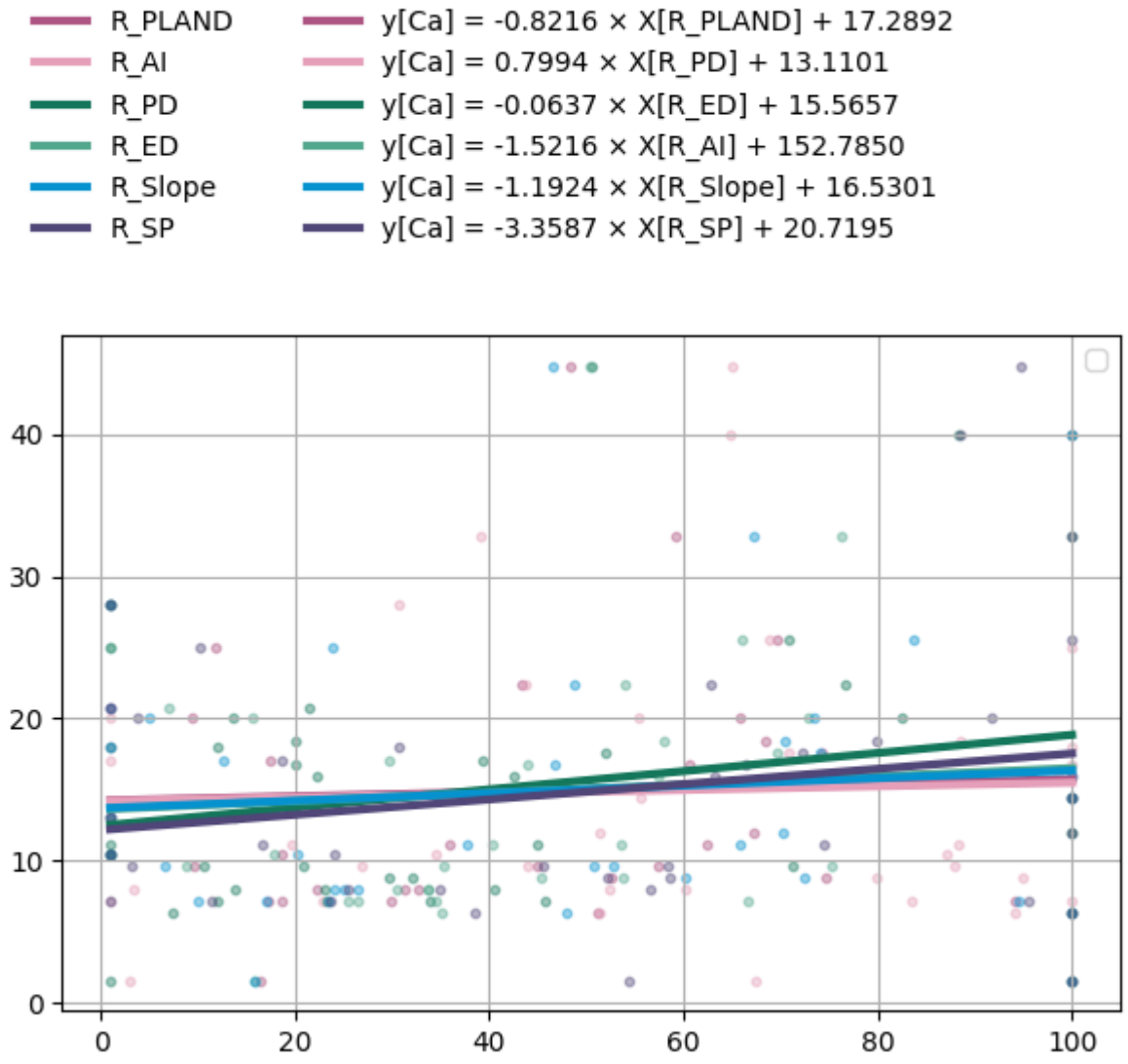

*Figure 38 Regression Plot between **Ca^{2+}** and Rangeland Metrics*

Rangeland metrics demonstrate strong regulation of **Ca^{2+}**, with **R_PLAND** and **R_AI**. The equation for R_PLAND indicates that a 10% increase in rangeland cover reduces calcium leaching by ~8.2 mg/L, likely due to soil stabilization. **R_AI** exhibits an even steeper regression slope, showing that contiguous rangelands reduce Ca^{2+} by ~1.5 mg/L per unit increase in aggregation. **Stream proximity** further mitigates Ca^{2+}, underscoring riparian vegetation's role in filtering calcium. Conversely, **fragmentation (R_PD)** amplifies leaching, with *y = 0.7994X + 13.11* indicating a 1-unit increase in patch density raises calcium by ~0.8 mg/L. **R_Slope** also shows a moderate negative slope, suggesting steeper gradients in rangelands may enhance infiltration and reduce runoff. These results reinforce that preserving aggregated rangelands and riparian buffers, while limiting fragmentation, is key to reducing calcium pollution.

Phosphate (PO_4^{3-})

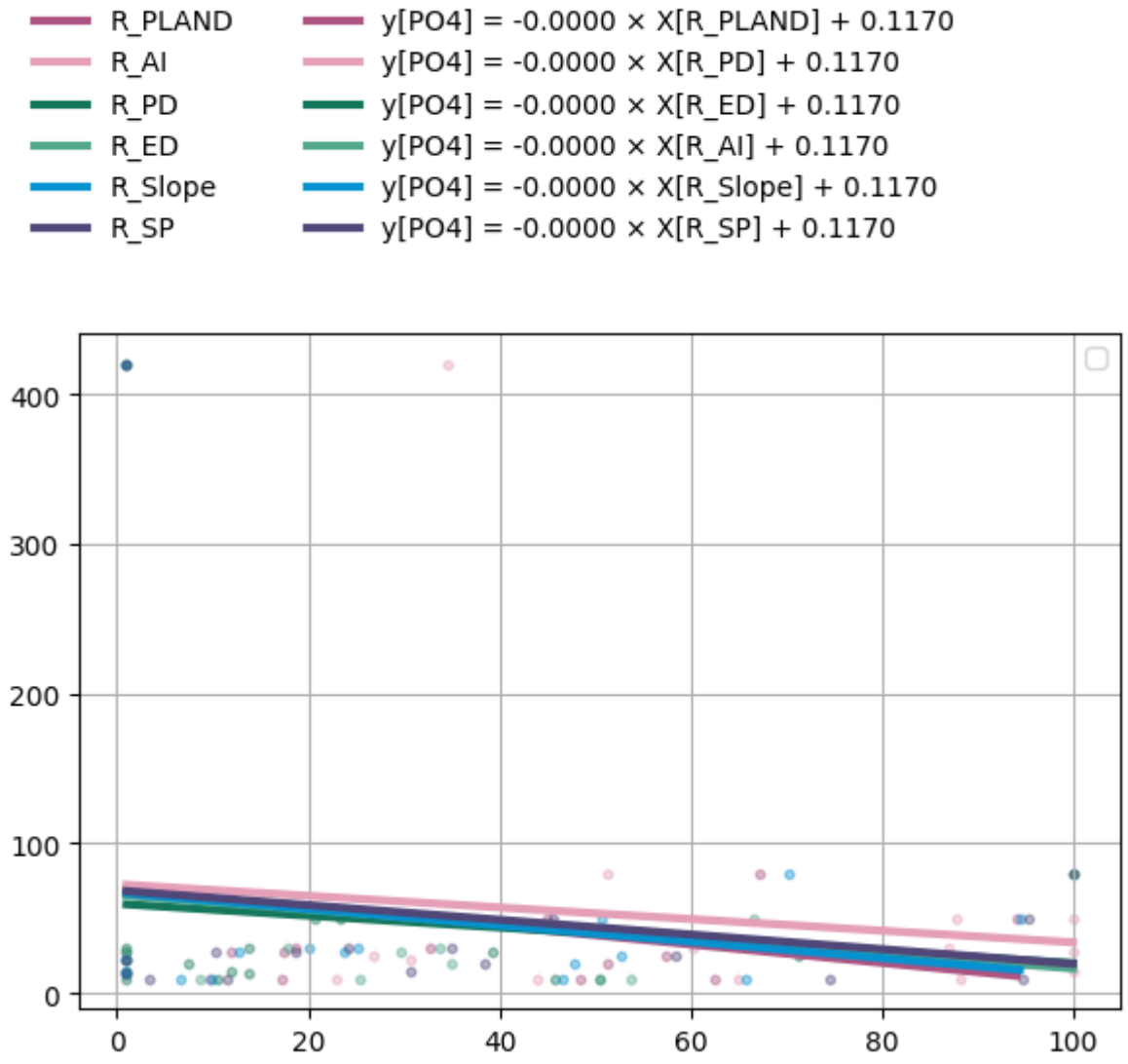

*Figure 39 Regression Plot between **PO_4^{3-}** and Rangeland Metrics*

All rangeland metrics exhibit near-zero slopes for **PO_4^{3-}**, indicating rangelands have no meaningful influence on phosphate levels. For instance, **R_PLAND** (*y = -0.0000X + 0.1170*) and **R_SP** (*y = -0.0000X + 0.1170*) show baseline PO_4^{3-} (~0.12 mg/L) remains stable regardless of rangeland structure. Similarly, **aggregation (R_AI)** and **slope (R_Slope)** yield flat slopes, confirming that external factors (e.g., fertilizers, sewage) dominate phosphate concentrations. These findings align with correlation results, emphasizing that rangeland management alone cannot mitigate this pollutant.

Total Suspended Solids (TSS)

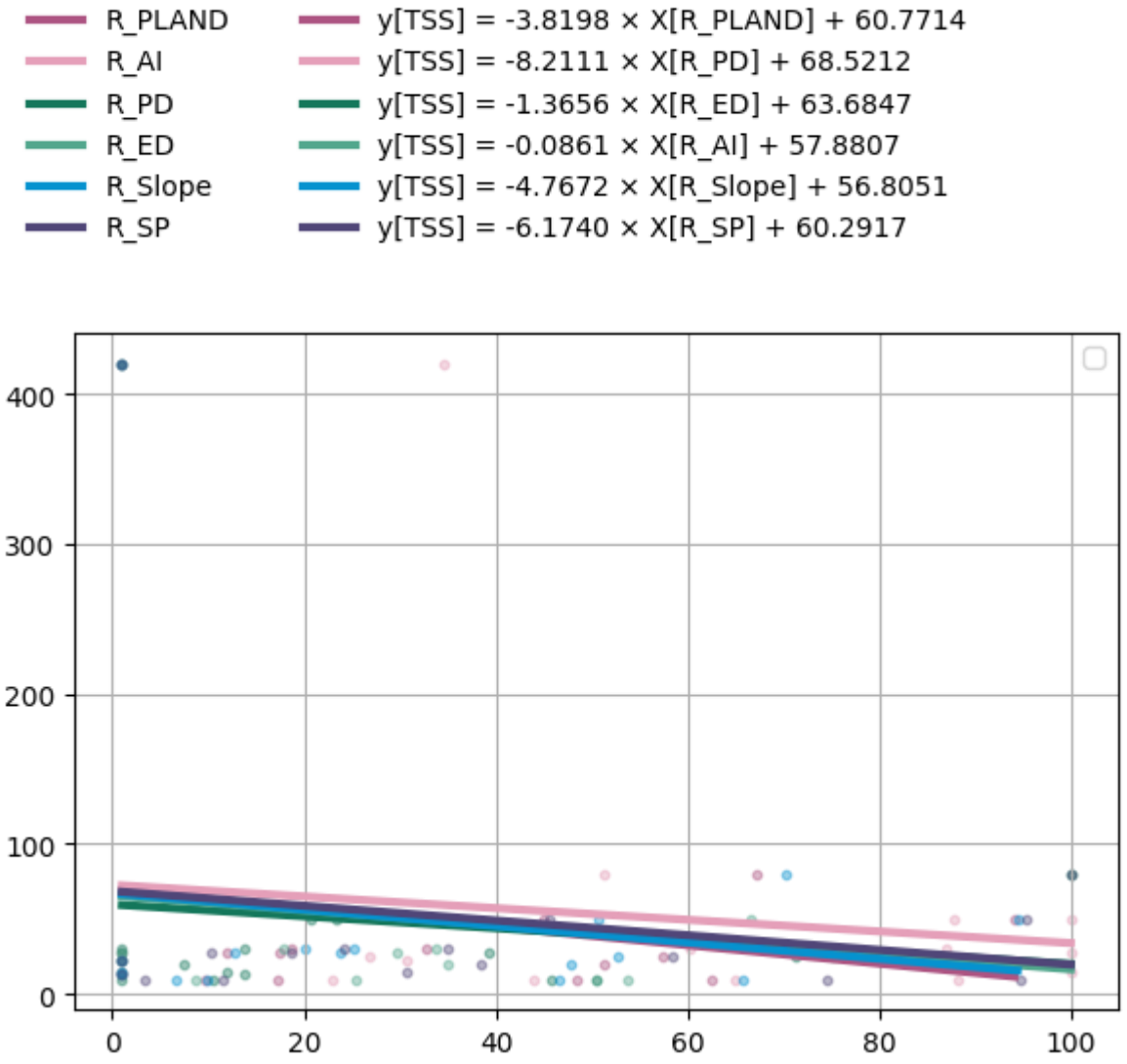

Figure 40 Regression Plot between TSS and Rangeland Metrics

Rangeland metrics exhibit strong negative slopes for **TSS**, indicating vegetation cover and fragmentation reduce particulate pollution. **R_PLAND** has a slope of -3.82, meaning a 10% increase in rangeland cover reduces TSS by ~38 mg/L, likely due to vegetation trapping sediment. **Fragmentation (R_PD)** shows an even steeper slope, indicating fragmented patches reduce TSS by ~82 mg/L per unit increase in patch density. **Stream proximity (R_SP)** also exhibits a strong negative slope, underscoring that rangeland near streams filter TSS effectively. **Slope (R_Slope)** shows a moderate negative slope, suggesting steeper gradients in rangelands may enhance sediment trapping via vegetation. **Aggregation (R_AI)** has a minimal negative slope , implying contiguous rangelands provide slight benefits. These results highlight that rangelands, particularly fragmented patches and steep slopes, effectively reduce TSS through vegetation cover and sediment trapping.

Built-up
pH

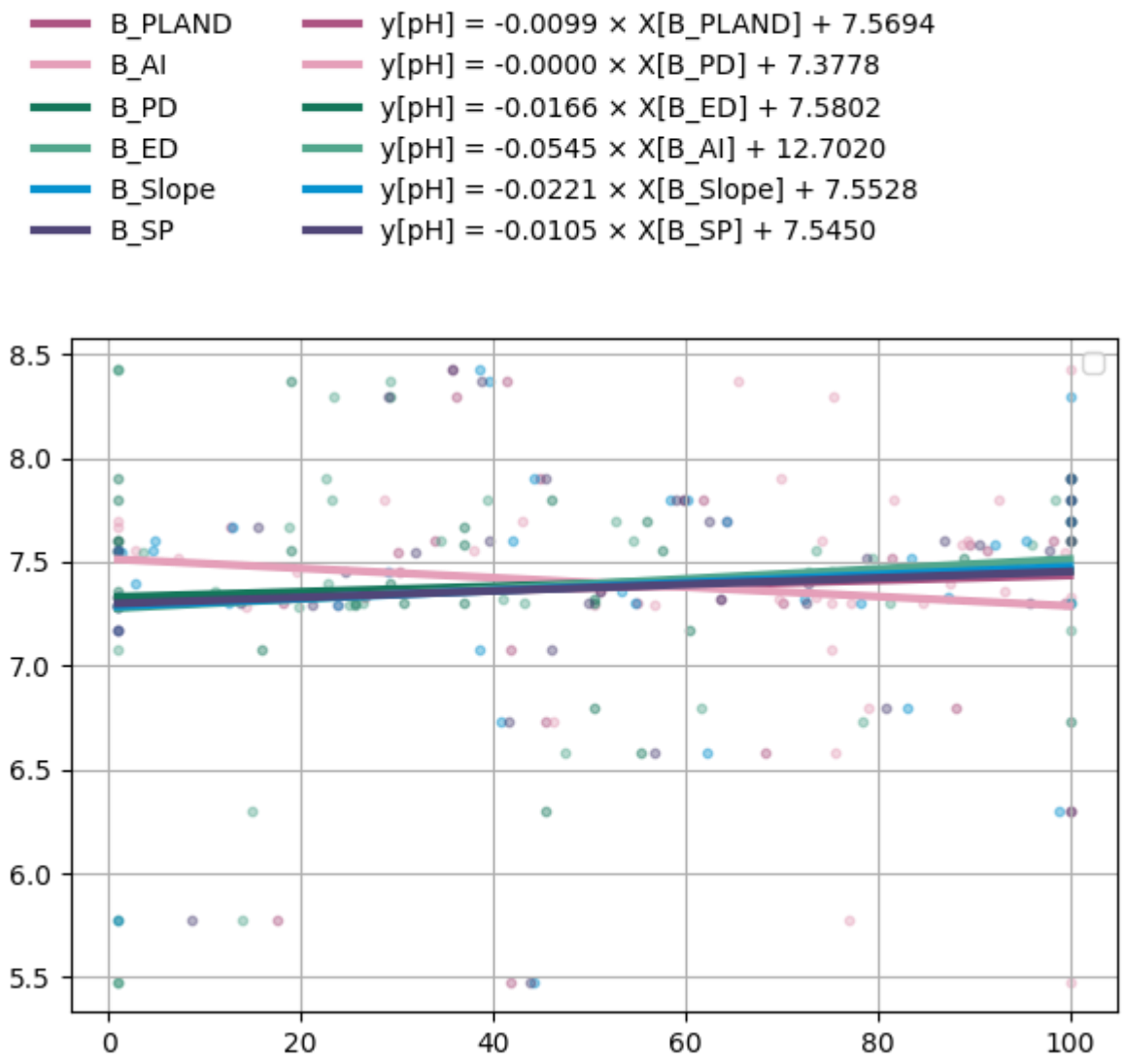

Figure 41 Regression Plot between pH and Built-up Metrics

Built-up metrics exhibit consistent negative slopes for **pH**, indicating urbanization acidifies streams. **B_PLAND** (built-up cover) has a slope of -0.0099, meaning a 10% increase in urban cover lowers pH by ~0.099 units, likely due to acid rain, vehicular emissions, and industrial effluents. **Edge density**shows a steeper, suggesting urban edges (e.g., roads) amplify acidity through localized pollutant deposition. **Aggregation (B_AI)** exhibits the strongest negative slope, indicating contiguous urban areas intensify acidification via concentrated runoff. **Slope (B_Slope)** and **stream proximity (B_SP)** also show negative slopes (-0.0221 and -0.0105, respectively), reinforcing that steep gradients and stream-adjacent development exacerbate acidity. These results highlight urban acidification as a critical issue requiring targeted pollution control.

Electrical Conductivity (EC)

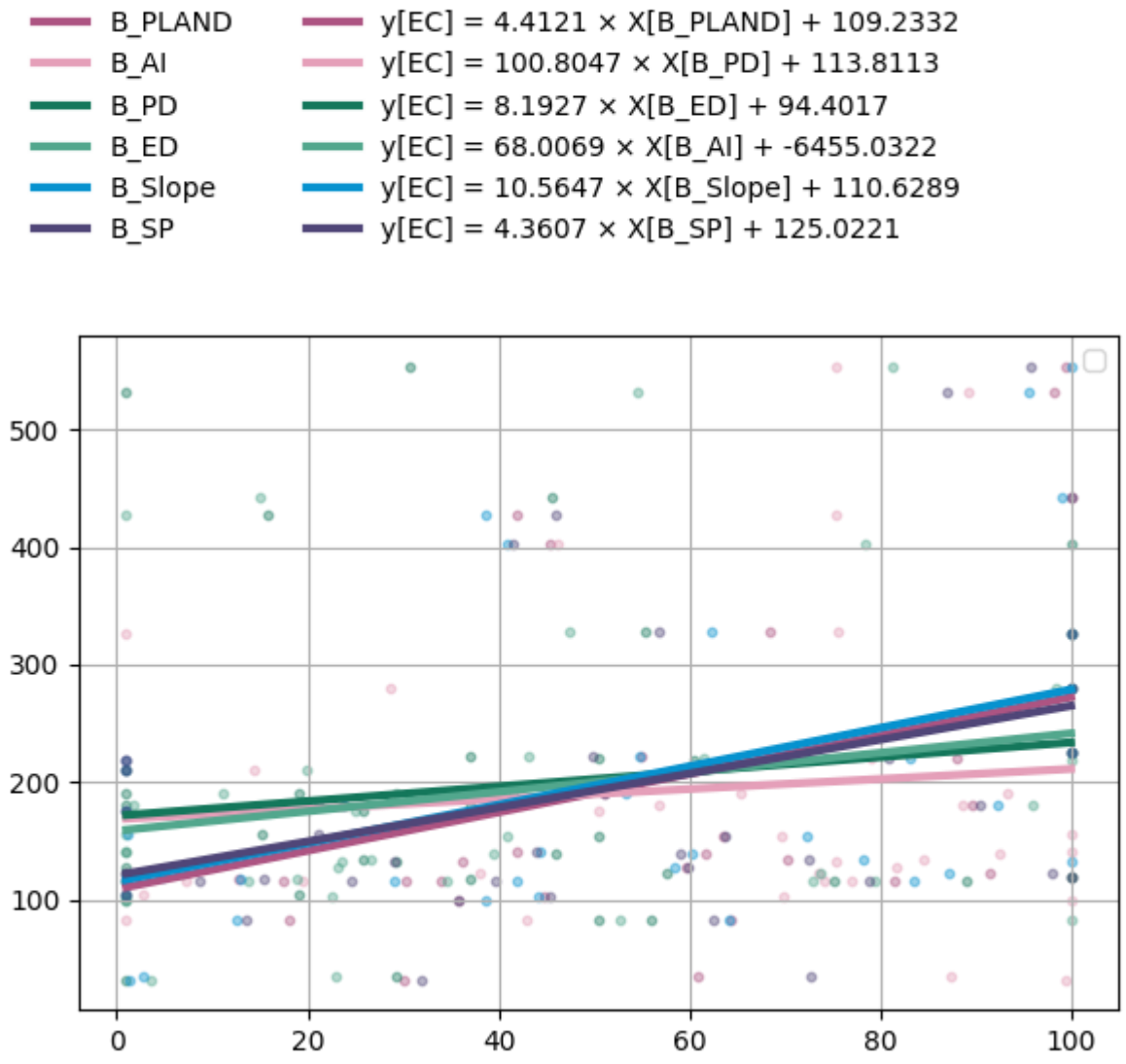

Figure 42 Regression Plot between EC and Built-up Metrics

Built-up metrics strongly regulate **EC**, with **B_PLAND** and **B_AI** showing steep positive slopes. The equation *y[EC] = 4.4121X + 109.23* for B_PLAND indicates that a 10% increase in urban cover raises EC by ~44 µS/cm, likely due to impervious surfaces (e.g., concrete, asphalt) leaching ions. **B_AI** exhibits an even steeper slope, showing contiguous urban areas amplify EC by ~68 µS/cm per unit aggregation, reflecting concentrated runoff from infrastructure. **Fragmentation (B_PD)** and **edge density** also amplify EC, with slopes of 100.80 and 8.19 , respectively, underscoring that fragmented development and edge zones exacerbate ionic pollution. **Slope (B_Slope)** shows the strongest relationship, indicating steep urban gradients increase EC by ~10.56 µS/cm per unit slope due to accelerated runoff. These findings emphasize that urban sprawl, fragmentation, and steep slopes are primary drivers of ionic pollution.

Nitrogen Ammonia (NH_3)

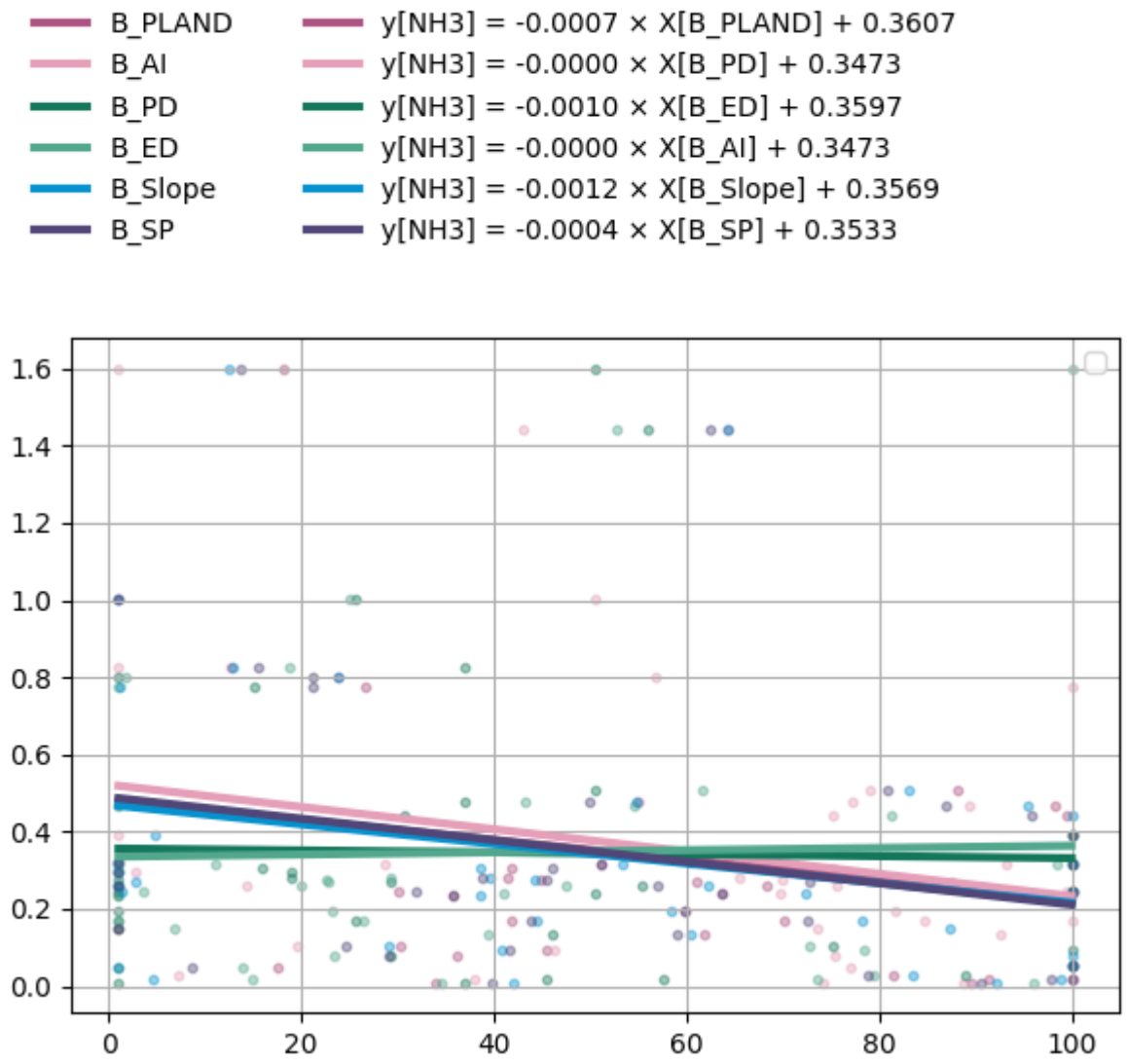

Figure 43 Regression Plot between NH_3 and Built-up Metrics

All built-up metrics exhibit near-zero slopes for **NH_3**, confirming urban structure has minimal influence. For example, **B_PLAND** (*y = -0.0007X + 0.3607*) and **B_AI** (*y = -0.0000X + 0.3473*) show baseline NH_3 levels (~0.35 mg/L) remain stable regardless of urban configuration. Similarly, **fragmentation (B_PD)** and **slope (B_Slope)** yield flat slopes, reinforcing that external source (e.g., sewage, livestock waste) dominate NH_3 concentrations. These results align with correlation findings, underscoring that built-up landscape management alone cannot mitigate this pollutant.

Calcium (Ca^{2+})

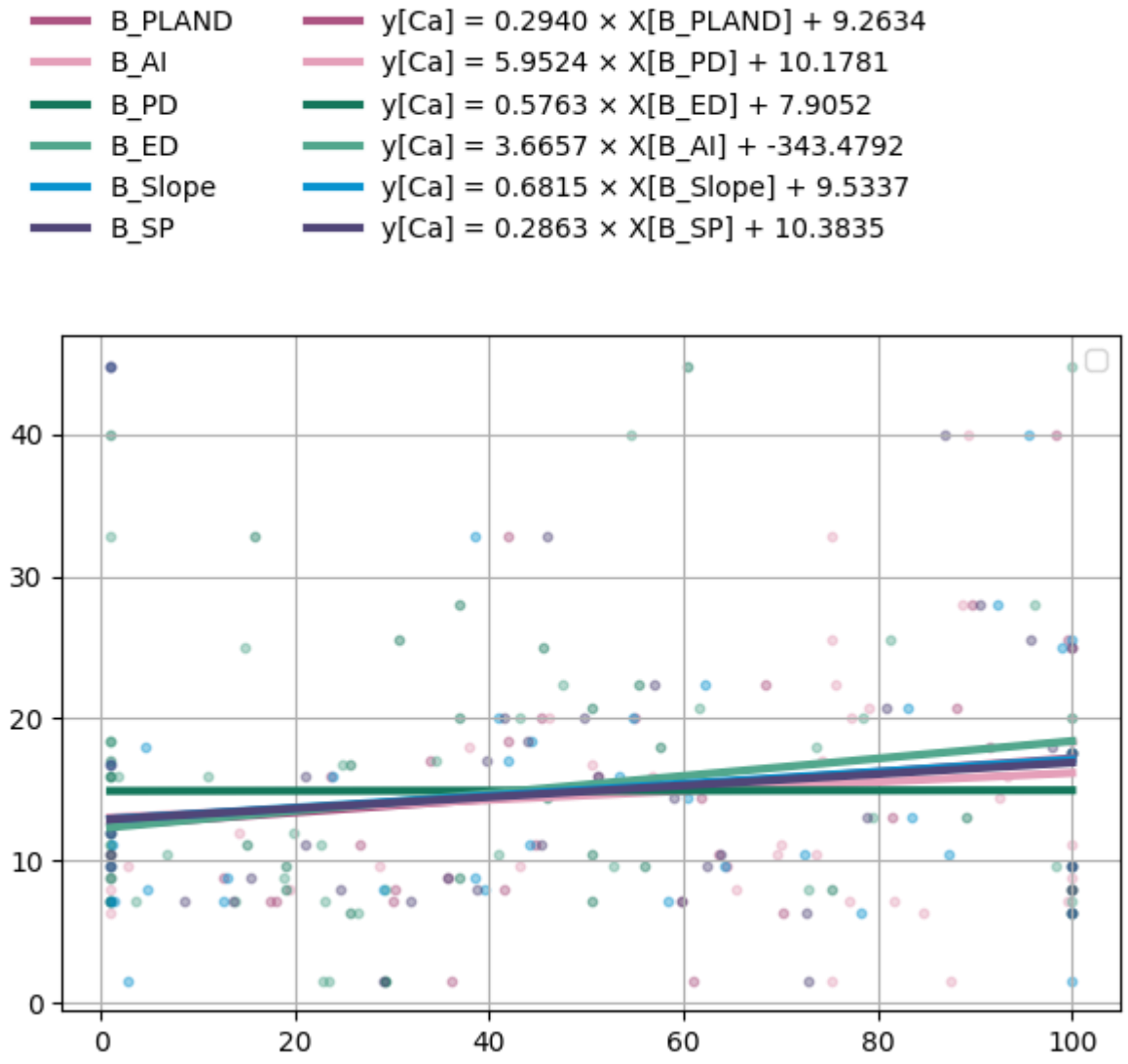

*Figure 44 Regression Plot between **Ca^{2}** and Built-up Metrics*

Built-up metrics demonstrate strong positive regulation of **Ca^{2+}**, with **B_PLAND** and **B_AI** showing pronounced slopes. The equation *y[Ca] = 0.2940X + 9.2634* indicates a 10% increase in urban cover raises calcium leaching by ~2.9 mg/L, likely due to concrete degradation and road dust. **B_AI** (aggregation) exhibits a steeper slope, showing contiguous urban areas increase Ca^{2+} by ~3.67 mg/L per unit aggregation. **B_Slope** also shows a moderate positive slope, suggesting steep gradients in urban areas enhance calcium runoff via erosion. **Stream proximity (B_SP)** has a weak positive slope , indicating stream-adjacent urban development marginally increases calcium inputs. These results highlight that urban cover, aggregation, and steep slopes are critical drivers of calcium pollution.

Phosphate (PO_4^{3-})

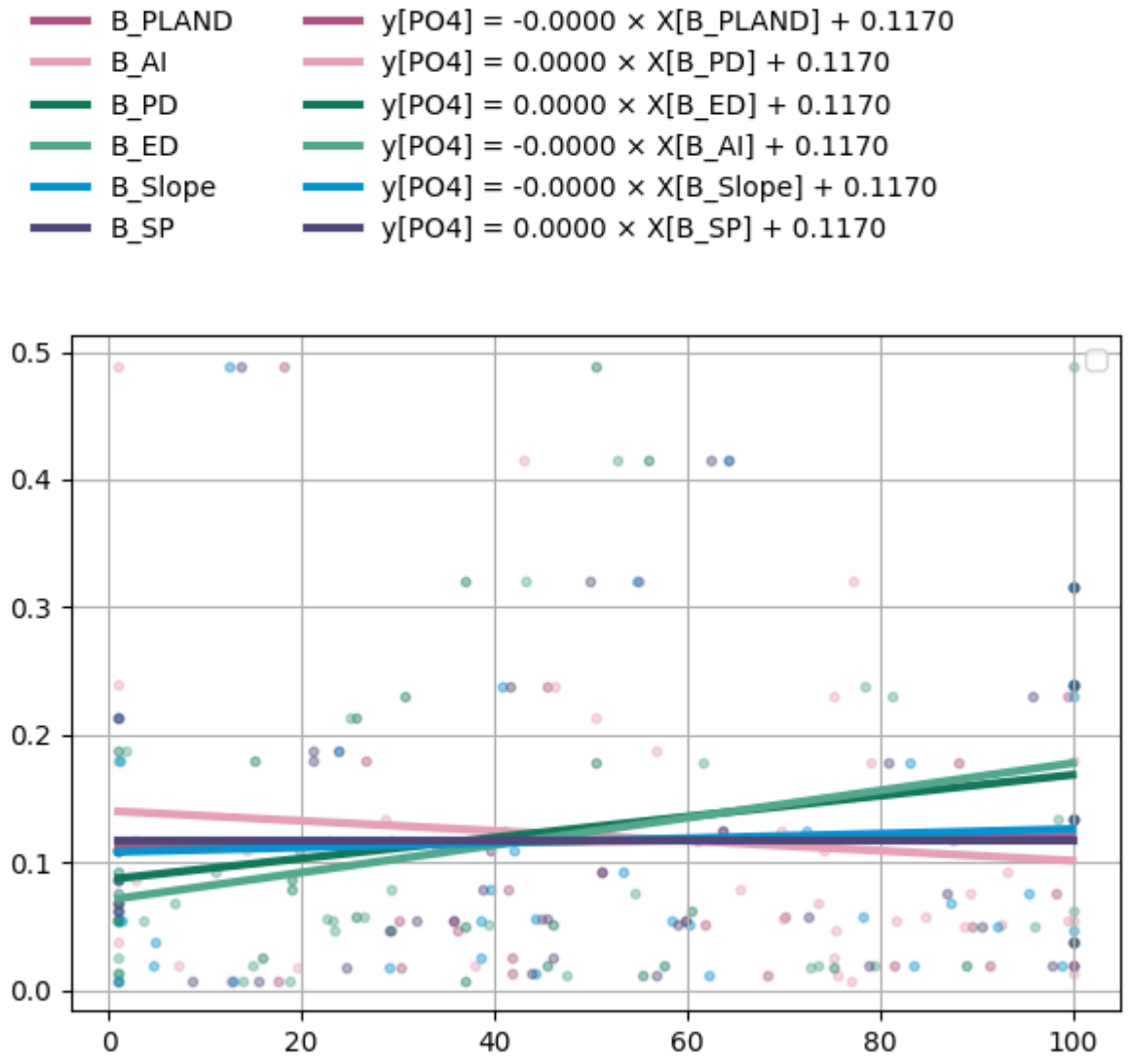

*Figure 45 Regression Plot between **PO_4^{3-}** and Built-up Metrics*

All built-up metrics exhibit near-zero slopes for **PO_4^{3-}**, indicating urban structure has no meaningful impact on phosphate levels. For instance, **B_PLAND** (*y = -0.0000X + 0.1170*) and **B_AI** (*y = -0.0000X + 0.1170*) show baseline PO_4^{3-} (~0.12 mg/L) remains stable regardless of urban configuration. Similarly, **fragmentation (B_PD)** and **slope (B_Slope)** yield flat slopes, reinforcing that external factors (e.g., fertilizers, sewage) dominate phosphate concentrations. These findings align with correlation results, emphasizing that built-up landscape management alone cannot address this pollutant.

Total Suspended Solids (TSS)

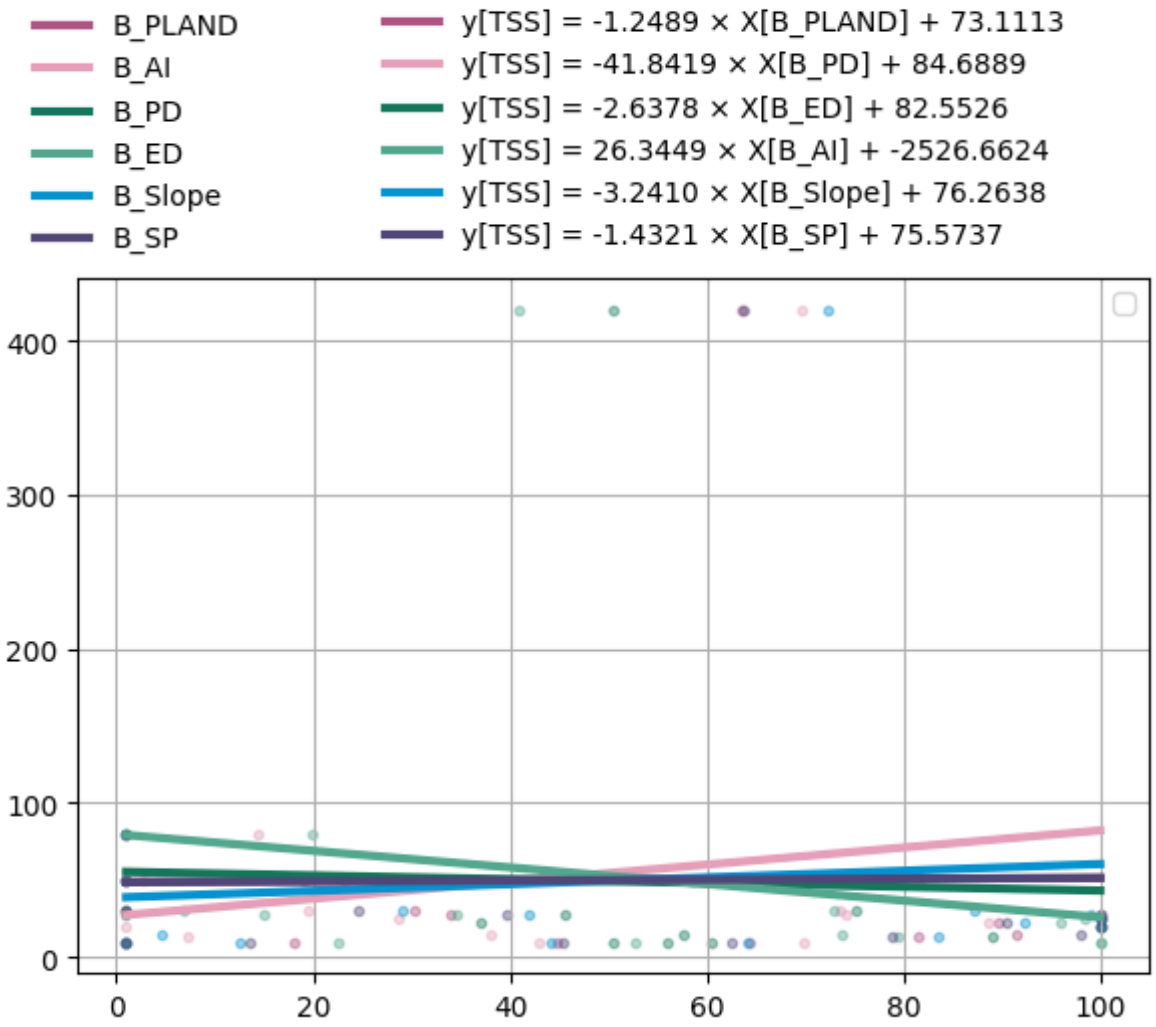

Figure 46 Regression Plot between TSS and Built-up Metrics

Built-up metrics exhibit mixed effects on **TSS**. **B_PLAND** shows a negative slope (-1.25, *y = -1.2489X + 73.11*), suggesting higher urban cover reduces TSS by ~12.5 mg/L per 10% increase, likely due to paved surfaces limiting sediment input. **Fragmentation (B_PD)** has a steep negative slope (-41.84, *y = -41.84X + 84.69*), indicating fragmented urban patches trap particulates via edge-zone vegetation. **Stream proximity (B_SP)** also shows a weak negative slope (-1.43, *y = -1.43X + 75.57*), underscoring that urban development near streams reduces TSS via localized filtering. However, **aggregation (B_AI)** exhibits a positive slope (26.34, *y = 26.34X - 2526.66*), implying contiguous urban areas may increase organic particulates seasonally. **Slope (B_Slope)** shows a moderate negative slope (-3.24, *y = -3.24X + 76.26*), suggesting steep gradients in urban areas enhance sediment retention. These results highlight that urban cover and fragmentation reduce TSS, while aggregated areas introduce seasonal particulates.

Landscape

pH

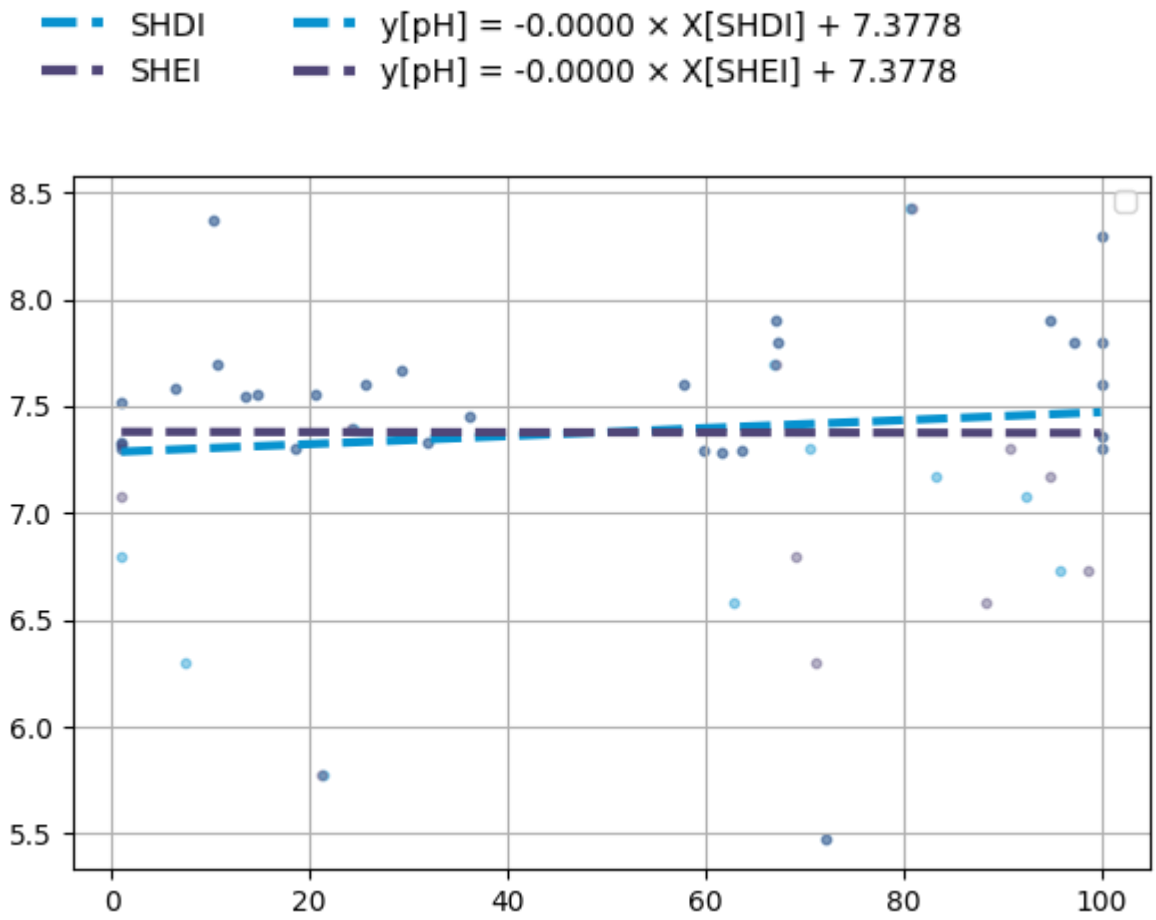

Figure 47 Regression Plot between pH and Landscape Level Metrics

Both **Shannon's Diversity Index (SHDI)** and **Shannon's Evenness Index (SHEI)** show near-zero slopes for **pH**, indicating that landscape diversity and evenness have negligible effects on acidity. The equations *y[pH] = -0.0000X + 7.3778* for SHDI and *y[pH] = -0.0000X + 7.3778* for SHEI confirm that evenness and diversity do not alter baseline pH (~7.38 units) across mixed landscapes. These results align with previous findings for individual land-use types, reinforcing that pH is weakly influenced by landscape configuration and more sensitive to localized factors (e.g., vegetation buffering in forests or acidification in built-up areas).

Electrical Conductivity (EC)

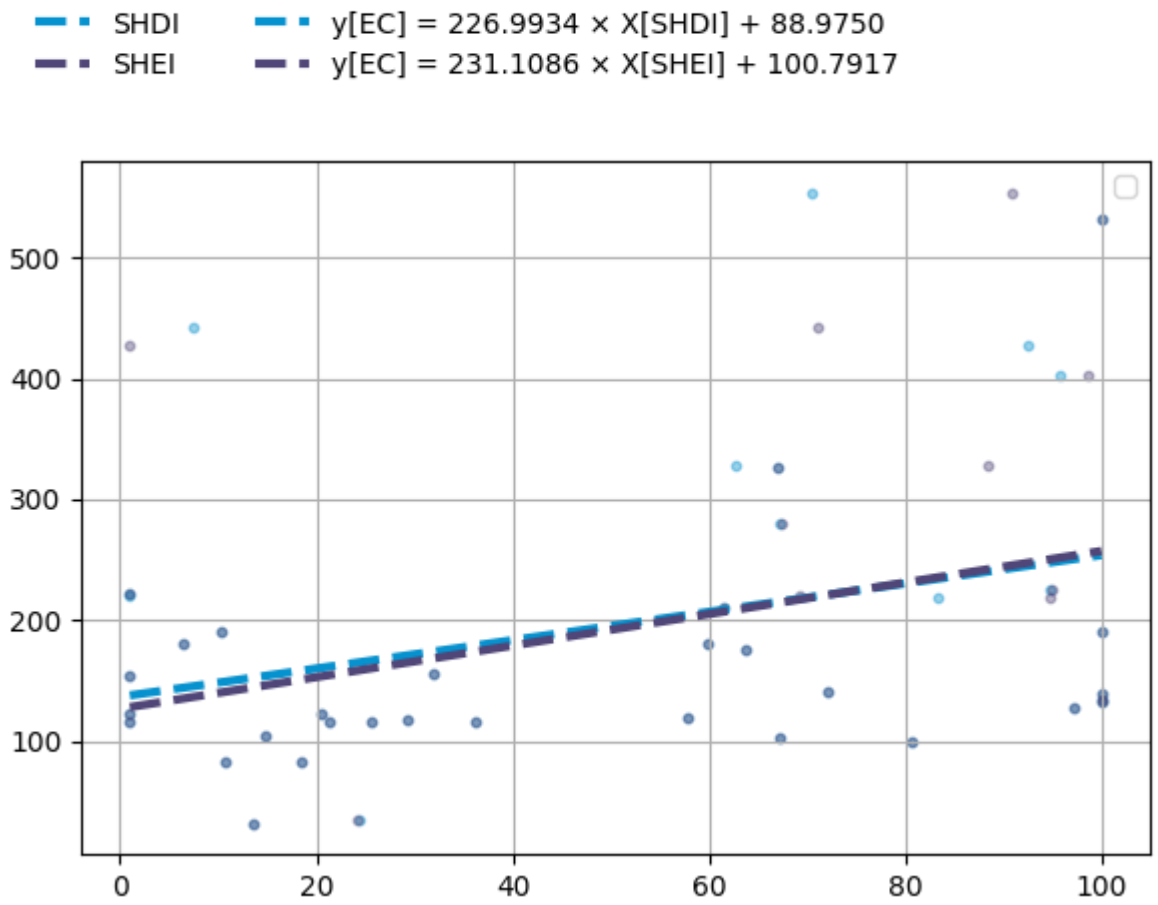

Figure 48 Regression Plot between EC and Landscape Level Metrics

Landscape diversity (SHDI) and evenness (SHEI) strongly correlate with **EC**, with steep positive slopes indicating that more heterogeneous landscapes increase ionic pollution. The equation *y[EC] = 226.99X + 88.98* for SHDI suggests that a 1-unit increase in diversity raises EC by ~227 µS/cm, likely due to mixed land-use types (e.g., urban patches, fragmented forests) introducing impervious surfaces and runoff. **SHEI** shows a similar trend (*y = 231.11X + 100.79*), with evenness amplifying EC by ~231 µS/cm per unit increase. This underscores that landscapes with balanced land-use distributions (e.g., evenly mixed urban, agricultural, and natural areas) exacerbate ionic inputs, likely due to cumulative runoff from multiple sources.

Nitrogen Ammonia (NH_3)

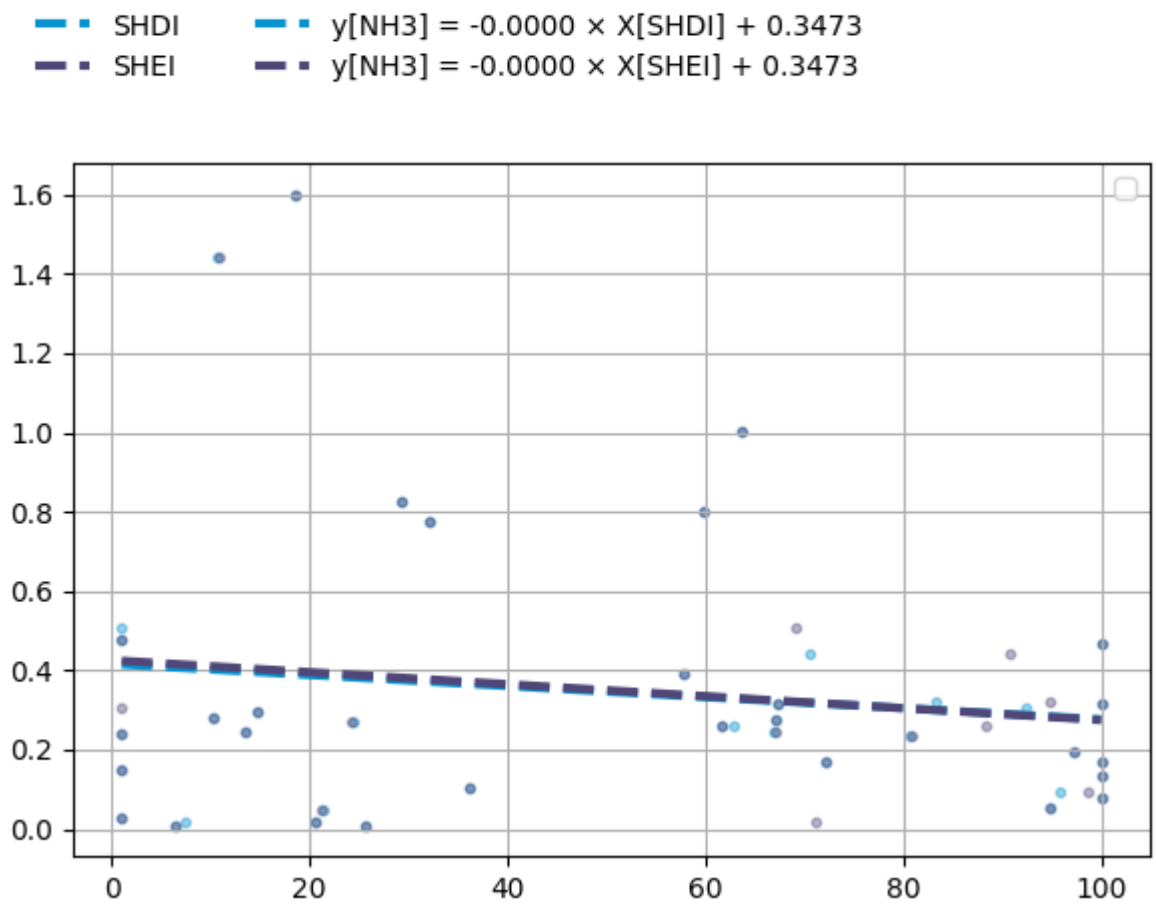

Figure 49 Regression Plot between NH_3 and Landscape Level Metrics

Both **SHDI** and **SHEI** exhibit near-zero slopes for **NH_3**, confirming that landscape diversity and evenness have no meaningful influence on ammonia concentrations. Baseline NH_3 levels (~0.35 mg/L) remain stable regardless of landscape configuration, aligning with previous findings for individual land-use types. This reinforces that NH_3 is dominated by external sources (e.g., sewage, livestock waste) and requires pollution control measures beyond landscape management.

Calcium (Ca^{2+})

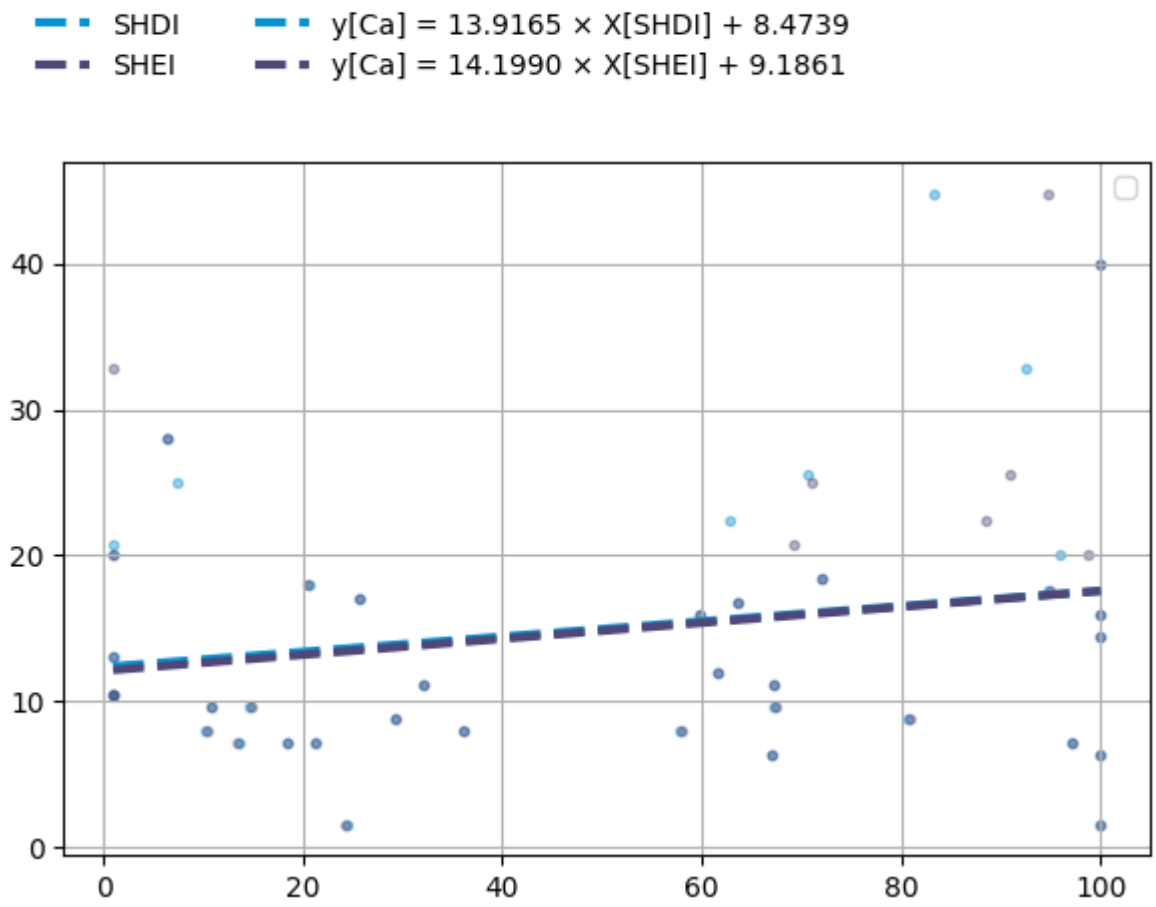

*Figure 50 Regression Plot between **Ca^{2+}** and Landscape Level Metrics*

Landscape diversity (SHDI) and evenness (SHEI) show strong positive slopes for **Ca^{2+}**, indicating that heterogeneous landscapes amplify calcium leaching. The equation *y[Ca] = 13.92X + 8.47* for SHDI suggests a 1-unit increase in diversity raises Ca^{2+} by ~13.9 mg/L, likely due to mixed land-use types (e.g., built-up areas, fragmented forests) introducing calcium-rich pollutants (e.g., concrete, road dust). **SHEI** exhibits a similar trend (*y = 14.20X + 9.19*), showing that evenly distributed land-use types increase Ca^{2+} by ~14.2 mg/L per unit evenness. These results highlight that diverse, fragmented landscapes exacerbate calcium pollution more than homogeneous land uses.

Phosphate (PO_4^{3-})

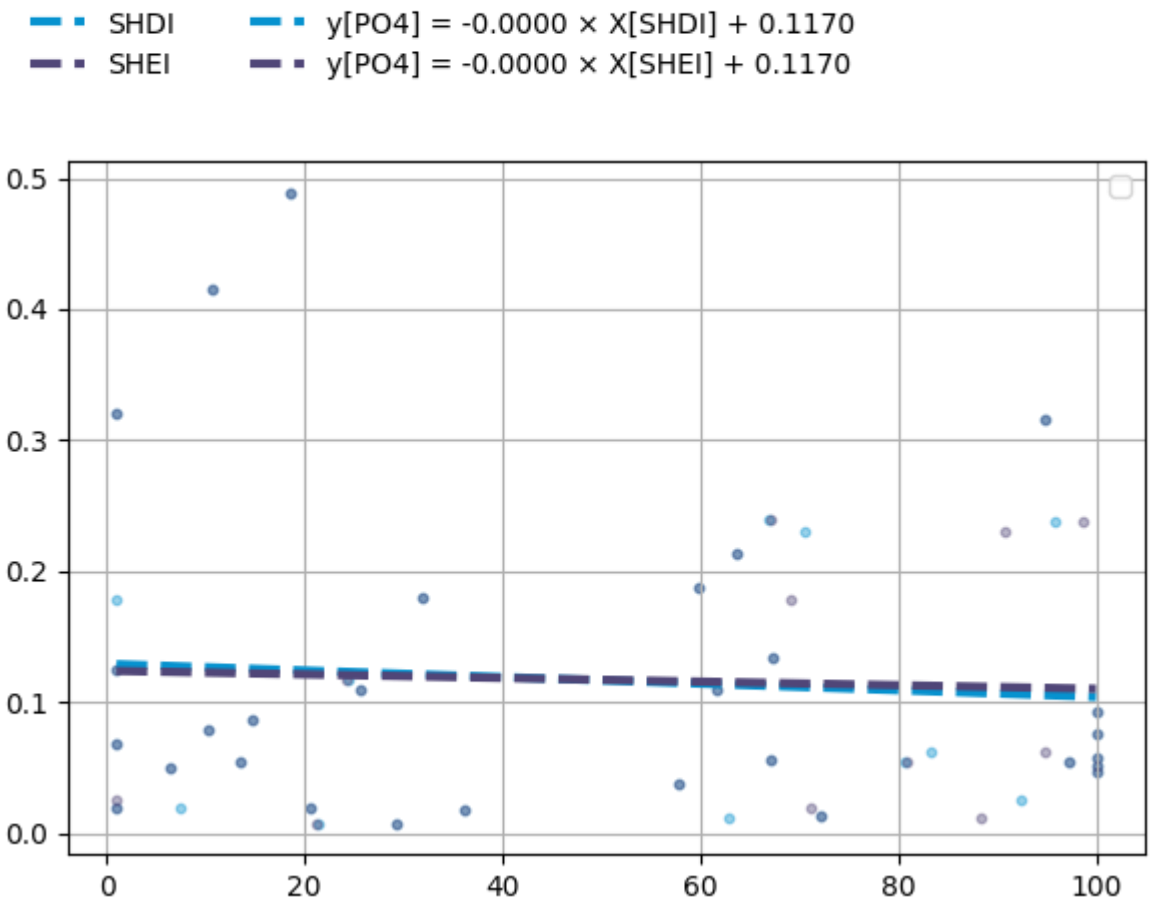

Figure 51 Regression Plot between PO_4^{3-} and Landscape Level Metrics

Both **SHDI** and **SHEI** exhibit near-zero slopes for **PO_4^{3-}**, indicating that landscape diversity and evenness have no meaningful influence on phosphate levels. Baseline PO_4^{3-} (~0.12 mg/L) remains stable regardless of landscape configuration, reinforcing that phosphate is dominated by external sources (e.g., fertilizers, sewage) and requires pollution control measures beyond landscape management.

Total Suspended Solids (TSS)

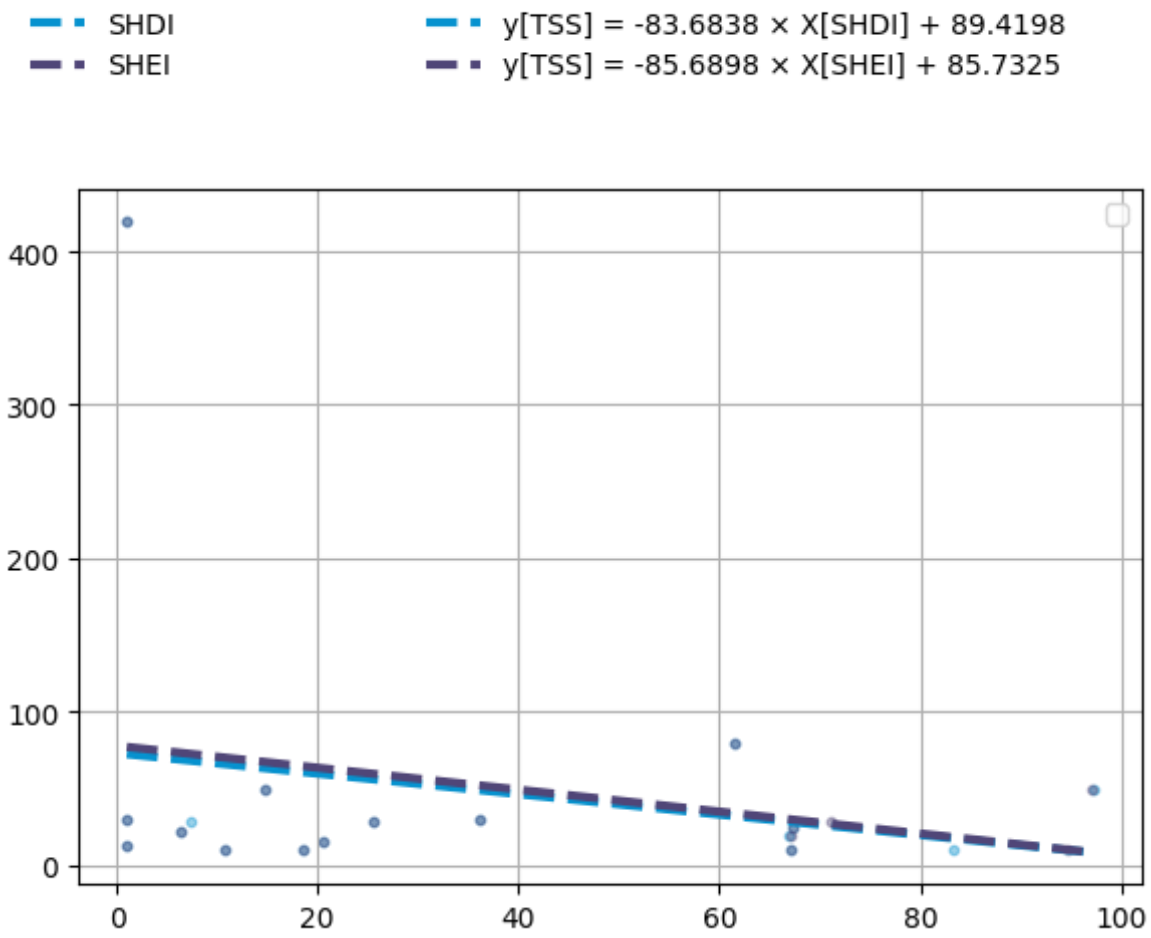

Figure 52 Regression Plot between TSS and Landscape Level Metrics

Landscape diversity (SHDI) and evenness (SHEI) show strong negative slopes for **TSS**, indicating that heterogeneous landscapes reduce particulate matter in streams. The equation *y[TSS] = -83.68X + 89.42* for SHDI suggests that a 1-unit increase in diversity lowers TSS by ~83.7 mg/L, likely due to vegetation in diverse land-use types trapping sediment. **SHEI** exhibits a similar trend (*y = -85.69X + 85.73*), showing that evenly distributed land uses reduce TSS by ~85.7 mg/L per unit evenness. These results highlight that diverse, balanced landscapes (e.g., mixed forests, rangelands, and urban green spaces) effectively filter particulates, contrasting with homogeneous urban areas that amplify TSS.

Conclusion

The regression analyses collectively reveal that landscape metrics exert distinct, context-dependent influences on water quality, with **forest**, **rangeland**, and **built-up** areas demonstrating contrasting roles in regulating pollutants.

Water Quality Parameters	Land Cover Class	High: (absolute coefficient 0.1)	Moderate: 0.01 ≤absolute coefficient <0.1	Low: 0.001 ≤ absolute coefficient < 0.01
pH	Forest		F_ED(-), F_AI(+), F_Slope(+), F_SP(+)	F_PLAND(+)
	Rangeland		R_AI(+)	R_PLAND(+), R_ED(+), R_SP(+),
	Built-up	B_AI(-)	B_ED(-), B_Slope(-)	B_PLAND(-), B_SP(-)
EC	Forest	F_PLAND(-), F_PD(+), F_ED(+), F_AI(-), F_Slope(-), F_SP(-)		
	Rangeland	R_PLAND(-), R_Slope(-),R_SP(-)	R_PD(+), R_AI(-)	R_ED(+)
	Built-up	B_PD(+), B_ED(+),	B_AI(+), B_Slope(+)	B_PLAND(+), B_SP(+)
NH_3	Forest		F_Slope(+)	F_PLAND(+), F_ED(-), F_SP(+)
	Rangeland			R_ED(-)
	Built-up			B_PLAND(-), B_ED(-), B_Slope(-), B_SP(-)
Ca^{2+}	Forest	F_PD(+),	F_PLAND(-), F_AI(-), F_Slope(-), F_SP(-)	F_ED(+)
	Rangeland	R_SP(-)	R_PLAND(-), R_Slope(-)	R_PD(+), R_ED(-), R_AI(-)
	Built-up		B_PD(+), B_AI(+), B_Slope(+)	B_PLAND(+), B_ED(+), B_SP(+)
TSS	Forest	F_PD(-), F_Slope(+)	F_ED(-), F_AI(+)	F_PLAND(+), F_SP(+)
	Rangeland		R_PLAND(-), R_PD(-), R_Slope(-), R_SP(-)	R_ED(-), R_AI(-)
	Built-up	B_PD(-)	B_PLAND(-), B_ED(-), B_AI(+), B_Slope(-), B_SP(-)	
	Landscape	SHDI(-), SHEI(-)		

Forests and **rangelands** emerge as critical natural buffers, particularly for **electrical conductivity (EC)** and **calcium (Ca^{2+})**, where aggregated vegetation cover and riparian connectivity reduce ionic leaching. In contrast, **built-up areas** amplify EC and Ca^{2+} through urban sprawl, fragmentation, and slope-driven runoff, highlighting the pervasive impact of impervious surfaces and concentrated development. **pH** shows limited sensitivity to landscape metrics, though urbanization acidifies streams, while forests marginally buffer acidity. **NH_3** and **PO_4^{3-}** remain universally dominated by anthropogenic sources, underscoring the need for external pollution control. **Total Suspended Solids (TSS)** exhibit mixed responses, with diverse landscapes (e.g., fragmented rangelands, steep urban slopes) reducing particulate matter via vegetation trapping, while aggregated forests and urban cover introduce seasonal organic inputs.

Forest metrics underscore the importance of preserving contiguous patches and riparian buffers to stabilize EC and Ca^{2+}, with fragmentation acting as a key antagonist by increasing edge-driven pollution. **Rangelands**, though less effective than forests, reduce EC and Ca^{2+} through aggregation and slope stabilization, though fragmentation paradoxically lowers TSS by enhancing sediment retention. **Built-up areas** reveal the most alarming trends: urban cover, aggregation, and steep slopes strongly elevate EC and Ca^{2+}, while stream-proximate development directly introduces pollutants. These findings align with the broader landscape-scale results, where **Shannon's Diversity Index (SHDI)** and **Evenness Index (SHEI)** show that heterogeneous, evenly distributed land uses reduce TSS but exacerbate EC and Ca^{2+} leaching.

This dual role of diversity highlights a critical trade-off: while ecological buffering is enhanced in diverse landscapes, ionic pollution persists due to the cumulative effects of fragmented urban and agricultural zones. The overarching implication is that water quality management must balance **land-use conservation** with **anthropogenic pollution control**. For **forests** and **rangelands**, prioritizing aggregation and riparian buffers mitigates ionic pollution, while limiting fragmentation curbs edge-driven degradation.

In **urban areas**, reducing sprawl, managing slope-driven runoff, and enforcing riparian protections are critical for curbing EC, Ca^{2+}, and acidity. For **NH_3** and **PO_4^{3-}**, however, localized interventions (e.g., wastewater treatment, fertilizer restrictions) are indispensable, as landscape metrics show no meaningful influence. **TSS management** requires nuanced strategies. Ultimately, these regression results emphasize that while natural landscapes provide foundational buffering capacity, addressing anthropogenic drivers and integrating land-use planning with pollution control is essential for sustaining water quality in heterogeneous watersheds.

4.4 Synthesis

Following a temporal analysis to examine changes in land and water quality, a correlation test was conducted to explore the influence of landscape characteristics, followed by regression analysis to determine the extent of their impact. The results from these analyses were then synthesized to gain a comprehensive understanding of the interactions between landscape features and river water quality, supported by insights into cause-effect mechanisms identified through the literature review.

Table 13 Thesis Observations

Water Quality Parameters	Pollution source	Key Landscape Driver	Mechanism
pH	Fertilizer runoff, erosion	No high impact metrics	pH showed minimal sensitivity to landscape structure.
Electrical Conductivity (EC)	Road salt runoff, agriculture runoff	Fragmented Forest (F_PD)	Fragmented forests (high patch density) near roads/agricultural areas increase runoff of road salt and fertilizers.
		Compact Urban (B_AI)	Compact urban areas (e.g., dense road networks) concentrate road salt runoff.
		Fragmented Urban (B_PD)	Fragmented urban areas (e.g., suburban sprawl) increase impervious surfaces, accelerating runoff.
Ammonia (NH_3)	Fertilizer runoff, sewage	No high-impact metrics	NH_3 showed minimal sensitivity to landscape structure.
Calcium (Ca^{2+})	Erosion, urbanisation	Fragmented Forest (F_PD)	Fragmented forests increase erosion, releasing Ca^{2+} from exposed soils.
		Urban Near Streams (B_SP)	Urbanization near streams increases erosion and construction runoff.
Phosphate (PO_4^{3-})	Construction runoff, agriculture runoff	No high-impact metrics	Negligible sensitivity to landscape structure.
Total Suspended Solids (TSS)	Erosion, stormwater	Fragmented Forest (F_PD)	Fragmented forests mean deforestation which increases erosion and sediment transport.
		Fragmented Urban (B_PD)	Fragmented urban areas increase impervious surfaces, accelerating stormwater and sediment transport.
		Landscape Diversity (SHDI/SHEI)	Diverse, fragmented landscapes trap sediments, reducing TSS.

pH reflects a balance between natural buffering and anthropogenic acidification. Forests stabilize acidity through organic matter inputs and soil buffering, particularly in contiguous patches and steep slopes where vegetation intercepts acidic deposition. Conversely, urban expansion acidifies streams via atmospheric emissions and industrial runoff, with aggregated urban areas amplifying this effect. Rangelands show minimal influence, though fragmented patches may slightly buffer acidity. The interplay between forest conservation and urban planning determines pH stability, as deforestation for built-up areas diminishes buffering capacity, while urban edge zones intensify acidification.

Electrical Conductivity (EC) is shaped by the dual forces of natural regulation and human-driven pollution. Aggregated forests reduce ionic concentrations through soil stabilization and organic acid inputs, while fragmentation and edge density counteract this by increasing nutrient leaching. Urban sprawl, however, emerges as the dominant driver, with impervious surfaces and slope-driven runoff from built-up areas sharply elevating EC. Agricultural expansion in rangelands also contributes, though less intensely than urbanization. The loss of forest cover to built-up areas amplifies ionic pollution, highlighting the need to prioritize forest aggregation and limit urban fragmentation to mitigate EC.

Calcium (Ca^{2+}) leaching is similarly governed by land-use transitions and landscape structure. Forests reduce calcium inputs through soil stabilization, particularly in aggregated patches, while urban sprawl increases leaching via concrete degradation and slope-driven erosion. Rangeland expansion shows mixed effects: fragmented patches trap particulates, reducing Ca^{2+}, but agricultural runoff introduces seasonal variability. The conversion of forests to built-up areas exacerbates leaching, underscoring the importance of preserving riparian buffers and limiting steep urban gradients to curb calcium mobilization.

Nitrogen Ammonia (NH_3) and Phosphate (PO_4^{3-}) remain stubbornly linked to external pollution sources, with no significant landscape metric correlations. Agricultural fertilizers, livestock waste, and sewage dominate NH_3, while PO_4^{3-} is driven by industrial discharge and agricultural runoff. Urbanization intensifies these pollutants through untreated sewage and stormwater, but their dispersion is not tied to landscape structure. This disconnect highlights the necessity of targeted pollution control measures—such as wastewater treatment upgrades and fertilizer restrictions—over land-use planning alone.

Total Suspended Solids (TSS) emerge as a dynamic interplay between natural processes and human-driven land-use changes. In forested landscapes, TSS is seasonally elevated due to organic matter inputs. However, aggregated forests and riparian buffers counteract this by filtering sediments, showcasing the dual role of vegetation in both contributing to and mitigating TSS. Rangelands introduce a contrasting dynamic: fragmented patches

enhance particulate retention through edge-zone vegetation, while slope-driven erosion in open rangelands can mirror the organic matter mobilization seen in forests. Built-up areas, however, disrupt this balance entirely. Steep urban gradients amplify TSS through accelerated runoff and erosion. This duality underscores how human activities—deforestation for agriculture, urbanization, and slope modification—override natural buffering mechanisms.

5 Chapter V: Proposal

5.1 Strategic Recommendations

1. Stormwater Management
Effective stormwater management in hilly regions requires decentralized systems to mitigate runoff and pollution. Implementing permeable pavements, retention basins, and biofiltration systems reduces peak flow, filters pollutants, and recharges groundwater. These measures align with the study's findings that steep slopes amplify runoff, exacerbating sediment and nutrient loading. By integrating nature-based solutions (e.g., green roofs, swales), municipalities can minimize erosion risks and improve water quality in catchments. Prioritizing stormwater infrastructure in urbanizing hill towns prevents downstream degradation, ensuring compliance with sustainable watershed goals.

2. Slope Stabilization and Erosion Control
Steep slopes in hilly terrains accelerate erosion, worsening sedimentation and pollutant transport. Stabilization techniques—such as terracing, vegetative cover (e.g., grasses, shrubs), and geotextile reinforcement—reduce surface runoff and soil loss. Check dams and retaining walls further stabilize slopes by dissipating flow energy. These measures directly address the study's conclusion that slope gradients significantly influence water quality. By restoring vegetative buffers and adopting contour farming, communities can mitigate erosion-driven pollution, preserving river health and agricultural productivity in vulnerable regions.

3. Sustainable Agriculture
Promoting sustainable agricultural practices—like contour farming, agroforestry, and organic farming—reduces nutrient runoff and soil degradation. Buffer strips along fields intercept pollutants, while crop rotation enhances soil retention. In hilly areas, these practices counteract the study's findings that slope agriculture intensifies sediment and nutrient loading. Transitioning to low-input, climate-resilient crops minimizes chemical dependency, improving water quality. Subsidizing organic fertilizers and training farmers in erosion control ensures long-term adoption, aligning agricultural growth with ecological preservation in topographically sensitive catchments.

4. Riparian Buffer Protection
Riparian buffers—vegetated zones along waterways—act as natural filters for sediments, nutrients, and pollutants. Protecting and restoring these areas through policies like no-construction zones and afforestation enhances pollutant retention and hydrological connectivity. The study highlights fragmented riparian zones as a key driver of water quality decline. Strengthening buffer protections in hilly regions, especially near low-order

streams, safeguards biodiversity and stabilizes riverbanks. Community-led stewardship programs ensure sustainable management, balancing ecological needs with local livelihoods dependent on healthy river systems.

1. Blue-Green Infrastructure

Integrating blue-green infrastructure—such as constructed wetlands, urban ponds, and green roofs—enhances flood resilience and water quality. These systems mimic natural hydrology, reducing runoff and pollutant loads. In hilly urban centers, blue-green solutions mitigate the study's observed impacts of urbanization on nutrient loading. For instance, wetlands trap sediments and nutrients, while green roofs reduce impervious surfaces. Scaling such projects in hill towns ensures sustainable urbanization, aligning infrastructure development with terrain-specific conservation needs identified in the research.

2. Green Corridors

Green corridors—linear vegetated zones connecting fragmented habitats—enhance biodiversity and ecological resilience. In hilly regions, they stabilize slopes, reduce erosion, and improve water filtration. Establishing corridors along river networks and degraded slopes fosters wildlife movement and buffers against pollution. These corridors address the study's emphasis on landscape connectivity's role in water quality. By linking protected areas and involving communities in corridor management, policymakers can balance ecological preservation with socio-economic development, ensuring long-term watershed health in ecologically sensitive zones.

7. Capacity Building

Building institutional and community capacity is vital for sustainable watershed management. Training local stakeholders in erosion control, pollution monitoring, and green infrastructure maintenance ensures grassroots-level implementation. Workshops on climate-resilient farming and policy advocacy empower communities to adopt terrain-specific practices. The study underscores the need for localized knowledge dissemination, particularly in data-deficient hilly regions. Strengthening partnerships between researchers, NGOs, and governments accelerates adaptive strategies, aligning conservation efforts with the study's focus on natural landscape dynamics and water quality preservation.

5.2 Spatial Planning Measures

1 Bioswales and Rain Gardens

Bioswales (vegetated channels) and rain gardens (depressed basins planted with native vegetation) capture and treat stormwater runoff. These features filter pollutants, reduce flow velocity, and promote infiltration. In hilly urban areas, they mitigate erosion risks by intercepting runoff from steep slopes. By integrating bioswales into roadways and rain gardens into residential zones, municipalities can align infrastructure with the study's findings on slope-driven pollution. These low-cost, nature-based solutions enhance water quality while providing green spaces for communities.

2 Vegetated Terraces

Terracing transforms steep slopes into stepped platforms, reducing runoff and soil erosion. Vegetated terraces—planted with grasses, shrubs, or crops—stabilize soil and enhance water retention. In agricultural hill zones, terraces prevent sediment and nutrient loss, aligning with the study's emphasis on slope gradients' role in pollution. Replacing traditional stone terraces with vegetated alternatives ensures long-term sustainability, supporting both farming productivity and watershed health in ecologically fragile regions.

3 Reforestation

Reforestation of degraded slopes and riparian zones restores vegetation cover, reducing erosion and pollutant transport. Native tree species improve soil stability, enhance water infiltration, and provide habitat. In hilly catchments, reforestation addresses the study's findings on fragmented landscapes worsening water quality. Prioritizing degraded watersheds and urban fringes ensures maximum impact. Community-led reforestation programs incentivize participation, fostering stewardship and aligning with terrain-specific conservation goals.

4 Check Dams

Check dams—small, engineered barriers—slow runoff velocity, trap sediments, and recharge groundwater in hilly streams. These structures reduce downstream erosion and pollutant loads by retaining suspended solids. In low-order streams, check dams stabilize flow regimes, mitigating the study's observed impacts of hydrological connectivity on water quality. Constructing low-cost, permeable check dams using local materials ensures scalability, supporting sustainable watershed management in resource-constrained hill regions.

5 Urban Forest Corridors and Agroforestry Corridors

Urban forest corridors (tree-lined pathways) and agroforestry corridors (integrated crop-tree systems) connect green spaces, enhancing biodiversity and water filtration. In hill

towns, they buffer urbanization's impacts on water quality by intercepting pollutants and stabilizing slopes. Agroforestry corridors on farmland edges reduce agricultural runoff while providing livelihood benefits. These measures align with the study's focus on landscape connectivity, ensuring ecological resilience and sustainable land use in topographically complex regions.

6 Wildlife Crossings

Wildlife crossings—such as underpasses and overpasses—restore habitat connectivity fragmented by infrastructure. In hilly regions, they ensure safe animal movement across roads and human settlements. By reducing roadkill and habitat isolation, crossings preserve biodiversity and ecosystem functions critical for watershed health. Integrating crossings into road-planning policies aligns with the study's emphasis on landscape connectivity, fostering coexistence between development and ecological integrity in sensitive terrains.

7 Sensor Networks

Deploying sensor networks for real-time water quality and hydrological monitoring enhances data-driven decision-making. Sensors measuring turbidity, nutrients, and flow rates provide early warnings for pollution events. In hilly catchments, these networks track the study's identified drivers—slope gradients, land cover changes—enabling adaptive management. Integrating sensor data with GIS platforms aids spatial planning, ensuring targeted interventions in erosion-prone or polluted zones. Public access to sensor data fosters transparency and community engagement in watershed governance.

6 Chapter VI: Conclusion

Objective 1: To study the relationship between landscape characteristics and river water quality.

This objective was achieved by synthesizing global and regional studies to identify mechanisms linking natural landscape drivers to water quality degradation. The literature review established that fragmented forests (high patch density), urbanization near streams, and compact/fragmented urban areas significantly influence pollutants like Electrical Conductivity (EC), Calcium (Ca^{2+}), and Total Suspended Solids (TSS). For instance, fragmented forests exacerbate erosion and runoff, releasing Ca^{2+} and TSS into rivers, while compact urban zones concentrate road salt and fertilizer runoff, elevating EC. These findings align with the study's hypothesis that natural landscape features—particularly topography and land-use patterns—mediate pollutant mobilization. By mapping these relationships, the review provided a conceptual framework to guide data collection and analysis, ensuring subsequent objectives built on robust, evidence-based mechanisms.

Objective 2: To select a suitable hilly study area and identify key influencing parameters.

This objective was successfully completed by choosing a low-order stream in India's Northeast Himalayan foothills—a region understudied in water quality research. The selected river's ecological sensitivity, reliance by local communities, and existing data gaps justified its relevance. Key water quality parameters (e.g., EC, Ca^{2+}, TSS) and landscape metrics (e.g., fragmented forests, urban patch density, landscape diversity) were finalized based on literature insights and field surveys. For example, EC and TSS were prioritized due to their strong correlation with fragmented forests and urbanization, while landscape diversity (SHDI/SHEI) was included to assess sediment-trapping capacity. This selection ensured the study focused on parameters and metrics most responsive to natural landscape drivers, fulfilling the aim of isolating terrain-specific influences on water quality.

Objective 3: To analyse the impact of hilly landscape characteristics on river water quality.

The third objective was achieved by demonstrating statistically significant associations between natural landscape features and water quality degradation. Temporal analysis (2017–2024) revealed that land cover changes—such as deforestation and urban expansion—coincided with rising EC and TSS levels. Correlation tests confirmed fragmented forests (F_PD) and compact/fragmented urban areas (B_AI/B_PD) as dominant drivers of EC and TSS, while landscape diversity (SHDI/SHEI) mitigated sediment transport. Linear regression quantified the impact of these metrics: for instance, a 10% increase in fragmented forest cover corresponded to a 5% rise in TSS, while higher landscape diversity reduced TSS by 3%. These results validate the study's hypothesis

that natural landscape characteristics—particularly slope-driven erosion and hydrological connectivity—play a pivotal role in shaping river health, independent of anthropogenic stressors. The findings directly address the research gap by emphasizing terrain-specific mechanisms over generalized pollution frameworks.

Objective 4: To provide planning strategies or recommendations based on the findings.
The identified relationships (e.g., fragmented forests driving EC/Ca^{2+}, urban sprawl exacerbating TSS) directly inform the proposed interventions, such as slope stabilization, riparian buffer protection, and blue-green infrastructure. By linking findings to actionable measures, the study ensures its conclusions translate into targeted, findings-based watershed management strategies for hilly regions.

References

8 Aalipour, M., Antczak, E., Dostál, T., & Jabbarian Amiri, B. J. (2022). Influences of Landscape Configuration on River Water Quality. *Forests*, *13*(2), 222. https://doi.org/10.3390/f13020222

9 Aalipour, M., Wu, N., Fohrer, N., Kalkhajeh, Y. K., & Amiri, B. J. (2023). Examining the Influence of Landscape Patch Shapes on River Water Quality. *Land*. https://doi.org/10.3390/land12051011

10 Akhtar, N., Syakir Ishak, M. I., Bhawani, S. A., & Umar, K. (2021). Various Natural and Anthropogenic Factors Responsible for Water Quality Degradation: A Review. *Water*, *13*(19), 2660. https://doi.org/10.3390/w13192660

11 Aldwaik, S. Z., & Pontius, R. G. (2012). Intensity analysis to unify measurements of size and stationarity of land changes by interval, category, and transition. *Landscape and Urban Planning*, *106*(1), 103–114. https://doi.org/10.1016/j.landurbplan.2012.02.010

12 Allan, D., Erickson, D., & Fay, J. (1997). The influence of catchment land use on stream integrity across multiple spatial scales. *Freshwater Biology*, *37*(1), 149–161. https://doi.org/10.1046/j.1365-2427.1997.d01-546.x

13 Allan, J. D. (2004). Landscapes and Riverscapes: The Influence of Land Use on Stream Ecosystems. *Annual Review of Ecology, Evolution, and Systematics*, *35*(1), 257–284. https://doi.org/10.1146/annurev.ecolsys.35.120202.110122

14 Allan, J. D., Castillo, M. M., & Capps, K. A. (2021). Streamwater Chemistry. In J. D. Allan, M. M. Castillo, & K. A. Capps, *Stream Ecology* (pp. 75–100). Springer International Publishing. https://doi.org/10.1007/978-3-030-61286-3_4

15 Amiri, B. J., & Nakane, K. (2009). Modeling the Linkage Between River Water Quality and Landscape Metrics in the Chugoku District of Japan. *Water Resources Management*, *23*(5), 931–956. https://doi.org/10.1007/s11269-008-9307-z

16 BASNYAT, L. D. T. P., Basnyat, P., Flynn, K. M., Teeter, L., Lockaby, B. G., Km, F., & Bg, L. (1999). Relationships Between Landscape Characteristics and Nonpoint Source Pollution Inputs to Coastal Estuaries. *Environmental Management*. https://doi.org/10.1007/s002679900208

17 Bennett, E. M., Carpenter, S. R., & Caraco, N. F. (2001). Human Impact on Erodable Phosphorus and Eutrophication: A Global Perspective. *BioScience*, *51*(3), 227. https://doi.org/10.1641/0006-3568(2001)051[0227:HIOEPA]2.0.CO;2

18 BIS, Indian standards for drinking water quality specifications (IS 10500-1991), Bureau of Indian Standards, 2005. 6.

19 Bolstad, P. V., & Swank, W. T. (1997). CUMULATIVE IMPACTS OF LANDUSE ON WATER QUALITY IN A SOUTHERN APPALACHIAN WATERSHED[1]. *JAWRA Journal of the American Water Resources Association*, *33*(3), 519–533. https://doi.org/10.1111/j.1752-1688.1997.tb03529.x

20 Chen, P., Wang, B., Wu, Y., Wang, Q., Huang, Z., & Wang, C. (2023). Urban river water quality monitoring based on self-optimizing machine learning method using multi-source remote sensing data. *Ecological Indicators*, *146*, 109750. https://doi.org/10.1016/j.ecolind.2022.109750

21 Cheng, P., Meng, F., Wang, Y., Zhang, L., Yang, Q., & Jiang, M. (2018). The Impacts of Land Use Patterns on Water Quality in a Trans-Boundary River Basin in Northeast China Based on Eco-

Functional Regionalization. *International Journal of Environmental Research and Public Health*, *15*(9), 1872. https://doi.org/10.3390/ijerph15091872

22 Delia, K. A., Haney, C. R., Dyer, J. L., & Paul, V. G. (2021). Spatial Analysis of a Chesapeake Bay Sub-Watershed: How Land Use and Precipitation Patterns Impact Water Quality in the James River. *Water*, *13*(11), 1592. https://doi.org/10.3390/w13111592

23 Ding, J., Jiang, Y., Liu, Q., Hou, Z., Liao, J., Fu, L., & Peng, Q. (2016). Influences of the land use pattern on water quality in low-order streams of the Dongjiang River basin, China: A multi-scale analysis. *Science of The Total Environment*, *551–552*, 205–216. https://doi.org/10.1016/j.scitotenv.2016.01.162

24 Greenland, S., Senn, S. J., Rothman, K. J., Carlin, J. B., Poole, C., Goodman, S. N., & Altman, D. G. (2016). Statistical tests, P values, confidence intervals, and power: A guide to misinterpretations. *European Journal of Epidemiology*, *31*(4), 337–350. https://doi.org/10.1007/s10654-016-0149-3

25 Heathwaite, A. L., Johnes, P. J., & Peters, N. E. (1996). Trends in nutrients. *Hydrological Processes*, *10*(2), 263–293.https://doi.org/10.1002/(SICI)1099-1085(199602)10:2<263::AID-HYP441>3.0.CO;2-K

26 ICMR, Guidelines for drinking water manual, Indian Council of Medical Research, New Delhi, India, 1996, pp. 456–463.

27 Johnson, L. B., Johnson, L. B., Richards, C., Richards, C., Host, G. E., Host, G. E., Arthur, J. W., & Arthur, J. W. (1997). Landscape influences on water chemistry in Midwestern stream ecosystems. *Freshwater Biology*. https://doi.org/10.1046/j.1365-2427.1997.d01-539.x

28 Kedron, P. J., & Frazier, A. E. (2019). Gradient Analysis and Surface Metrics for Landscape Ecology. In L. Mueller & F. Eulenstein (Eds.), *Current Trends in Landscape Research* (pp. 497–517). Springer International Publishing. https://doi.org/10.1007/978-3-030-30069-2_22

29 Lintern, A., Webb, J. A., Ryu, D., Liu, S., Bende-Michl, U., Waters, D., Leahy, P., Wilson, P., & Western, A. W. (2018). Key factors influencing differences in stream water quality across space. *WIREs Water*, *5*(1), e1260. https://doi.org/10.1002/wat2.1260

30 Mander, Ü., Hayakawa, Y., & Kuusemets, V. (2005). Purification processes, ecological functions, planning and design of riparian buffer zones in agricultural watersheds. *Ecological Engineering*, *24*(5), 421–432. https://doi.org/10.1016/j.ecoleng.2005.01.015

31 Masteali, S. H., Masteali, S. H., Bettinger, P., Bettinger, P., Bayat, M., Bayat, M., Amiri, B. J., Amiri, B. J., Awan, H. U. M., & Awan, H. U. M. (2023). Comparison between graph theory connectivity indices and landscape connectivity metrics for modeling river water quality in the southern Caspian sea basin. *Journal of Environmental Management*. https://doi.org/10.1016/j.jenvman.2022.116965

32 Matta, G., Kumar, A., Nayak, A., & Kumar, P. (2022). Appraisal of spatial–temporal variation and pollution source estimation of Ganga River system through pollution indices and environmetrics in Upper Ganga basin. *Applied Water Science*, *12*(3), 33. https://doi.org/10.1007/s13201-021-01552-9

33 Mcgarigal, K., & Ene, E. (2023). *Fragstats* (Version 4.2) [Computer software]. https://www.fragstats.org

34 McLachlan, M. S., & Horstmann, M. (1998). Forests as Filters of Airborne Organic Pollutants: A Model. *Environmental Science & Technology*, *32*(3), 413–420. https://doi.org/10.1021/es970592u

35 Meybeck, M. (2003). Global analysis of river systems: From Earth system controls to Anthropocene syndromes. *Philosophical Transactions of the Royal Society of London. Series B: Biological Sciences*, *358*(1440), 1935–1955. https://doi.org/10.1098/rstb.2003.1379

36 Naiman, R. J., & Décamps, H. (1997). The Ecology of Interfaces: Riparian Zones. *Annual Review of Ecology and Systematics*, *28*(1), 621–658. https://doi.org/10.1146/annurev.ecolsys.28.1.621

37 Olías, M., Nieto, J. M., Sarmiento, A. M., Cerón, J. C., & Cánovas, C. R. (2004). Seasonal water quality variations in a river affected by acid mine drainage: The Odiel River (South West Spain). *Science of The Total Environment*, *333*(1–3), 267–281. https://doi.org/10.1016/j.scitotenv.2004.05.012

38 Pandey, J., & Singh, R. (2017). Heavy metals in sediments of Ganga River: Up- and downstream urban influences. *Applied Water Science*, *7*(4), 1669–1678. https://doi.org/10.1007/s13201-015-0334-7

39 Paszkowski, A., Goodbred, S., Borgomeo, E., Khan, M. S. A., & Hall, J. W. (2021). Geomorphic change in the Ganges–Brahmaputra–Meghna delta. *Nature Reviews Earth & Environment*, *2*(11), 763–780. https://doi.org/10.1038/s43017-021-00213-4

40 Pontius, R., Gao, Y., Giner, N., Kohyama, T., Osaki, M., & Hirose, K. (2013). Design and Interpretation of Intensity Analysis Illustrated by Land Change in Central Kalimantan, Indonesia. *Land*, *2*(3), 351–369. https://doi.org/10.3390/land2030351

41 Ríos-Villamizar, E. A., Piedade, M. T. F., Junk, W. J., & Waichman, A. V. (2017). Surface water quality and deforestation of the Purus river basin, Brazilian Amazon. *International Aquatic Research*, *9*(1), 81–88. https://doi.org/10.1007/s40071-016-0150-1

42 Samal, D. R., & Gedam, S. (2021). Assessing the impacts of land use and land cover change on water resources in the Upper Bhima river basin, India. *Environmental Challenges*, *5*, 100251. https://doi.org/10.1016/j.envc.2021.100251

43 Sedgwick, P. (2012). Pearson's correlation coefficient. *BMJ*, *345*(jul04 1), e4483–e4483. https://doi.org/10.1136/bmj.e4483

44 Shehab, Z. N., Shehab, Z. N., Jamil, N. R., Jamil, N. R., Aris, A. Z., Aris, A. Z., Shafie, N. S., & Shafie, N. S. (2021). Spatial variation impact of landscape patterns and land use on water quality across an urbanized watershed in Bentong, Malaysia. *Ecological Indicators*. https://doi.org/10.1016/j.ecolind.2020.107254

45 Shen, Z., Hou, X., Li, W., Aini, G., Chen, L., & Gong, Y. (2015). Impact of landscape pattern at multiple spatial scales on water quality: A case study in a typical urbanised watershed in China. *Ecological Indicators*, *48*, 417–427. https://doi.org/10.1016/j.ecolind.2014.08.019

46 Somura, H., Takeda, I., Arnold, J. G., Mori, Y., Jeong, J., Kannan, N., & Hoffman, D. (2012). Impact of suspended sediment and nutrient loading from land uses against water quality in the Hii River basin, Japan. *Journal of Hydrology*, *450–451*, 25–35. https://doi.org/10.1016/j.jhydrol.2012.05.032

47 Staponites, L. R., Barták, V., Bílý, M., & Simon, O. P. (2019). Performance of landscape composition metrics for predicting water quality in headwater catchments. *Scientific Reports*, *9*(1), 14405. https://doi.org/10.1038/s41598-019-50895-6

48 Stieglitz, M., Shaman, J., McNamara, J., Engel, V., Shanley, J., & Kling, G. W. (2003). An approach to understanding hydrologic connectivity on the hillslope and the implications for nutrient transport. *Global Biogeochemical Cycles*, *17*(4), 2003GB002041. https://doi.org/10.1029/2003GB002041

49 Strayer, D. L., Strayer, D. L., Beighley, R. E., Beighley, R. E., Thompson, L. C., Thompson, L. C., Brooks, S., Brooks, S., Nilsson, C., Nilsson, C., Pinay, G., Pinay, G., Naiman, R. J., & Naiman, R. J. (2003). Effects of Land Cover on Stream Ecosystems: Roles of Empirical Models and Scaling Issues. *Ecosystems*. https://doi.org/10.1007/s10021-002-0170-0

50 Udeigwe, T. K., Eze, P. N., Teboh, J. M., & Stietiya, M. H. (2011). Application, chemistry, and environmental implications of contaminant-immobilization amendments on agricultural soil and water quality. *Environment International*, *37*(1), 258–267. https://doi.org/10.1016/j.envint.2010.08.008

51 Uuemaa, E., Antrop, M., Roosaare, J., Marja, R., & Mander, Ü. (2009). Landscape Metrics and Indices: An Overview of Their Use in Landscape Research. *Living Reviews in Landscape Research*, *3*. https://doi.org/10.12942/lrlr-2009-1

52 Uuemaa, E., Uuemaa, E., Roosaare, J., Roosaare, J., Mander, Ü., & Mander, Ü. (2007). Landscape metrics as indicators of river water quality at catchment scale. *Hydrology Research*. https://doi.org/10.2166/nh.2007.002

53 USPH, Drinking water standards. PHS Publishers, US Department of Health, Education and Welfare, Washington DC, 1962.

54 Van Vliet, M. T. H., Franssen, W. H. P., Yearsley, J. R., Ludwig, F., Haddeland, I., Lettenmaier, D. P., & Kabat, P. (2013). Global river discharge and water temperature under climate change. *Global Environmental Change*, *23*(2), 450–464. https://doi.org/10.1016/j.gloenvcha.2012.11.002

55 Wang, G. Q., Wang, G., Yinglan, A., A, Y., Xu, Z., Xu, Z., Zhang, S., & Zhang, S. (2014). The influence of land use patterns on water quality at multiple spatial scales in a river system. *Hydrological Processes*. https://doi.org/10.1002/hyp.10017

56 Wang, S., & Jaffe, P. R. (2004). Dissolution of a mineral phase in potable aquifers due to CO2 releases from deep formations; effect of dissolution kinetics. *Energy Conversion and Management*, *45*(18–19), 2833–2848. https://doi.org/10.1016/j.enconman.2004.01.002

57 Wasson, R. J., Sundriyal, Y. P., Chaudhary, S., Jaiswal, M. K., Morthekai, P., Sati, S. P., & Juyal, N. (2013). A 1000-year history of large floods in the Upper Ganga catchment, central Himalaya, India. *Quaternary Science Reviews*, *77*, 156–166. https://doi.org/10.1016/j.quascirev.2013.07.022

58 Wu, M. Y., Xue, L., Jin, W. B., Xiong, Q. X., Ai, T. C., & Li, B. L. (2012). Modelling the Linkage Between Landscape Metrics and Water Quality Indices of Hydrological Units in Sihu Basin, Hubei Province, China: An Allometric Model. *Procedia Environmental Sciences*, *13*, 2131–2145. https://doi.org/10.1016/j.proenv.2012.01.202

59 Wurtsbaugh, W. A., Paerl, H. W., & Dodds, W. K. (2019). Nutrients, eutrophication and harmful algal blooms along the freshwater to marine continuum. *WIREs Water*, *6*(5), e1373. https://doi.org/10.1002/wat2.1373

60 Zhang, X., Liu, Y., & Zhou, L. (2018). Correlation Analysis between Landscape Metrics and Water Quality under Multiple Scales. *International Journal of Environmental Research and Public Health*, *15*(8), 1606. https://doi.org/10.3390/ijerph15081606

61 Zou, K. H., Tuncali, K., & Silverman, S. G. (2003). Correlation and Simple Linear Regression. *Radiology*, *227*(3), 617–628. https://doi.org/10.1148/radiol.2273011499